

NTIA Case Study: Adjacent-Band Coexistence Between 5G Base Station Transmitters and Air Traffic Control Radar Receivers

**Frank H. Sanders
Geoffrey A. Sanders
Brian D. Nelson
Robert L. Sole
Oscar Valle-Colon**



Technical Report

NTIA Case Study: Adjacent-Band Coexistence Between 5G Base Station Transmitters and Air Traffic Control Radar Receivers

**Frank H. Sanders
Geoffrey A. Sanders
Brian D. Nelson
Robert L. Sole
Oscar Valle-Colon**



U.S. DEPARTMENT OF COMMERCE

Alan Davidson
Assistant Secretary of Commerce for Communications and Information
National Telecommunications and Information Administration

December 2024

DISCLAIMER

Certain commercial equipment and materials are identified in this report to specify adequately the technical aspects of the reported results. In no case does such identification imply recommendation or endorsement by the National Telecommunications and Information Administration, nor does it imply that the material or equipment identified is the best available for this purpose.

FOREWORD

This report tells the story of more than just a routine radiofrequency electromagnetic compatibility (EMC) and coexistence problem and its solution. It is, more fundamentally, a case study in how to approach these kinds of problems in a systematic way, using a scientific-engineering method to find an answer even though the answer, in this case, was completely unexpected.

The authors, especially the lead author over the last four and a half decades, have heard calls for a one-size-fits-all, cookbook solution for approaching these kinds of problems, an approach that can be implemented by minimally trained personnel with a minimum amount of available equipment and shoestring-level funding. That goal is unrealistic and unattainable. There is no substitute for knowledgeable and experienced personnel, supplied with adequate equipment.

Successionally, it is crucially important for newer engineers to study with more experienced engineers, while they have a chance to overlap in the work force. The lead author feels especially strongly about this need for succession provisions and considerations, as he will be retiring in November 2024, after more than 45 years of Federal Government service in which he has worked on dozens of these sorts of cases.

On the equipment side, the most important need is not necessarily for the latest or most expensive gear, although good equipment should be made available for the work. Rather, the most important aspect is that the people who are using the equipment should understand exactly how their machines work; what the machines' limitations are; and how to properly interpret the machines' outputs. That is how forward progress is made and costly mistakes are avoided.

Although making an EMC cookbook is an illusory goal, general guidelines for approaching these sorts of studies can be defined and described. That is what this report does, using this particular EMC coexistence problem as an illustration.

The fundamental basis of all such work must always be a solid grasp of the scientific method by the people who are working on it. Following Karl Popper, this method never proves a hypothesis. It always seeks, contrarily, to *disprove* its hypotheses. Disproven hypotheses are used to build alternatives which are, in their turn, subjected to further attempted disproofs.

Failure to disprove a hypothesis strengthens it, leading to another, logically developmental, step along the same path. But again, these hypotheses are never, in and of themselves, proven. They are only, and at most, not disproved.

Our engineering hypotheses for radio interference problems must be constructed creatively, using known facts while seeking to extend them into unknown territory. In this case study, we used initially known facts to construct what we believed was an initially solid hypothesis for the cause of observed and reported radar receiver interference that was clearly causally connected to adjacent band 5G base station transmitter operations. Our initial interference hypothesis was for a routine type of problem, with a routinely encountered physical mechanism.

Working to disprove ourselves, we were greatly surprised and rather pleased when we succeeded! The revealed interference mechanism was completely unexpected. Moreover, it was novel, one that we had never previously seen in four and a half decades of experience with such cases.

In this report's case study format, we note, too, that we have followed a suggestion made years ago by a noted ITS mathematician, the late Dr. George Hufford. George felt that too many scientific and engineering studies were published showing only successes, and that too few (really not any) studies were published which described, for educational purposes, researchers' wrong turns and mistakes. He volunteered that a *Journal of Failed Studies and Erroneous Results* would be productive and useful for scientific and engineering communities.

This case study honors Dr. Hufford's suggestion. The largest point of this study is not the interference mechanism that we found, along with its resolution, as interesting, useful and critically important as they are for obtaining better coexistence between legacy safety-of-life air traffic control radar receivers and newly introduced adjacent-band 5G transmitter base stations.

Rather, it is to show our readers that the scientific method, used properly, will lead to accurately revealed physical truth, despite contrary, pre-conceived expectations. We scientist-engineers do not seek to be proven right. We seek to prove ourselves wrong. Because that is how we learn.

In this report we happily describe how we have, in this instance, succeeded in proving ourselves wrong.

CONTENTS

Foreword.....	iii
Figures.....	viii
Tables.....	xiii
Abbreviations/Acronyms.....	xiv
Executive Summary.....	xv
1. Introduction.....	2
1.1 Background.....	2
1.2 NTIA Involvement and Work Program Goal Development.....	4
1.3 Work Program Development: General.....	6
1.4 Work Program Development: Specific.....	7
1.5 Pause for Interference-Mechanism Discussion.....	9
1.6 Work Program.....	10
2. Measurements of Adjacent-band B41 5G Signals Inside an ASR-9 Receiver.....	12
2.1 Initial 5G Signal-Response Measurements Inside the ASR-9 Receiver.....	12
2.2 Pause for Field Notebooks.....	14
2.3 Establishment of the Interference Mechanism and Source.....	15
2.4 Radar Receiver Initial Interference-Effects Measurements.....	16
2.5 Further RF Beam-Switch and STC-Stage Interference-Effects Testing at the FAA Technical Center.....	22
2.6 Results of Interference-Effects Testing at the FAA Technical Center.....	23
2.6.1 Attempted Power-Overload: Results.....	23
2.6.2 Fourier Spectrum-Spreading Interference-Effects Results.....	23
3. Controlled-condition Measurements of Radiated 5G Base Station Emission Spectra.....	28
3.1 Adequacy of Base Station Spectrum Certification Emission Spectra.....	29
3.2 5G CoW Base Station Radiated-Emission Setup at Table Mountain.....	29
3.2.1 Physical Radiated Measurement Location and Geometry.....	29
3.2.2 RSMS Measurement System Hardware.....	33
3.2.3 RSMS Measurement System Calibration.....	34
3.2.4 RSMS Measurement System Software.....	34
3.2.5 RSMS-5G Measurement Software Including Stepped-Frequency Algorithm.....	36
3.2.6 Stored Emission Spectra and Supporting Associated Data.....	38
3.2.7 Local ASR-9 Signals at Table Mountain.....	38
3.2.8 Local B41 5G Signals.....	39
3.3 5G Base Station Transmitters.....	40
3.3.1 64T64R MIMO Array Designs, Briefly.....	40
3.3.2 5G MIMO Beam Elevation Angle Range and Control.....	42
3.3.3 Table Mountain 5G CoW Configurations.....	43
3.4 5G Radiated Emission Data from Table Mountain.....	44
3.4.1 Baseline (Background) Spectrum Environment.....	44
3.4.2 5G Base Station Emission Spectra as a Function of Channel Bandwidth.....	46
3.4.3 5G Base Station Emission Spectrum Channel-Width Discussion.....	49

3.4.4 5G Base Station Antenna Beam-Muting Experiment	50
3.4.5 5G Base Station Antenna Beam-Muting Discussion	53
3.4.6 5G Base Station Antenna Beam Downtilting Experiment	54
3.4.7 5G Base Station Antenna Beam Azimuth-Rotation Experiment	54
3.4.8 5G Transmitter Base Station Channel PRB Blanking.....	55
4. Coexistence Analysis	56
4.1 Power-Decoupling Approaches	56
4.2 Desirability of Proactive Power-Decoupling Coordination.....	56
4.3 Wireless Carriers Need to Know Where to Power-Decouple.....	56
4.4 Computation Approach for Spectrum Coexistence Coordination-Zone Development	57
4.5 Example Coordination Outputs	58
5. Conclusions and Recommendations	62
6. Lessons Learned.....	64
7. References.....	65
Acknowledgements.....	66
Appendix A : ASR-9 Receiver Characteristics Measurements	68
Appendix B : Test Plan for ASR-9 Receiver-Response Characterization Measurements at the FAA Technical Center	71
B.1 Background	71
B.2 Objectives.....	72
B.3 Approach	72
B.3.1 Data Collection	72
B.3.2 FAA, NTIA/ITS, and NTIA/OSM Participation	73
B.3.3 Classification of the Work	73
B.4 Data Collection Measurements	73
B.4.1 Measurement Location	73
B.4.2 Measurement Procedures.....	74
B.4.3 Note on Controlling the 5G Signal Input-Power to the Radar Receiver.	76
B.4.4 Note on Determining ASR-9 Receiver Overload-Power Thresholds, If Overload is Observed	76
B.5 ASR-9 Receiver Measurements	76
B.5.1 Measurement 1: Locating and Documenting a Receivable Band-B41 (2590–2690 MHz) 5G Base Station Coupling into the ASR-9 at Highest Available Power (AP-1 tap point).....	76
B.5.2 Measurement 2: Measure and Document the 5G Unwanted Emission Power Levels in the Spectrum Above 2700 MHz (AP-1 tap point).....	79
B.5.3 Measurement 3: Measure and Document the 5G Unwanted Emission Power Levels in the Spectrum Above 2700 MHz (AP-2 tap point).....	81
B.5.4 Measurement 4: Measure and Document the 5G Unwanted Emission Power Levels in the Spectrum Above 2700 MHz (AP-3 tap point).....	84
B.5.5 Measurement 5: Measure and Document the 5G Unwanted Emission Power Levels in the Spectrum Above 2700 MHz (AP-4 tap point).....	86

B.5.6 Measurement 6: Measure and Document the Radar Receiver’s Bandpass Filter plus LNA Output (and Check for Radar Receiver LNA Overload) (AP- 5 tap point).....	88
B.5.7 Measurement 7: Measure and Document the 5G Signal in the Radar Receiver’s IF Stage (AP-6 tap point)	93
B.6 Data Analysis	95
B.7 Timeline	95
Appendix C : Test Plan for ASR-9 Receiver-Response Characterization Measurements at the FAA Technical Center	96
C.1 Bench Testing.....	96
C.2 ASR-9 IF Characterization.....	97
C.3 Additional Testing.....	98
C.4 Test Matrix.....	98
Appendix D : Measurements Demonstrating the Interference Mechanism between 5G Base Station Transmitters and ASR-9 Receivers.....	100
Appendix E : 5G Base Station Spectrum Certification Measurement Discussion	106

FIGURES

Figure 1. ASR-9 with an airliner and 5G (plus other links) cellular tower. Photo: F. Sanders.....	3
Figure 2. The diagram illustrates different forms of interference effects in radar station PPI screens. Blue wedge-shaped strobes and yellow ring-around circular patterns indicate individual drop-out zones; multiple strobes create what are called “rising sun” patterns.....	4
Figure 3. General-purpose electromagnetic compatibility flow-chart approach for developing coexistence between any two radio systems.....	6
Figure 4. Sub-set of specific work program stages needed for this case study.	8
Figure 5. Simplified block diagram of the ASR-9 receiver, including the option for a weather-surveillance processing (WSP) feed to air traffic controllers.....	12
Figure 6. Two pages from the lead author’s field notebook, documenting the unexpected findings at the radar receiver’s first measurement point, on the first day of field work.....	15
Figure 7. Peak power measured at AP-1 at the waveguide beam switch input, from the southerly 5G base station tower.	17
Figure 8. Peak power measured at AP-2, waveguide beam switch output, the same way as in Figure 7. Blue curve is the normal radar receiver condition. Brown curve (spikes including 2850 MHz due to local radars) is with the ad hoc bandpass filter inserted at AP-1, the waveguide beam switch input. The brown curve’s dramatic drop in the radar band demonstrates interference is caused by 5G signal power in its own licensed band.	18
Figure 9. Comparative power measurements at the beam switch output, with no attenuation there, <i>versus</i> 34 dB of RF input attenuation. Improvement is 40 dB at 2700 MHz, identical to what was earlier achieved with the <i>ad hoc</i> bandpass filter. (Note, signal analyzer noise is at -98 dBm.).....	18
Figure 10. Frequency-domain power measurement (peak-detected in 1 MHz) at the radar receiver’s LNA output with 34 dB of RF attenuation at the beam switch’s input.....	19
Figure 11. Power measured in the time domain at the output of the radar receiver, with 34 dB of 5G attenuation at the beam switch input.....	20
Figure 12. Initial, <i>ad hoc</i> waveguide beam-switch test for controlled-condition interference generation in the presence of an input CW-modulated RF signal, at the FAA Technical Center. The switch is spreading the single-frequency CW input across a substantial portion of spectrum.....	21

Figure 13. Comparison of a time-gated (no beam switch) carrier wave’s Fourier spectrum spreading with the output of an ASR-9 beam switch that was given a CW input. The stand-alone CW signal’s pulsing was adjusted to the same parameters as the beam switch’s operational cycle.25

Figure 14. Fourier spreading into the radar band of a live, local B41 5G base station signal at the FAA Technical Center, through a work bench-mounted beam switch; STC stage; and in-series combination of beam switch and STC stage.26

Figure 15. Overview of the Department of Commerce Table Mountain field site. The Pliocene-Pleistocene alluvial-outwash mesa is flat and level, with short-grass vegetation. The mesa center is 40°07’50.3” N, 105°14’40.6” W. Elevation is 1701 m (5574 ft) MSL.30

Figure 16. 5G base station CoW and RSMS geometry at Table Mountain.31

Figure 17. View of 5G Radio-A base station CoW during radiated emission measurements at Table Mountain, looking westward.....31

Figure 18. View of the NTIA mobile, self-contained RSMS during radiated emission measurements at Table Mountain, looking eastward.32

Figure 19. Block diagram schematic of the RSMS measurement system used to measure radiated emissions from the 5G Radio-A and Radio-B base stations at Table Mountain.33

Figure 20. Diagram of 64T64R MIMO array architecture and beam-directing capability.40

Figure 21. A MIMO 64T64R transmitter-receiver box for 5G base station. It is an integrated, weather-sealed unit with connectors on the lower edge for power and data.41

Figure 22. Azimuthal computed radiation pattern for a 3 GHz band MIMO array antenna in narrow-beam mode. Courtesy and permission of MITRE.41

Figure 23. Elevation computed radiation pattern for a 3 GHz band MIMO array antenna in narrow-beam mode. Note the -1.5 degree downtilt. Courtesy and permission of MITRE.42

Figure 24. Baseline (background) ASR-9 and 5G environmental emissions at Table Mountain relative to a foreground B41 5G base station being measured in this case study.45

Figure 25. 5G base station Radio-A radiated emission spectrum, 100 MHz channel bandwidth.46

Figure 26. 5G base station Radio-A radiated emission spectrum, 90 MHz channel bandwidth.....	46
Figure 27. 5G base station Radio-A radiated emission spectrum, 80 MHz channel bandwidth.....	47
Figure 28. 5G base station Radio-A radiated emission spectrum, 60 MHz channel bandwidth.....	48
Figure 29. 5G base station Radio-A radiated emission spectrum, 20 MHz channel bandwidth.....	48
Figure 30. 5G base station Radio-B radiated emission spectrum, 100 MHz channel bandwidth.	49
Figure 31. Example of a 5G antenna beam-muting simulation prediction. Maximum decoupling in the muted-beam direction is -15 dB, due to sidelobe contributions from adjacent beams.	51
Figure 32. 5G Radio-A array Beams 2 and 5 muted.....	52
Figure 33. 5G Radio-A array Beams 2 and 3 muted.....	52
Figure 34. 5G antenna beam downtilt experiment, -10° versus no downtilt.	54
Figure 35. Power-decoupling effect of mechanically off-rotating the 5G Radio-B MIMO array in azimuth by 70 degrees.....	55
Figure 36. First step: Define a coexistence radar station with a simulation radius.	59
Figure 37. Second step: Define a 5G base station grid spacing within the simulation zone.	59
Figure 38. Third step: Compute KML contours for multiple power-mitigation levels.	60
Figure 39. Illustrative dummy example of coexistence contours for B41 5G base station transmitters and ASR-9 radar receivers across the U.S.	61
Figure A-1. Measured bandpass filter response for the ASR-9 receiver.	68
Figure A-2. Measured frequency-domain response of the ASR-9 receiver IF stage. The IF is about 720 kHz wide at its 3-dB points.	69
Figure A-3. ASR-9 vertical-plane antenna patterns and beam coverage.....	70
Figure B-1. Locations of the ASR-9 and two local 5G base station transmitters.	74

Figure B-2. Simplified block diagram schematic of the ASR-9/WSP receiver.....	75
Figure B-3. Flow diagram for the order in which the measurements will be performed.....	75
Figure B-4. Sketch of what we expect to see in the first measurement.	77
Figure B-5. Sketch of what we expect to see in the second measurement (at AP-1).....	79
Figure B-6. Sketch of what we expect to see in the measurement at AP-2.	82
Figure B-7. Sketch of what we expect to see in the measurement at AP-3.	84
Figure B-8. Sketch of what we expect to see in the measurement at AP-5.	86
Figure B-9. Sketch of what we expect to see in the measurement at AP-5, frequency domain.....	88
Figure B-10. Sketch of what we expect to see in the measurement at AP-5, time domain.....	89
Figure B-11. What we expect to see (or not see) in the final measurement, at AP-6.	93
Figure C-1. Simplified block diagram of the ASR-9 with test points shown in red.....	97
Figure D-1. The beam switch was well-behaved with a CW input as high as +8 dBm total power.....	100
Figure D-2. Chopping a single-frequency wave into pulses in the time domain forces an infinitely large family of output waves to form across the entire spectrum.	101
Figure D-3. A radar beam switch converts a carrier wave to a spread spectrum when it activates.....	102
Figure D-4. Comparison of a time-gated (no beam switch) carrier wave's Fourier spectrum spreading with the output of an ASR-9 beam switch with a CW input.	102
Figure D-5. Comparison of beam switch alone to switch plus STC. Null result.....	103
Figure D-6. Linearity of the Fourier spectrum spreading with input power levels.	104
Figure D-7. Fourier spreading of a local, live 5G base station signal by a beam switch operated on the bench at the FAA Technical Center.....	104

Figure E-1. Edge-of-band certification measurement for a 5G base station's (70 + 50) MHz transmission mode. Dynamic range (60 dB) annotation added by the authors.....106

Figure E-2. Spurious emissions certification measurement result for the radio's (70 + 50) MHz transmission mode. ASR-band frequency and FCC limit-level annotations added by the authors.....107

TABLES

Table 1. Differential diagnostics for radio interference mechanisms.	9
Table 2. Interference-effects test results for ASR-9 receiver components.	27
Table 3. Outcome status (yes or no) of radiated measurements performed with OEM support on 5G Radio-A and Radio-B base station transmitter CoWs at Table Mountain.	28
Table 4. Manufacturer-specified electronic elevation beam scanning limits for 5G MIMO Arrays, relative to the MIMO broadside axis.	43
Table 5. Dummy coexistence numerical inputs (for illustrative purposes only)	58

ABBREVIATIONS/ACRONYMS

5G NR	Fifth Generation New Radio
64T64R	64 transmit and 64 receive elements (each element having two dipoles)
AAS	active antenna system
AGL	height above (relative to) local ground level
ASR(-9)	Airport Surveillance Radar (Model 9)
ATC	air traffic control
B41	Wireless Band n41 (2496–2690 MHz; specifically, 2590–2690 MHz in this study)
dB	decibel
dB_i	decibels relative to isotropic
dB_m	decibels relative to a milliwatt
DL	downlink (base station to user equipment)
DR	dynamic range (of spectrum measurement equipment)
EIRP	effective isotropic radiated power
EMC	electromagnetic compatibility
FAA	Federal Aviation Administration
FCC	Federal Communications Commission
FDR	frequency dependent rejection
IF	intermediate frequency of a heterodyned receiver
IPC	interference protection criterion (or criteria) for a receiver
ITS	Institute for Telecommunication Sciences (of NTIA)
KML	(formerly) Keyhole Markup Language
KkW	kilowatt(s)
LNA	low noise amplifier
MHz	megahertz
MIMO	multiple input multiple output (phased array antenna)
n41 Band	2590–2690 MHz (for wireless communication links)
NAS	National Air Space
NTIA	National Telecommunications and Information Administration
OEM	original equipment manufacturer (of 5G base station radios)
OoB	out-of-band
PA	power amplifier (in a transmitter)
PRB	physical resource block of a 5G radio channel
RF	radio frequency
RMS	root mean square (averaging)
RSMS	NTIA’s radio spectrum measurement system
STC	sensitivity time control (of a radar receiver)
TDD	time division duplex
TMRQZ	Table Mountain Radio Quiet Zone (north of Boulder, Colorado)
UE	user equipment (e.g., wireless mobile phone)
UL	uplink (user equipment to base station)
U.S.	United States
YIG	yttrium iron garnet electronically-tuned radiofrequency bandpass filter

EXECUTIVE SUMMARY

This NTIA Technical Report is a case study in radio spectrum coexistence between sensitive, legacy safety-of-life air traffic control radar receivers and newly introduced, adjacent-spectrum 5G base station transmitters. As a case study, this report describes not only the What of a particular coexistence challenge and its solution. It also describes the How of the work that went into the study. The What is straightforward (albeit we do describe a novel interference mode, heretofore not seen or at least not previously reported or documented). This report's What and How are intended to benefit the wider spectrum management and engineering community; the telecommunications industry; government regulatory agencies; American taxpayers; the U.S. Congress and the White House.

For the What, we show that circuit switches in the radar receivers, when they (in effect) chop adjacent-spectrum 5G signals into what amount to time-pulses, thereby spread the 5G signal power across the radar receiver's spectrum band and thereby cause interference effects. This spectrum spreading is an inevitable and physically unavoidable consequence of localizing power in time: The tighter the time localization, the wider must be the spread in the power's frequencies. The non-zero product of the time-pulse widths and the spectrum-spread widths is built into the physics of waves and, ultimately, of the very fiber of the mathematics by which our Universe operates.

This unintentional interference situation was, surely, never anticipated by the engineers who designed these radars in the 1980s, when the adjacent spectrum was quiet. It was likewise unanticipated when the radar-adjacent spectrum band was recently auctioned and broadcast-power 5G base stations began to be deployed across the country, including, randomly and accidentally, near susceptible air traffic control radar stations.

This is where we arrive at this report's How. We describe an *ad hoc*, and highly successful, collaboration among multiple Federal Government agencies and the U.S. telecommunications industry (and one telecom company in particular) to aggressively approach reported interference problems at multiple radar sites; perform a major series of difficult measurements; analyze and diagnose the problem; and arrive at a description of the problem and the potential steps for solving it. Potential solutions are described in the conclusion section.

The key to this entire effort was the flexibility, willingness, and imagination of the government and industry participants to solve the air traffic control electromagnetic coexistence problem first and to be concerned about administrative agreements later. None of this would have been possible without the existence of highly trained and knowledgeable cadres of experienced electromagnetic engineers across U.S. Government and Industry. Nor would it have been possible without the pre-existence of sophisticated, specialized hardware and software that have been developed in our own agency, NTIA, through decades of steady Congressional support.

The people, equipment, organizations, and mutual technical and administrative support that have made this report's case study a success were not dreamed into existence overnight. They were already waiting when the interference problem arose. We look forward to sustaining this same kind of work, the next time this sort of problem (inevitably) arises.

NTIA CASE STUDY: ADJACENT-BAND COEXISTENCE BETWEEN 5G BASE STATION TRANSMITTERS AND AIR TRAFFIC CONTROL RADAR RECEIVERS

Frank H. Sanders, Geoffrey A. Sanders,¹ Brian D. Nelson, Robert L. Sole,² and Oscar Valle-Colon³

Introduction of Fifth Generation New Radio (5G NR) base station transmitters into 2590–2690 MHz in the U.S., adjacent to the spectrum band 2700–2900 MHz used by air traffic control radars, has resulted in interference effects in some safety-of-life Airport Surveillance Radar receivers, especially the Model 9 (ASR-9). This report describes work performed by the National Telecommunications and Information Administration (NTIA); the Federal Aviation Administration (FAA); the wireless carrier T-Mobile; and two 5G equipment manufacturers to understand and resolve this coexistence challenge. Although the problem initially appeared to be due to 5G unwanted emissions within the radar band, detailed work shows that this is not the typical case. Instead, a novel spectrum-spreading effect within the radar receivers generates power from adjacent-band 5G input signals on the receivers' tuned, radar-band frequencies. This occurs despite the receivers being equipped with robust radiofrequency (RF) bandpass filtering. The effect is generated by solid-state RF switches in the receivers. The spectrum spreading is due to ordinary physics of the switches' time-chopping of adjacent-band input 5G waveforms. Possible solutions are presented. This report is written as an illustrative case study, emphasizing not only the technical problem but also the study's underlying scientific and engineering process.

Keywords: 5G; 5G NR; 5G emissions; 5G emission spectrum; 5G radiation; 5G spectrum bands; air traffic control radars; airport surveillance radars; electromagnetic coexistence; electromagnetic compatibility; national air space safety; radar receiver interference; radio spectrum coexistence; radio spectrum compatibility; wireless coexistence with radars

¹ Sanders and Sanders are with the Institute for Telecommunication Sciences (ITS), National Telecommunications and Information Administration (NTIA), 325 Broadway St., U.S. Department of Commerce, Boulder, Colorado 80305.

² Nelson and Sole are with the NTIA Office of Spectrum Management (OSM), 1401 Constitution Ave. NW, Washington, D.C., 20230.

³ Valle-Colon is with the Federal Aviation Administration (FAA), 800 Independence Ave. S.W., Washington, District of Columbia, 20591.

1. INTRODUCTION

1.1 Background

The Federal Communications Commission (FCC) has authorized [1] the frequency band 2496–2690 MHz (called the “wireless n41 band” or simply “B41” in this report)⁴ for use by Fifth Generation New Radio (5G NR, called simply 5G in this report) base stations and associated user equipment (UEs, colloquially “cellphones”) in the United States (U.S.). This authorization has had the effect of putting broadcast power-class (200 watts transmitter power multiplied by 25 decibels of transmitter antenna gain = 56 kilowatts = +78 dBm effective isotropic radiated power (EIRP) total-channel power in 100 MHz) radiated signals into the radio spectrum immediately below the lower edge of the 2700–2900 MHz band used by the Federal Aviation Administration (FAA) for air traffic control (ATC) airport surveillance radars (ASRs).⁵ ASRs play a critically important role in the National Air Space (NAS) management system.

This new radio spectrum coexistence condition (that is, high-power communication-system transmitters newly deployed in spectrum adjacent to a radar band) has introduced interference effects in radar receivers at some ASR stations. Specifically, ASR Model 9 (ASR-9) radars have experienced interference effects at about thirty⁶ NAS radar station locations around the U.S., associated and correlated with the azimuths of nearby adjacent-band, B41 5G base stations (Figure 1). Wedge-shaped interference-effects target⁷ drop-out zones in the radar stations’ receiver displays, called strobes, are generated on radar plan position indicator (PPI) screens as sketched in Figure 2. ASRs being classed as safety-of-life NAS systems, strobes in their PPI target and weather displays are a serious problem.

Prior to NTIA’s involvement in this study, the described interference was already associated by the FAA with B41 radiated power in a 100-MHz wide channel between 2590 and 2690 MHz from some Massive Multiple Input Multiple Output (MIMO) Radio 5G base stations located in close physical proximity to ASR-9 stations.

⁴ The 2.5 GHz band, which extends from 2496 to 2690 MHz, is comprised of twenty channels designated for Educational Broadband Service (EBS), thirteen channels designated for commercial Broadband Radio Service (BRS), and a number of small guard band channels. EBS licensees are authorized to operate on the A, B, C, D, and G channel groups, with each group comprised of three 5.5-MHz-wide channels in the lower or upper band segment and a single 6 MHz-wide channel in the middle band segment. See [1] for additional details.

⁵ The ASR channel plan uses radar frequencies spaced every five megahertz across the band, from 2705 MHz to 2895 MHz. Each ASR-9 station operates on only a single tuned radio channel at a time.

⁶ Unlike depictions in popular, dramatic portrayals in movies and television, definitive identification and characterization of interference in radar receivers can be an involved process. The estimate of thirty ASR-9 stations experiencing interference associated with adjacent band 5G base station transmitters is believed by the authors to be conservative.

⁷ “Target” is established jargon for radar-displayed dots or blips corresponding to objects detected in space by radars. It is not used here in the military sense of the word.

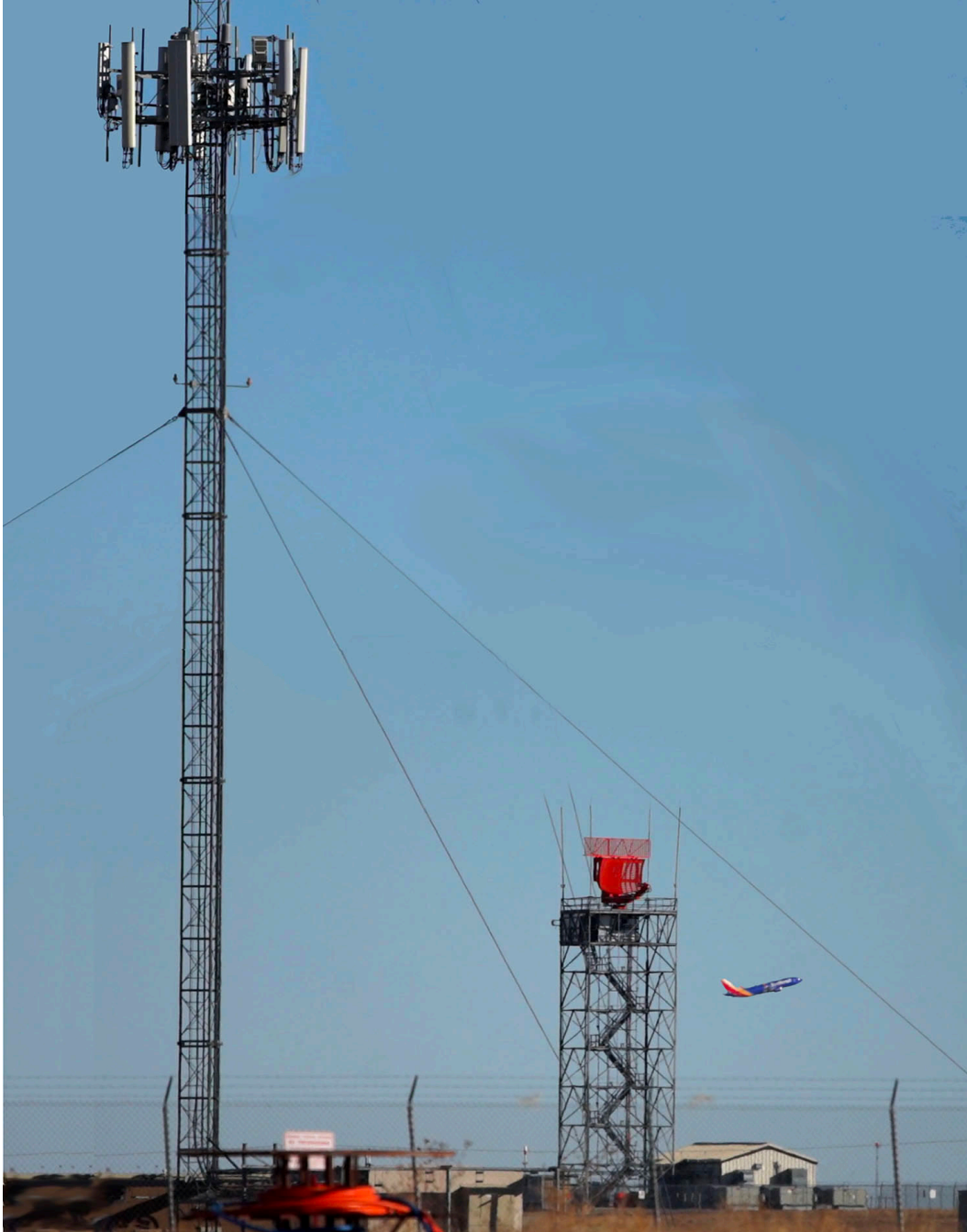


Figure 1. ASR-9 with an airliner and 5G (plus other links) cellular tower. Photo: F. Sanders.

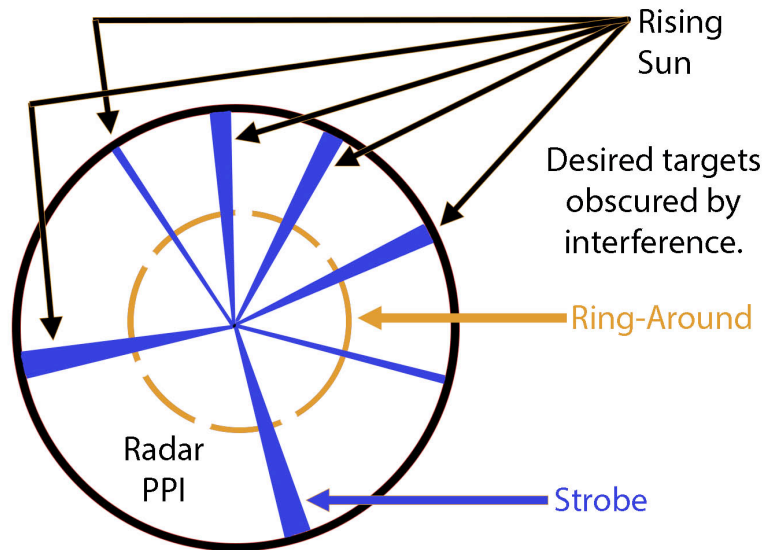


Figure 2. The diagram illustrates different forms of interference effects in radar station PPI screens. Blue wedge-shaped strobes and yellow ring-around circular patterns indicate individual drop-out zones; multiple strobes create what are called “rising sun” patterns.

Addressing the numerical dimensions of the problem now and as it may evolve in the near future, the FAA operates 131 ASR-9 stations across the U.S. The Department of Defense (DoD) operates four electronically equivalent GPN-27 radar stations. The FCC’s 2.5 GHz Auction 108 of September 2022 made thousands of licenses available for new B41 deployments in the spectrum immediately adjacent to (on frequencies just below) the lower radar band-edge at 2700 MHz. After the U.S. Senate subsequently passed the 5G Spectrum Authority Licensing Enforcement (SALE) Act (HR-5677) in December 2023, the FCC released the auctioned 2.5 GHz licenses for station-equipment deployments and operations. That allowed license-winning wireless carriers to physically build-out and enhance their 5G networks across the U.S. with newly deployed B41 5G transmitters.

The number of released licenses as of February 2024 was 7,872, of which 91 per cent (7,156) went to a single wireless carrier, T-Mobile US Inc. (“T-Mobile”). The number of physically deployed B41 5G transmitter base stations is larger than the number of licenses, as each license can represent multiple transmitters. Since airports may require many base stations to support the flying public’s telecommunication needs, FAA ASR-9 or DoD GPN-27 radar stations will be likely to have one or more adjacent-band B41 base stations located nearby.

1.2 NTIA Involvement and Work Program Goal Development

As this is a case study, we describe here how we came to be involved in this case; what goals we set; and what our approach was for achieving those goals. NTIA is the radio spectrum regulatory organization for all U.S. Federal Departments and their sub-agencies. Complementarily to NTIA, the FCC is the Federal Government’s spectrum regulatory organization for all non-Federal radio

systems.⁸ NTIA chairs the regulatory Interdepartment Radio Advisory Committee (IRAC), which counts all Federal Departments and many of their sub-agencies as its membership. When a Federal agency encounters a spectrum interference or coexistence problem, it may utilize its internal spectrum management and engineering staff to address it.

However, it is common for agencies to contact NTIA if such problems involve other agencies or the private sector. Such contacts can be via the working-level Technical Subcommittee (TSC) of the IRAC, or they can be directly to NTIA (commonly via NTIA's Office of Spectrum Management (OSM)) or NTIA's Boulder, Colorado laboratory, the Institute for Telecommunication Sciences (ITS).

In this case, the problem was initially diagnosed by the FAA as involving private sector 5G base station transmitters. FAA engineering staff worked early on with T-Mobile engineers to examine and understand the situation.⁹ A substantial amount of important baseline information about the characteristics of the interference and the conditions under which it was occurring was collected in this initial study stage.

FAA technical staff subsequently reached out directly to one of the authors (F. Sanders) in November 2023. Based on a long-standing, historically important inter-agency relationship, this illustrates the fact that the spectrum management and engineering discipline is specialized. It involves a relatively small number of people, even at the national level, and even in a country the size of the U.S. Many, perhaps most, of these people either have existing working relationships or only have one or two degrees of separation from each other. It is also a field that tends toward career longevity, with experience levels that are often fairly high. If somebody in one organization needs to make a telephone call to someone else in another group who might be able to make a knowledgeable contribution to a problematic situation, then they can (and usually do) do it. Formal organizational-administrative arrangements can be followed-up later, if necessary.

The organizations that were soon brought together to examine and resolve this problem were, by November 2023, the FAA; NTIA (specifically ITS and OSM); and T-Mobile. T-Mobile in turn had strong business and technical-level contacts and relationships with its original equipment manufacturers (OEMs) from whom it procures B41 5G base stations.¹⁰

NTIA involvement was funded from Congressional allocations.¹¹ The pre-existence of that funding allowed a rapid agency response, as opposed to the much-longer timeline that would have resulted if it had been necessary to set up a new project with its own cumbersome funding

⁸ NTIA, in the Department of Commerce, is an Executive Branch agency that ultimately answers to the U.S. President. The FCC is an independent agency that is overseen by the U.S. Congress. Spectrum management responsibilities are thus bifurcated between the Executive and Congressional Branches of U.S. government.

⁹ We note the remarkable level of high-quality cooperation and support that T-Mobile has provided to FAA and NTIA throughout this study. None of the work described in this case study would have been possible without the assistance generously provided by this carrier.

¹⁰ The wireless carrier deploys two models of 5G base stations in B41, from two OEMs. In this report, these are identified as OEM-A and OEM-B; their respective 5G base station models are designated 5G Radio-A and 5G Radio-B in this report.

¹¹ Specifically, the Radio Spectrum Measurement Science Operations Project and the FACTS 5G Project.

development, between NTIA and FAA. NTIA also utilized technical resources that had already been developed over previous decades using appropriated funds. Again, in this situation where timeliness and alacrity of response were needed, there would have been no time or capability for such sophisticated technical development work on a short-notice, *ad hoc* basis.

1.3 Work Program Development: General

We have been asked over the years for a cookbook method for approaching and resolving these sorts of spectrum interference and coexistence cases. There is no one-size-fits-all approach. But in this case study, we provide an initially broad approach concept, within which individual cases can likely be accommodated. We use this broad-to-narrow approach to illustrate how we narrowed the initial study area into the tasks of a specific Work Program for this effort.

Ultimately, this case and others like it amount to developing a coexistence *modus vivendi* between any two radio systems. In Figure 3, we show a general-purpose electromagnetic compatibility (EMC) flow-chart approach for developing coexistence between any two radio systems.

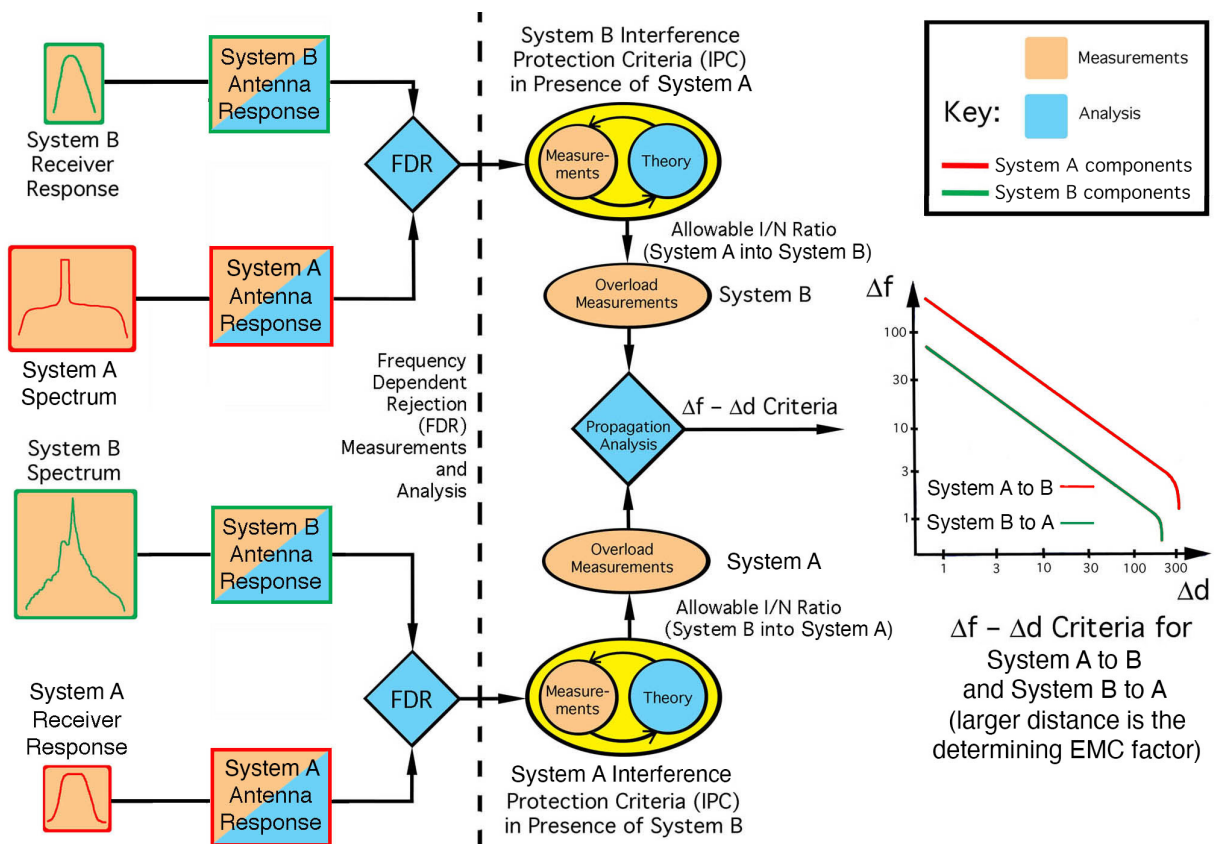


Figure 3. General-purpose electromagnetic compatibility flow-chart approach for developing coexistence between any two radio systems.

In the figure, the two systems' emission power spectra, receiver frequency responses and antenna responses (frequency and direction dependent antenna gain) are used to determine their mutual frequency dependent rejection (FDR).

The FDR are then used with further measurements (if needed) and theory to determine interference protection criteria (IPC) for each system's receiver in the presence of the other system's radiated emissions. For radars, this is typically an interference-to-noise ratio, in which the interference term, I , is power from the interfering signal in the receiver bandwidth of the radar receiver, and the noise term, N , is the radar receiver's internal noise floor. The acceptable I/N levels for radar receivers are often in the neighborhood of -6 dB [2], although other levels can be argued depending on radar type and ambient conditions, as for example in [3].

Non-linear conditions in receivers causing 'overload' should be assessed for situations in which one system's transmitted signals may cause overload in the other system's receiver. Propagation conditions between the systems need to be accounted, ranging from line-of-sight, free space conditions to, possibly, over-the-horizon conditions.

From all of these steps, numerical criteria and graphical curves are developed using an analytical engine for the amount of frequency separation (Δf) needed between the systems as a function of their physical separation distance (Δd). Depending on antenna directionality, it may also be possible to specify angular separation. There will be one such set of separation criteria for System A transmissions into System B receivers, and another for System B transmissions into System A receivers. Since one side of this pairing will inevitably be stricter than the other, the more-strict pairing will in effect be the ultimate criterion for frequency-distance separation between the systems, as depicted in Figure 3.

This is an idealized and exhaustive (in multiple senses of the word) scenario, which will not be expected to be entirely realized in individual real-world operations. Not all of the steps and stages in Figure 3 will ordinarily be incorporated into a coexistence work program for any two radio systems. But the work stages in the figure are, in effect, a checklist for all of the factors that *should* be potentially considered in any final, implemented coexistence work program.

1.4 Work Program Development: Specific

In this case study, we winnowed the general process of Figure 3 into the sub-set of Figure 4.

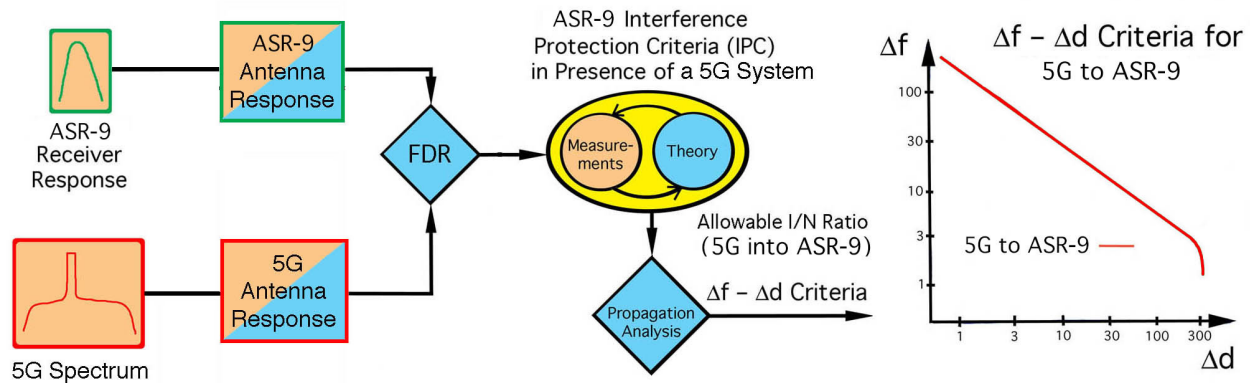


Figure 4. Sub-set of specific work program stages needed for this case study.

Half of the general process was immediately eliminated, as radar transmitter interference into 5G base station receivers has not been an issue for spectrum coexistence engineering.¹² This left the following work program stages to be performed: Obtain the ASR-9 receiver response to B41 5G base station signals; measure the B41 5G base station transmitter emission spectra with large dynamic range (at least 100 dB) under controlled conditions; measure, further, any 5G transmitter spectrum coexistence features; and process the results into numerical criteria or curves for required Δf - Δd separations, as depicted in Figure 3. (Since the 5G B41 channel is fixed, the only Δf factor will be the tuned frequency of any given ASR-9 station, from 2705 MHz upward.)

The work program's field work stages, two as it turned out, were thereby defined. One would be measurement of the B41 5G base station Radios A and B. That work would be performed by transporting each of those radios, as cells on wheels (CoWs) to the Department of Commerce Table Mountain Radio Quiet Zone (TMRQZ) field site north of Boulder. The CoWs would be set up and their radiated emission spectra and spectrum coexistence features would be measured by the NTIA-ITS Radio Spectrum Measurement System (RSMS).

The other work program field stage would be characterization of the ASR-9 receiver responses to B41 5G signals. That would need to be performed at the FAA's Atlantic City Technical Center,¹³ with an engineering ASR-9 exposed to high-power B41 5G signals from a pair of nearby B41 5G base station towers.

The wide dynamic range radiated emission spectrum measurements would be straightforward for NTIA to accomplish. The ASR-9 receiver-response measurements however would require

¹² We do note that, in another NTIA-ITS study, we have documented (unpublished) conditions under which 5G base station receiver front-end LNAs can, and do, overload due to out-of-band radar emissions. We have seen this in bench tests and from airborne radar flights, and have replicated it at our TMRQZ with radiation from a purpose-built radar-pulse transmitter. But 5G receivers do not experience harmful interference from this overload when it is limited to the on-target dwell time of a search radar's main beam, on the order of fifteen to thirty milliseconds, repeating at intervals of every few (e.g., five or ten) seconds. Continuous exposure of 5G receivers to high-power radar pulses does disrupt the receivers, but we know of no conditions under which search radars would continuously boresight 5G receiver stations.

¹³ In Egg Harbor Township, New Jersey.

substantial advance consideration and planning. One large factor in planning those measurements would be the assessment of the particular interference mechanism affecting the radars in the presence of adjacent band 5G signals. The solution to these EMC problems always depends on which mechanism is occurring. We therefore momentarily digress for this sub-topic.

1.5 Pause for Interference-Mechanism Discussion

There are two commonly occurring¹⁴ physical mechanisms for interference in radar receivers and satellite earth station receivers. These are 1) unwanted, unintentional, out-of-band (OoB) spectral emissions from a transmitter that happen to occur on the frequency of a radar receiver; and 2) non-linear overload effects within a radar receiver, resulting from the receiver’s radiofrequency (RF) front end coupling power from a transmitter tuned outside the radar’s spectrum band, or at least not operating on the radar’s tuned frequency.¹⁵ The first case is the one that most people probably think of when they imagine radio interference. The other case, of overload from off-tuned signals, is less obvious and more physically complex.

It is crucially important to know which mechanism is occurring in any given reported interference situation, because the problem’s ultimate resolution will depend on which situation is occurring. If the problem is OoB emissions from a transmitter, then the solution is improved transmitter filtering, or some other method that increases spectrum roll-off in the radar band or at least on given radar receiver frequencies.

If the problem, conversely, is a non-linear overload effect in the radar receiver, then the solution can only be improved with receiver filtering, or some other physical decoupling of the radar receiver. (This has historically been a persistent source of confusion in addressing EMC problems between systems.) In any event, non-linear receiver effects mean that improvements in the transmitter’s emission spectrum will be ineffective. Table 1 provides differential diagnostics for these two radio interference mechanisms.

Table 1. Differential diagnostics for radio interference mechanisms.

Diagnostic	Indicated Interference Mechanism
Receiver has robust RF front end spectrum filtering	Transmitter OoB emissions on receiver frequency
Receiver lacks effective RF filtering	Receiver non-linear overload
Interference effects become more pronounced as receiver frequency approaches transmitter frequency	Transmitter OoB emissions on receiver frequency

¹⁴ There are other interference mechanisms. These include intermodulation in densely built transmitter environments; and the so-called rusty-bolt effect in which a transmitted signal impinging on a corroded joint in a metal structure, with the joint acting as a diode, re-radiates on harmonic frequencies. And so on. But here we focus on the mechanisms commonly involving radars.

¹⁵ Receiver overload is sometimes called “receiver blocking.”

Diagnostic	Indicated Interference Mechanism
Interference effects are not dependent on frequency separation between transmitter and receiver	Receiver non-linear overload
Transmitter OoB emission levels are relatively high	Transmitter OoB emissions on receiver frequency
Transmitter OoB emission levels are relatively low	Receiver non-linear overload

In this case study, we knew from the outset, from previous spectrum coexistence work with ASR-9s, that the radar receivers incorporate effective, robust RF front end filtering, i.e., filtering ahead of their RF low noise amplifiers (LNAs). We had ourselves measured the ASR-9 RF and intermediate frequency (IF) bandpass filter responses on a workbench in an FAA laboratory years earlier (see Appendix A) and found them both to have narrow passbands (individually tuned for each ASR-9 tuned channel), with effectively steep spectrum roll-offs.

Initial interference case reports from FAA field sites indicated that the interference occurrences were concentrated among ASR-9s that were tuned in the lower part of the radar spectrum band, especially between 2705–2750 MHz, although sometimes at higher frequencies around 2800 MHz in the middle of the band. Few or no interference cases were being reported for radars tuned much above 2800 MHz. These two factors, per Table 1, implied that the interference was most likely due to 5G OoB emissions in the lower part of the radar spectrum band.

An unaccounted differential factor, the third one in Table 1, was the 5G base station transmitter emission spectra. As discussed below and in Appendix E, we found the OEMs’ FCC-compliance spectrum emission data to be insufficient.

Based on this preliminary technical analysis (known effective radar receiver filtering present and a concentration of interference among low-tuned radars in the radar band), plus a preliminary, *ad hoc* NTIA emission-spectrum measurement that was performed on a field-deployed 5G Radio-A base station in Boulder in January 2024, there were substantive (but not definitive) indications that the interference mechanism was most likely due to coupling of unwanted, OoB 5G base station emissions on frequencies above 2700 MHz, co-channel to ASR-9 receivers. The ASR-9 receiver-response measurements at Atlantic City would be tailored to look for that mechanism but would still accommodate the possibility of non-linear receiver responses.

What we were not prepared for but eventually discovered by proving our own initial hypothesis to be wrong, was that a heretofore unanticipated, novel interference mechanism was operating in the ASR-9 receivers. This mechanism was not OoB interference; nor was it any sort of receiver overload; nor was it any non-linear rusty-bolt effect. (We do note that OoB and non-linear interference effects might occur at some radar sites; these do not seem to be the predominant problem in this case study, however.)

1.6 Work Program

The work program for this case study thus became:

- 1) Perform ASR-9 receiver-response measurements on an engineering ASR-9 at the FAA's Atlantic City Technical Center to determine the interference mechanism. This would require cooperation from the wireless carrier, T-Mobile, utilizing two of its nearby B41 5G base station towers as interfering transmitters.¹⁶
- 2) Perform radiated, controlled-condition, wideband, wide dynamic range (100 dB or more) emission spectrum measurements at the TMRQZ on the two B41 5G base station models as CoWs, Radio-A and Radio-B, used by the numerically dominant wireless carrier in the band
- 3) Perform radiated measurements on the same CoWs to understand and demonstrate 5G-technology spectrum coexistence features that might be of use
- 4) Analyze the collected data from (1) and (2), and then propose a technical method for preventing additional, future cases of the interference
- 5) Develop Lessons Learned to prevent similar situations in the future
- 6) Publish the work for the benefit of the spectrum management and engineering communities, American taxpayers, the telecommunications industry, the U.S. Congress, and the White House¹⁷

¹⁶ The Test Plan for Atlantic City is provided in Appendix B. This plan documents, for this case study, the substantial level of effort and planning that goes into these sorts of measurements in support of coexistence EMC studies like this one.

¹⁷ ITS does not consider our work to have been completed until it has been published, to the extent that project circumstances permit. Unpublished work provides no benefit to the technical community, other agencies, Congress, the White House, or taxpayers, and contributes nothing to the historical record.

2. MEASUREMENTS OF ADJACENT-BAND B41 5G SIGNALS INSIDE AN ASR-9 RECEIVER

2.1 Initial 5G Signal-Response Measurements Inside the ASR-9 Receiver

Figure 5 shows a simplified block diagram of the ASR-9 radar receiver. Access Points (APs) for the receiver-response testing and indicated, numbered 1 to 6. “STC” is sensitivity time control, a radar receiver feature in which a high-speed, solid-state, variable RF attenuator switches rapidly from high attenuation to low attenuation during the initial pulse-echo reception phase following each transmitted pulse. The radar’s frequency was low in the band, at 2725 MHz.

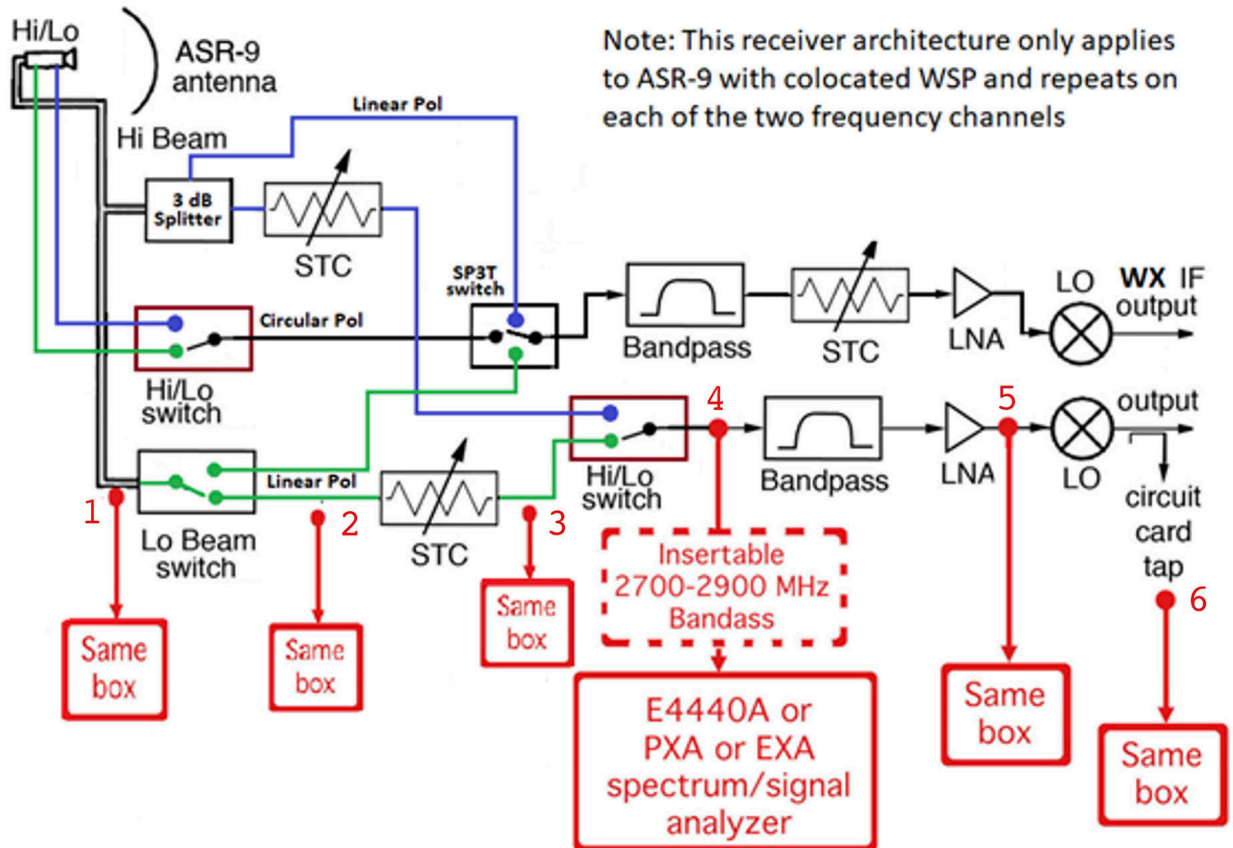


Figure 5. Simplified block diagram of the ASR-9 receiver, including the option for a weather-surveillance processing (WSP) feed to air traffic controllers.

Prior to the measurements, T-Mobile had aligned the local 5G antennas onto the radar’s azimuth, to ensure maximal interference potential. One tower was 2.3 km away and the other was 4.1 km away, on separate azimuths. Both base stations, themselves on high towers, were boresighted line-of-sight on the radar antenna, itself 17 m (57 ft) above ground level.

With reference to the full Test Plan (Appendix B), the measurement process was, briefly:

- 1) Stop the radar antenna's rotation and align it on a nearby B41 5G base station tower, running one of the 100 MHz channel-width radio models that was known to be associated with interference in ASR-9 receivers.¹⁸
- 2) Connect an E4440A spectrum analyzer (which as it turned out, was what we shipped to the Technical Center from Boulder) at AP-1 in Figure 5, and use it to observe both the licensed B41 5G emission spectrum, 2590–2690 MHz, and any receivable unwanted, OoB adjacent-band emissions.

Note that, at AP-1, we were monitoring the radar receiver's waveguide well ahead of the receiver's RF bandpass filter. We saw the B41 (2590–2690 MHz) 5G channel at -20 dBm, peak-detected, in 1 MHz resolution bandwidth.¹⁹ This corresponds to 10 dB less power, -30 dBm, when root-mean square (RMS) average-detected in 1 MHz. This translates in turn, in the full 100 MHz channel bandwidth of the 5G signal, to -10 dBm average power; or 0 dBm in the full 100 MHz 5G channel width, peak-detected.

(As a slight but necessary digression, we note here some critically important considerations about the time-domain, statistical behavior of 5G signals versus the detection modes used to measure them. As documented in detail in [4], pp. 32–39, 5G signals have Gaussian statistics. This means that the difference between their peak-detected and RMS average-detected power levels is 10 dB. Ideally, we would pick a single detection mode for 5G measurements and use it throughout our work, including in our report. Unfortunately, for 5G we have to use, and reference, both detection modes and both power levels. This is because 5G signals, with their on-and-off time domain duplexed (TDD) switching in the time domain, are best and most reliably power-measured with peak detection. Plus, radar receivers respond to the peak levels of the 5G signals. But RMS average levels also need to be specified, because 5G transmitter power levels are specified in terms of their time-averaged power output, not their peak power output.)

We had expected at this point to see OoB emissions from the 5G base stations at frequencies above 2700 MHz. Given that our spectrum analyzer, like all such machines, had about 60 dB of instantaneous dynamic range, we were not surprised to initially *not* have seen the 5G OoB emissions, as we would expect that those emissions would be more than 50 dB down from the 5G on-tuned emissions, and we were close to the analyzer's overload-power point in the 5G in-channel emission power.

So, we inserted a high-performance FAA bandpass filter, 2700–2900 MHz, into the radar receiver waveguide, and therefore in front of our signal analyzer as well. The FAA filter decoupled our equipment from the out-of-band (for the radar) 5G intentional emissions but would pass any OoB emissions on frequencies above 2700 MHz. With the intentional 5G

¹⁸ It is next to impossible to perform these sorts of measurements, with repeatable results, if the radar beam is scanning across the interference azimuth. A typical dwell interval for this sort of search radar will be 10 milliseconds, once every 4.7 seconds, if the radar antenna is rotating. That momentary flicker of interference every few seconds is inadequate for good measurements.

¹⁹ The 1 MHz signal analyzer measurement bandwidth was used because it approximated the radar receiver's bandwidth of about 720 kHz. (The power difference between 720 kHz and 1 MHz is 1.4 dB.) Maximum E4440A resolution bandwidth is 8 MHz; all measurement power levels were kept well below the analyzer's overload point.

emissions eliminated, we were able to bring the dynamic range window of our signal analyzer downward by tens of decibels. We were now sensitive enough to see power at levels about 100 dB lower than the 5G intentional, in-channel emissions. We now expected to see the 5G OoB emissions above 2700 MHz. based on the 5G emissions data we had at the time. Later 5G emission measurements showed that the OoB emissions were more than 90 dB lower than the intentional emissions.

We did not see any such 5G unwanted emissions, however.

This was, we shall say here in this case study at this time, unexpected. It may be said that, just as battle plans do not survive first contact with the enemy, similarly no spectrum test plan is likely to survive first contact with its own measurements. This (non-)result was illustrative of that philosophy.

We subsequently, and rapidly (within the first day's work) established several facts, all unexpected. One was that the 5G unwanted emissions above 2700 MHz were 80 dB or more below the 5G in-channel power levels; another was that substantial noise-like power was observed within the radar receiver, in the lower part of the radar's spectrum band, in definite correlation with the presence of the 5G intentional emissions in the B41 channel below the radar band edge; the third was that those noise-like emissions were *not* being produced by the B41 5G base station; the fourth was that the noise-like emissions were originating in a radar receiver solid-state RF waveguide beam switch (about which, more below).

2.2 Pause for Field Notebooks

As this is a case study, we pause to note that it is critically important to carefully document field work and lab work in a notebook, as shown in Figure 6. The notes need to be made as the work progresses. EMC study results can depend on how well these notes are taken.

Notebooks travel in pockets, requiring no power source or operating system. They are physically robust and can survive storage for millennia. In the lead author's opinion, hand-written notes on paper translate human understanding better than sterile, digital keyboard inputs; they incorporate drawings easily; and they can be amended on-the-fly, with modifications that do not obscure first passes in the work. *The act of writing notes allows the writer to stop, think, and analyze what he/she is doing, while the work is in progress.* And notes document, for the benefit of later analysis and report-writing, what happened, in terms that were current at the moment of the work. The lead author sometimes references notebooks from years ago, in response to inquiries or to review what he did in some study.

There is no substitute for well-written field notebooks. They have been the lead author's secret weapon in 45 years of EMC studies. Anyone who seeks to competently do this sort of work needs to keep these kinds of notes.

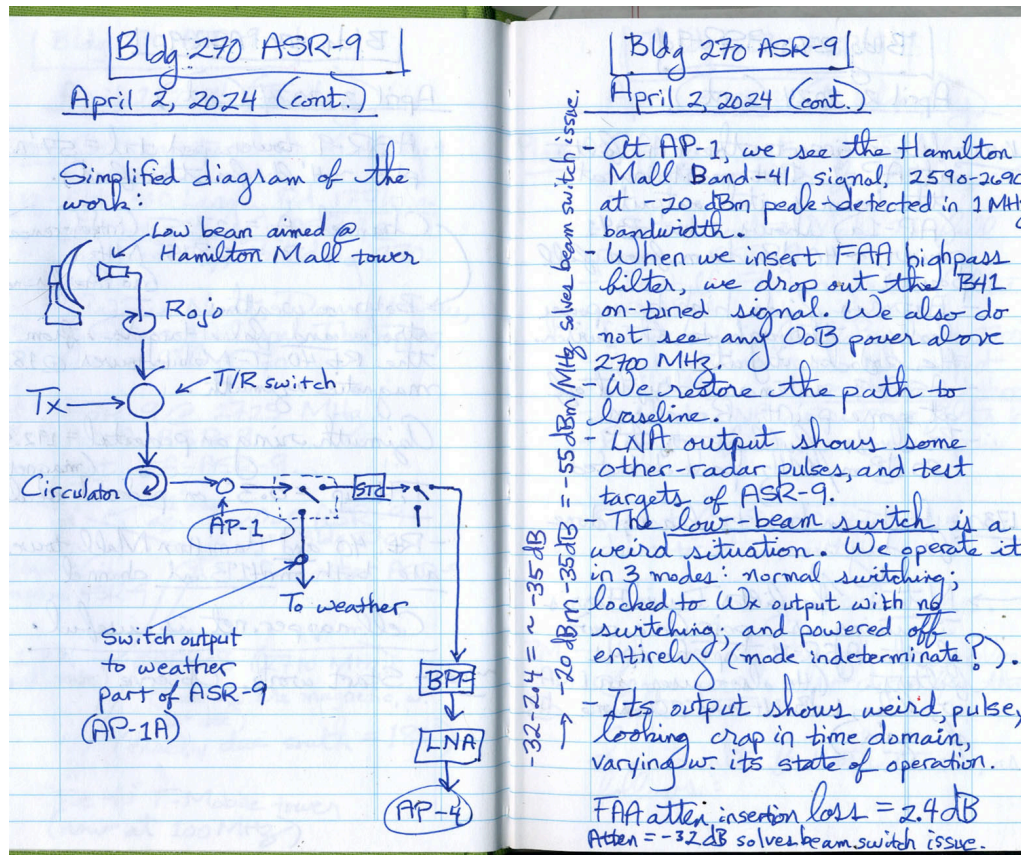


Figure 6. Two pages from the lead author’s field notebook, documenting the unexpected findings at the radar receiver’s first measurement point, on the first day of field work.

2.3 Establishment of the Interference Mechanism and Source

Over the course of the first two days of work, radar receiver interference measurements were performed on B41 5G signals from both of the local base stations, with the physical geometries as described above. The power levels coupled into the radar receiver RF front end, just below the rotary joint, were in both cases measured at -20 dBm/MHz peak-detected, or -30 dBm/MHz root mean square (RMS) average-detected.

Interference results from both towers were identical. At levels of 80 dB below the 5G intentional emissions, no 5G power was observed in the radar band at frequencies above 2700 MHz (which was 10 MHz above the upper edge of Channel B41, at 2690 MHz) at this power level or higher.²⁰

So, 5G unwanted-emission power in the OoB spectrum region, above 2700 MHz, was not high enough power level to indicate co-channel interference in the radar receiver. The radar receiver

²⁰ Those 5G OoB levels above 2700 MHz were subsequently measured exactly, for both of the 5G base station models deployed by T-Mobile in the band, via controlled-condition measurements on CoWs at the Table Mountain Radio Quiet Zone north of Boulder.

did however generate noise-like power internally, on its own frequencies and concentrated in the lower part of the radar band, in response to the 5G intentional emissions in the B41 channel below 2700 MHz. This was a surprising condition.

Referencing Figure 5, the so-called Lo-Beam solid-state waveguide beam switch, which is located electronically just below the rotary joint but which is in front of (and therefore not filtered by) the radar receiver's built-in RF bandpass filter, was generating the interference power in the radar receiver, distributed mostly in the lower portion of the radar spectrum band. Because the beam switch generated this interference power within the radar receiver's own frequency band, the downstream RF bandpass filter passed the energy onward into the LNA and from there into the radar's heterodyned intermediate frequency (IF) stage, then onward through the signal processing stages, and thence to air traffic controllers' screens.

Because the switch alternates its outputs to the radar's target PPI and the weather display when operating in linear polarization, both displays are affected by the switch's interference outputs. In addition, when the weather receiver path is operating in circular polarization, the Hi/Lo switch (see Figure 5, the component above the Lo-Beam switch and below the 3 dB splitter) generates an interference output. Therefore, the weather and target products are both affected. Figures 7 to 12 show the pertinent results from the work on the ASR-9 receiver at the Atlantic City Technical Center

2.4 Radar Receiver Initial Interference-Effects Measurements

Figure 7 shows the adjacent band 5G signal from one of the local base station towers, as measured through the radar receiver's RF front end at AP-1, at the waveguide beam switch input. The dynamic range of the measurement is 60 dB, which is typical for spectrum analyzers and signal analyzers. Further work showed the 5G emissions in the radar band were nearly 100 dB down; confirmation measurements under controlled conditions were subsequently performed with 5G CoWs at the TMRQZ.

Figure 8 shows power measured at AP-2, the output of the waveguide beam switch. There are two curves in the figure differentiated by the presence of an ad hoc 2700–2900 MHz bandpass filter inserted at AP-1. This filter, which attenuates the 5G signal in its own band by a minimum 40 dB but passes the 5G signal in the radar band with little attenuation, is needed to determine whether the interfering signal is 5G OoB emissions or generated within the receiver by the waveguide beam switch. The uppermost curve (blue) is the normal radar receiver condition without this ad hoc filter and the bottom curve (brown) is with it.

If the beam switch is transparent to the signal passing through it we would expect a brown curve that is an attenuated version of the blue curve in the 2496–2690 MHz B41 band and an unattenuated version of the blue curve in the 2700–2900 MHz radar band. What is odd about Figure 7. Peak power measured at AP-1 at the waveguide beam switch input, from the southerly 5G base station tower. is that the brown curve has significant attenuation in the radar band. The brown curves dramatic drop in power in the radar band demonstrates that the interference is caused by 5G signal power in its own band. This finding pointed us to our next logical step...

... which was to now determine the input-power threshold at which the beam switch began to produce these in-band to determine the 5G signal power at the input to the beam switch that produced interference in the radar receiver.²¹ Then the IPC threshold could be decided upon. To measure this threshold,²² we replaced the bandpass filter with a variable attenuator. We then incrementally increased RF attenuation until we saw the interference vanish, or at least minimized.²³ Figure 8 shows the result of this measurement.

We subsequently decided that an additional decibel of decoupling, for a total of 35 dB of RF attenuation (inclusive of the attenuator's insertion loss of 2.4 dB), was more effective in deleting the interference output from the beam switch. We use that value subsequently in this report and in our analyses.

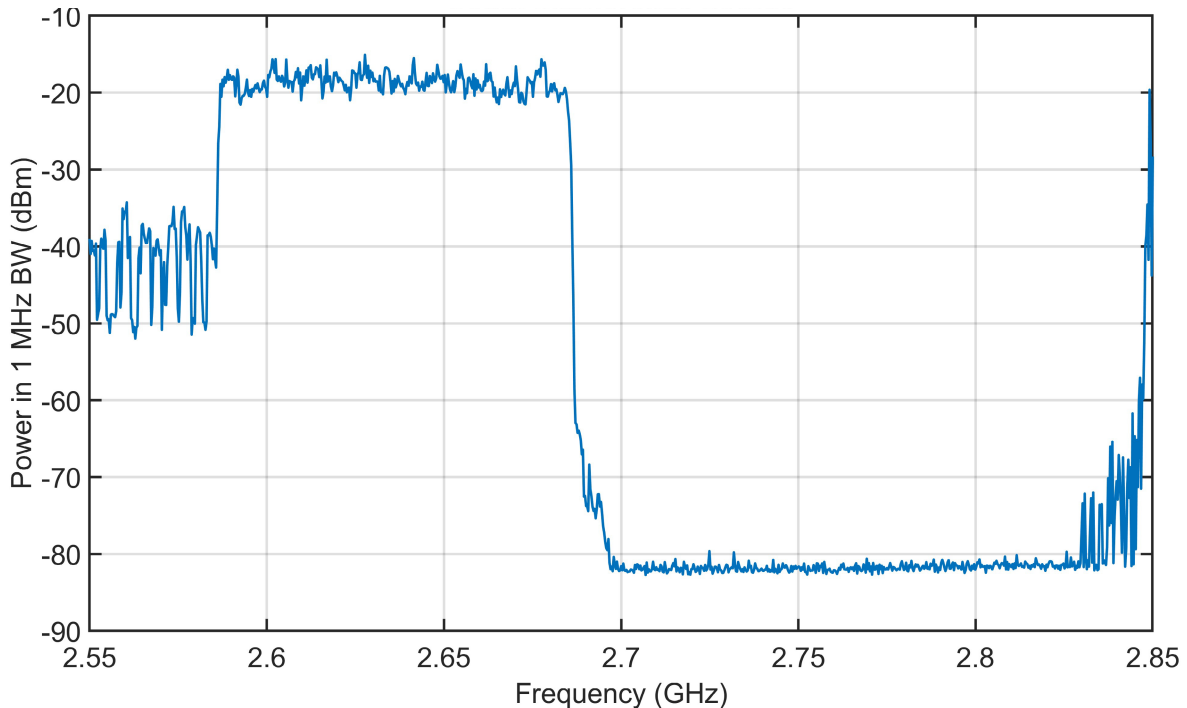


Figure 7. Peak power measured at AP-1 at the waveguide beam switch input, from the southerly 5G base station tower.

²¹ We note, as this is a case study, that this is an example of the flexibility that may be required when the planned work must deviate into previously unanticipated territory due to unexpected developments in the measurement results.

²² This illustrates another reason to do this sort of work at an engineering facility, and not at a field site. The FAA radar engineering facility had laboratory-grade equipment such as the variable RF attenuator with its waveguide couplings. No such thing would have been available at a field site, nor would we have imagined, in advance, needing to bring such an item to a field site from our Boulder lab. Overnighting one from Boulder to a field site would have delayed the rest of the work by one or two working days.

²³ The attenuation values that are quoted here are inclusive of the attenuator's measured (baseline) insertion loss of 2.4 dB.

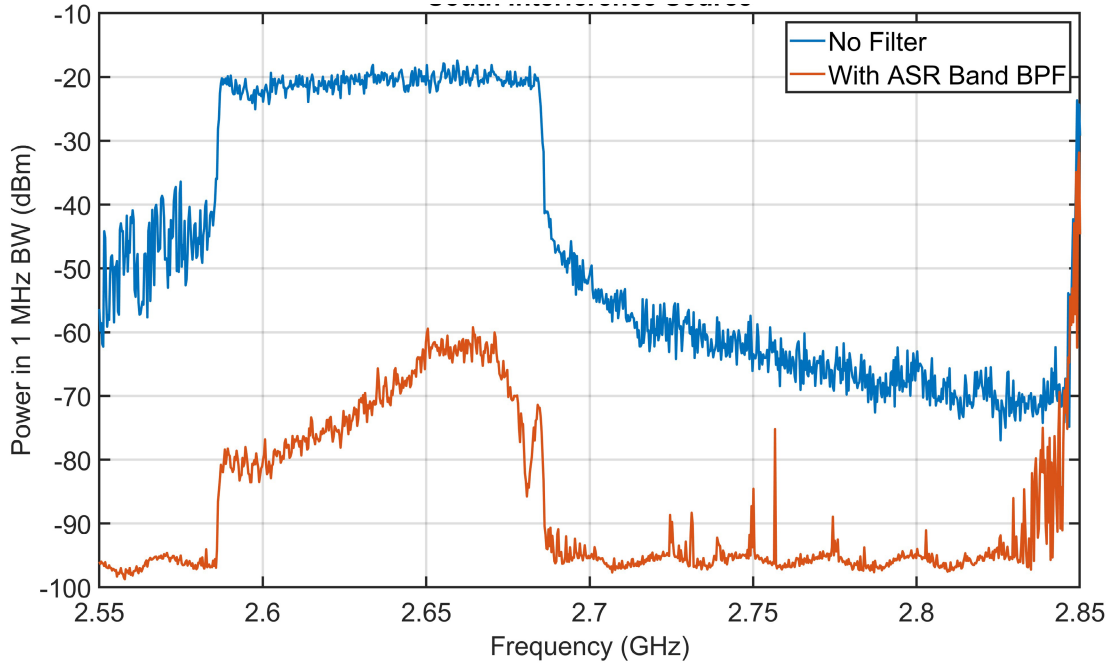


Figure 8. Peak power measured at AP-2, waveguide beam switch output, the same way as in Figure 7. Blue curve is the normal radar receiver condition. Brown curve (spikes including 2850 MHz due to local radars) is with the ad hoc bandpass filter inserted at AP-1, the waveguide beam switch input. The brown curve's dramatic drop in the radar band demonstrates interference is caused by 5G signal power in its own licensed band.

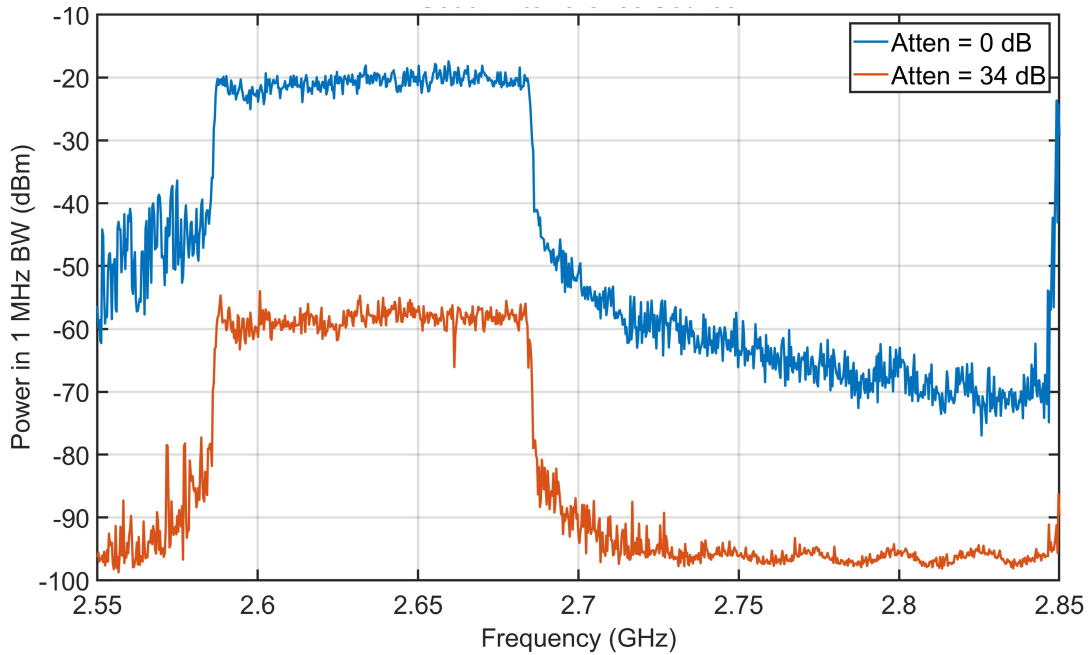


Figure 9. Comparative power measurements at the beam switch output, with no attenuation there, versus 34 dB of RF input attenuation. Improvement is 40 dB at 2700 MHz, identical to what was earlier achieved with the *ad hoc* bandpass filter. (Note, signal analyzer noise is at -98 dBm.)

Having found a reduced-power input that mostly or entirely eliminated the interference outputs from the beam switch, we then transitioned our measurement equipment downstream in the radar receiver, to AP-5 at the LNA output (see Figure 5). Figure 10 shows the frequency-domain behavior in the LNA's output with the reduced 5G power at the beam switch's input. This is a peak-detected spectrum made with the signal analyzer's maximum-hold trace mode over a long (several minutes) integration dwell. The individual frequency-domain spikes appeared at sporadic intervals.

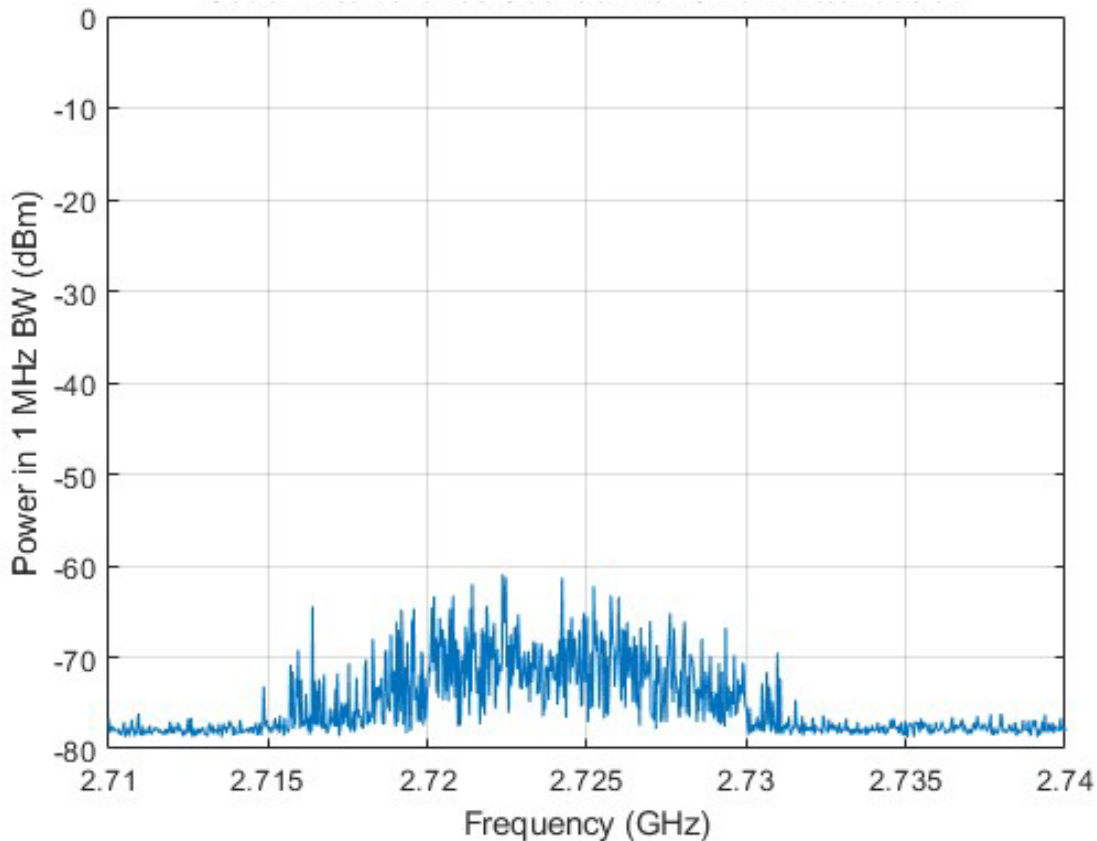


Figure 10. Frequency-domain power measurement (peak-detected in 1 MHz) at the radar receiver's LNA output with 34 dB of RF attenuation at the beam switch's input.

When we transitioned the signal analyzer to the time domain and observed the LNA's output with the same peak detection in the same (1 MHz) resolution bandwidth, we obtained the result shown in Figure 11. In intervals of 100 milliseconds, which equates to about ten radar antenna-scan beam-dwell intervals, no switch-generated noise spikes occurred. Watching the LNA output through longer time intervals, we observed that the noise spikes would occur at intervals on the order of a few seconds apart.

This confirmed that most or all of the interference effect had been eliminated by reducing the 5G signal input power by 35 dB (as reconsidered from the 34 dB where the above figures' data were taken). That 35 dB power reduction had brought the 5G power at the beam switch input down from the original overload level of -30 dBm/MHz RMS average-detected, to -65 dBm/MHz RMS average-detected or -45 dBm *total* average 5G 100 MHz channel power.

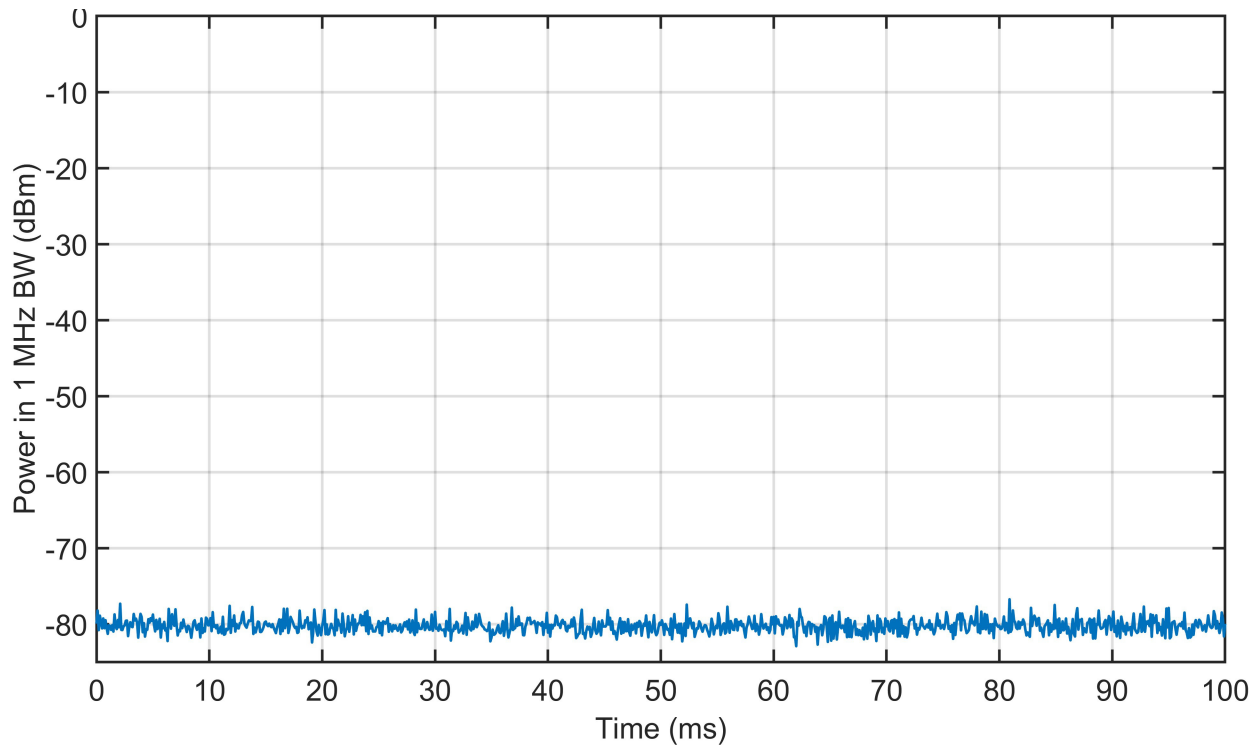


Figure 11. Power measured in the time domain at the output of the radar receiver, with 34 dB of 5G attenuation at the beam switch input.

An additional measurement observation was performed near the end of our first round of work at the Atlantic City engineering facility. For this, FAA engineers²⁴ produced a spare waveguide beam switch²⁵ from the radar’s inventory, identical to the radar receiver’s *in situ* beam switch. Breadboarding a voltage controller for the switch and configuring an RF input commensurate with the power levels that the local 5G towers were coupling into the radar receiver, he set up the bench test shown in Figure 12.

For a signal input, we initially used a simple RF carrier wave (CW). Later testing (in September 2024, see below) used signals with closer fidelity to 5G, and even the actual 5G base station signals from the local towers. But because this was a simple initial test intended to demonstrate that we could reproduce the interference effect under a controlled bench-test condition, the simple CW input RF signal was an adequate first step.

What we immediately saw, but did not immediately understand for its implications, was substantial spectrum-spreading of the input CW signal (which itself was only a single frequency, and which would look like a vertical line on a spectrum analyzer screen). This wideband

²⁴ Mr. Aatman Nandi and Mr. Sampson Afuape.

²⁵ Westinghouse Model XSW-101, manufacturer’s date-plate 1987. These were built at the Linthicum, Maryland Westinghouse plant, now Northrop Grumman, during the radars’ production in the 1980s. These switches are based on PIN diode circuit technology.

spectrum spreading at the switch's output is seen on the spectrum analyzer screen display in the upper-left background of Figure 12.

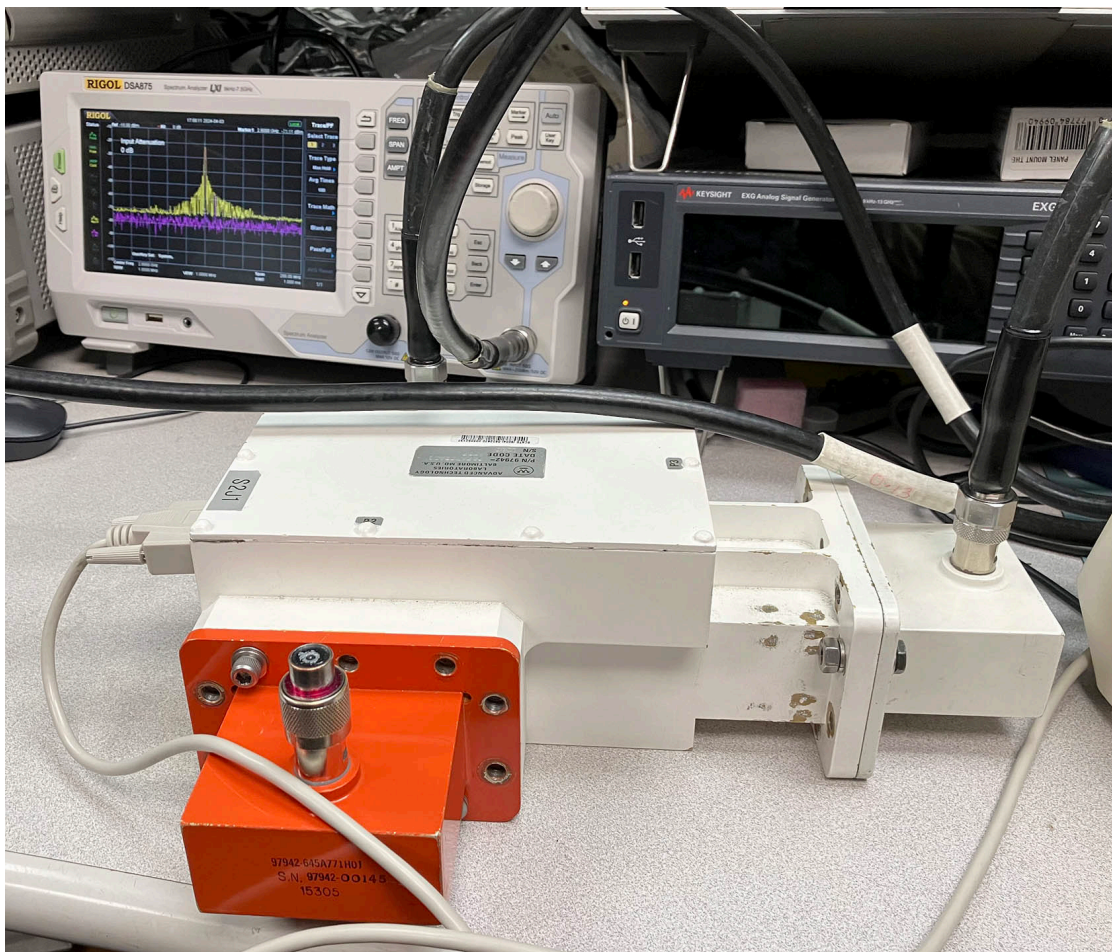


Figure 12. Initial, *ad hoc* waveguide beam-switch test for controlled-condition interference generation in the presence of an input CW-modulated RF signal, at the FAA Technical Center. The switch is spreading the single-frequency CW input across a substantial portion of spectrum.

FAA engineers²⁶ who had configured the test commented that the spreading looked like the Fourier-wave display of a carrier wave that was being pulsed. They were correct. It was then that we realized that the RF beam-switch, as it moved between its positions, was in effect pulsing the carrier wave and causing inevitable spectral spreading, as discussed further in Appendix D. This observation became the basis of unraveling the interference mechanism between 5G base station transmissions and ASR-9 radar receivers.

We varied the CW signal's input power. We observed that the spectrum spreading effect became more and less pronounced as the input signal power was increased and decreased. We realized that the spectrum-spreading effect of the RF beam switch was becoming visible in the radar receiver because of the high power level at which the adjacent-band 5G signal was coupling into

²⁶ Mr. Aatman Nandi and Mr. Sampson Afuape.

the radar receiver. And we saw that, although the effect could occur at lower signal-input power levels, it was becoming small in the radar receiver, relative to the radar receiver's internal noise level, when the input 5G power level from the nearby base station towers was reduced by 35 dB, as noted above.

We note here, and reiterate in the report's Conclusions section, that when these radars were designed and deployed in the 1980s, the adjacent bands were essentially radio-quiet ([5]–[8]).²⁷ The radar receivers were designed to accommodate signals from other, in-band radars, and from military radars, weather radars and maritime surface search and navigation radars in the next-higher frequency bands of 2900-3100 MHz and 3100-3700 MHz.

They were never designed to coexist with high-power (broadcast-power-class) transmitters in the next-lower, frequency-adjacent spectrum band of 2500–2700 MHz. The design engineers of 1987 surely never anticipated the eventual, routine deployment of 50 kW EIRP transmitters on towers as close as 0.5 km from these radar stations. Even if they were aware of this spectrum-spreading characteristic of these solid-state beam switches (and we will probably never know, as those engineers are not available to speak with, a third of a century later), they would have regarded the possibility of that kind of input power occurring in the adjacent radio band as outlandishly unlikely.

We observe, as this is a case study, that prior to the deployment of 5G in B41 in the U.S., no technical work²⁸ was done by spectrum regulators to establish coexistence parameters between the newly deployed 5G communication base stations and the safety-of-life radar receivers in the adjacent spectrum band. This despite the fact that it would not have been unreasonable to anticipate that some receiver-interference effects might occur when thousands of new, high-power transmitters were being deployed in close physical proximity and close spectrum proximity²⁹ to decades-old receiver designs that pre-dated the advent of such high-power transmitters in the adjacent spectrum.

2.5 Further RF Beam-Switch and STC-Stage Interference-Effects Testing at the FAA Technical Center

As noted above, high-power adjacent-band radio signals were not anticipated when the ASR-9 radars were designed and deployed in the 1980s. Key RF components in the receiver which are not protected by the RF bandpass filter are several RF beam switches and the STC stage, as shown in Figure 5.

Having established in April 2024 that one of these beam switches, at least, was generating its own spread-spectrum output in the presence of high-power adjacent-band 5G signal inputs, three

²⁷ Prior to the FCC auction, the 2650–2690 MHz band was lightly used by wireless carriers for WiMAX base stations. Before that, it was used for point-to-point transmissions for education applications.

²⁸ That we were aware of.

²⁹ The frequency difference between the upper edge of B41, at 2690 MHz, and the lowest ASR frequency, at 2705 MHz, is 15 MHz. The fractional difference is only $(15/2700) = 0.0056 = 0.56$ percent. From a technical standpoint, that is a very small difference in frequency, called the radio guard-band size.

of the authors³⁰ returned to the FAA technical Center to work with FAA engineers³¹ to conclusively resolve the extent, if any, to which any non-linear power-overload effects were occurring in these receiver front-end components; and to quantify and conclusively determine the cause and effects of the receiver's beam switch-induced Fourier spectrum-spreading that had been briefly observed in the *ad hoc* bench testing of April. Appendix C provides the Test Plan for this additional testing.³²

2.6 Results of Interference-Effects Testing at the FAA Technical Center

2.6.1 Attempted Power-Overload: Results

Regarding power-overload effects and testing in the beam switches and the STC stage, the critical power threshold for inducing overload in the receiver's RFR front end, ahead of the LNA's protective RF bandpass filter, is +6 dBm of total input power.

It is possible, under circumstances of exceptionally close physical proximity and strong antenna beam coupling, for adjacent band 5G input signals to reach this power level in the radar receiver, and to thereby induce overload effects in the RF beam switches (Figure 5) and the STC stage. To reach this power level, 5G base stations would need to couple even more strongly into the radar receivers than was the case during the Atlantic City Technical Center work, where the total 5G RF channel power in-coupled at the beam switch inputs was -10 dBm RMS average-detected = 0 dBm peak-detected.

Recognizing that there could nevertheless be other locations where local geometries between 5G base station transmitter antennas and radar receiver antennas could reach or exceed this overload level, we point to the Fourier spectrum spreading effect (discussed immediately below), which occurs at lower input-power levels. With the spectrum-spreading effect occurring at lower thresholds than the power overload effect, any radar station that is protected from the spectrum spreading phenomenon will also be protected from higher-threshold power-overload effects. We therefore leave off the discussion of power overload and move to the spectrum spreading problem.

2.6.2 Fourier Spectrum-Spreading Interference-Effects Results

The full set of measurements, tests and results for Fourier spectrum spreading in the radar receivers' RF front end beam switches and STC stages is provided in Appendix D. We summarize the work and results here.

³⁰ G. Sanders, B. Nelson and O. Valle-Colon.

³¹ A. Nandi and O. Valle-Colon.

³² We include this plan in this case study to further illustrate the large amount of work, time, planning and funding that are required to perform and complete these kinds of EMC coexistence studies.

First, the physical phenomenon: Any continuously running time-domain signal that is chopped into pulses has, definitionally, had its energy or power³³ compartmentalized into time-localized packets. Time localization automatically forces the wave frequencies of the input power to spread out across the spectrum, even if the original input was a single-frequency wave, a so-called carrier wave. *This spectrum spreading is not a non-linear effect.* It is a completely linear signal processing effect, based on ordinary wave physics.

The spectrum spreading can be viewed in multiple ways. In classical-mechanics physics, its basis is the non-commutative character of the time and energy (equivalent to frequency) operators and domains. In wave physics, its basis is the fact that finitely long time-domain pulses can only be constructed from infinitely many distinct sine-wave components, as described in Fourier analysis. There is even a quantum-mechanical interpretation, which is that (analogously to the classical-wave non-commutative characteristics of time and energy operators) the product of the forced time localization (the pulse width, Δt) and the smallest-possible, simultaneously specifiable energy localization (ΔE , functionally equivalent to frequency, $\Delta E = (h \cdot \Delta f)$)³⁴ must necessarily always be non-zero: $(\Delta t \cdot h \Delta f) \geq h$, or simply, $(\Delta t \cdot \Delta f) \geq 1$. For example, a one-microsecond pulse's energy must occupy a spectrum bandwidth of at least one megahertz.

In this report, we call this effect Fourier spreading. The radar receiver has several beam switches in its RF front end, ahead of the RF bandpass filter (Figure 5). Each of these switches sees the B41 5G adjacent-band intentional emissions, and chops it into, effectively, a series of pulses. This spreads the 5G signal's upper-frequency edge at 2690 MHz upward in frequency, into the radar receiver's spectrum band of 2700–2900 MHz. In Figure 13, we show the spreading of a carrier wave that was run through the beam switch in one of our bench tests, and compare it to a carrier wave that was not run through the beam switch, but instead was pulsed with the same time-domain values as the beam switch's effective time-chopping. The identical results demonstrate that the spreading out of the beam switch is in fact due to Fourier spreading, and not to any non-linear phenomenon related to any sort of power overload.³⁵

³³ Power being energy flow rate; that is, the amount of energy passing a point per unit time.

³⁴ Where h is Planck's Constant.

³⁵ Note that the CW power level, at -36 dBm, was 42 dB below the beam switch's power-overload point.

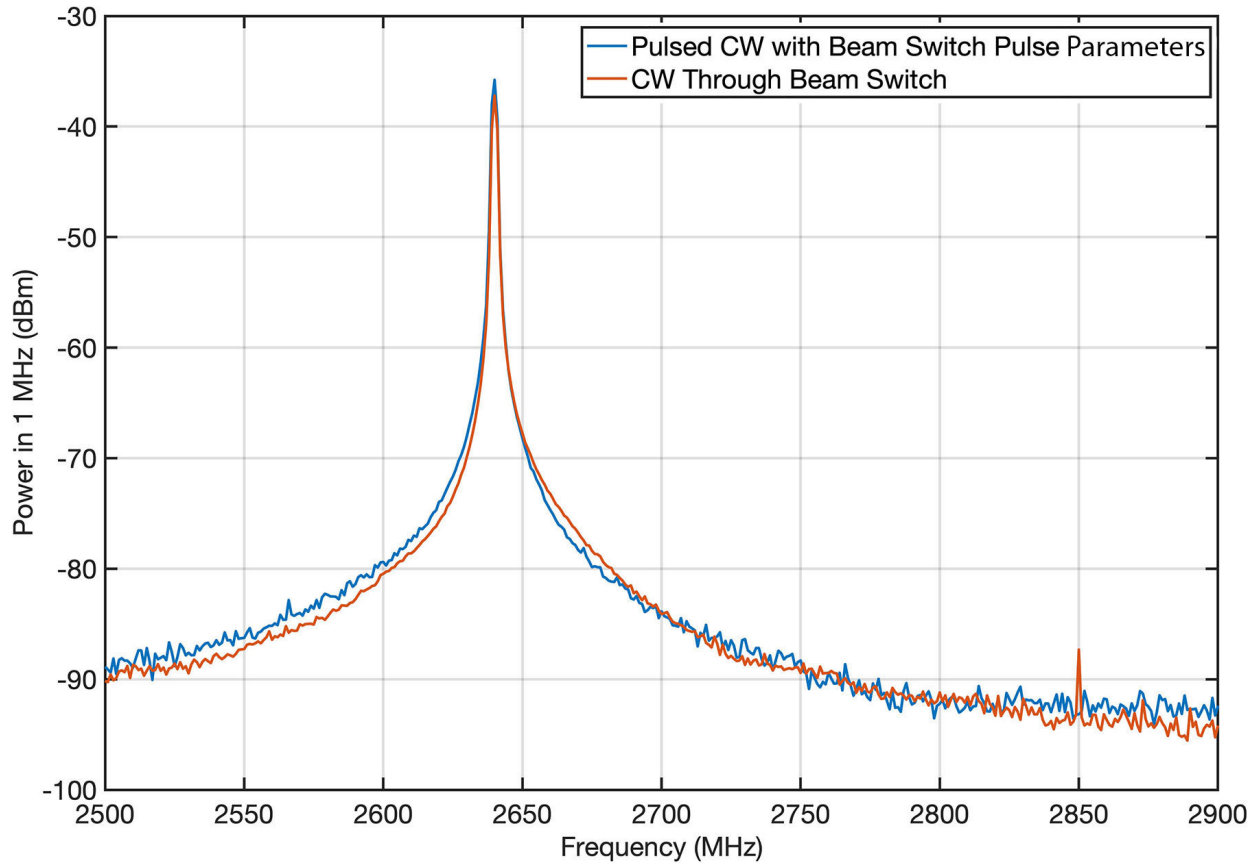


Figure 13. Comparison of a time-gated (no beam switch) carrier wave's Fourier spectrum spreading with the output of an ASR-9 beam switch that was given a CW input. The stand-alone CW signal's pulsing was adjusted to the same parameters as the beam switch's operational cycle.

In an ultimate demonstration of the Fourier spreading of the 5G signal by a beam switch in the radar receiver, we actually ported the B41 5G signal from one of the Technical Center's nearby 5G base station towers into the radar via its (hand-aligned and locked-down) antenna and then ran that signal into a beam switch on the work bench in the Technical Center's lab area. The result is shown in Figure 13, for the beam switch only, the STC stage only (also on the work bench) and the beam switch and STC in series on the work bench, just as they are configured in the ASR-9 receiver's RF front end.

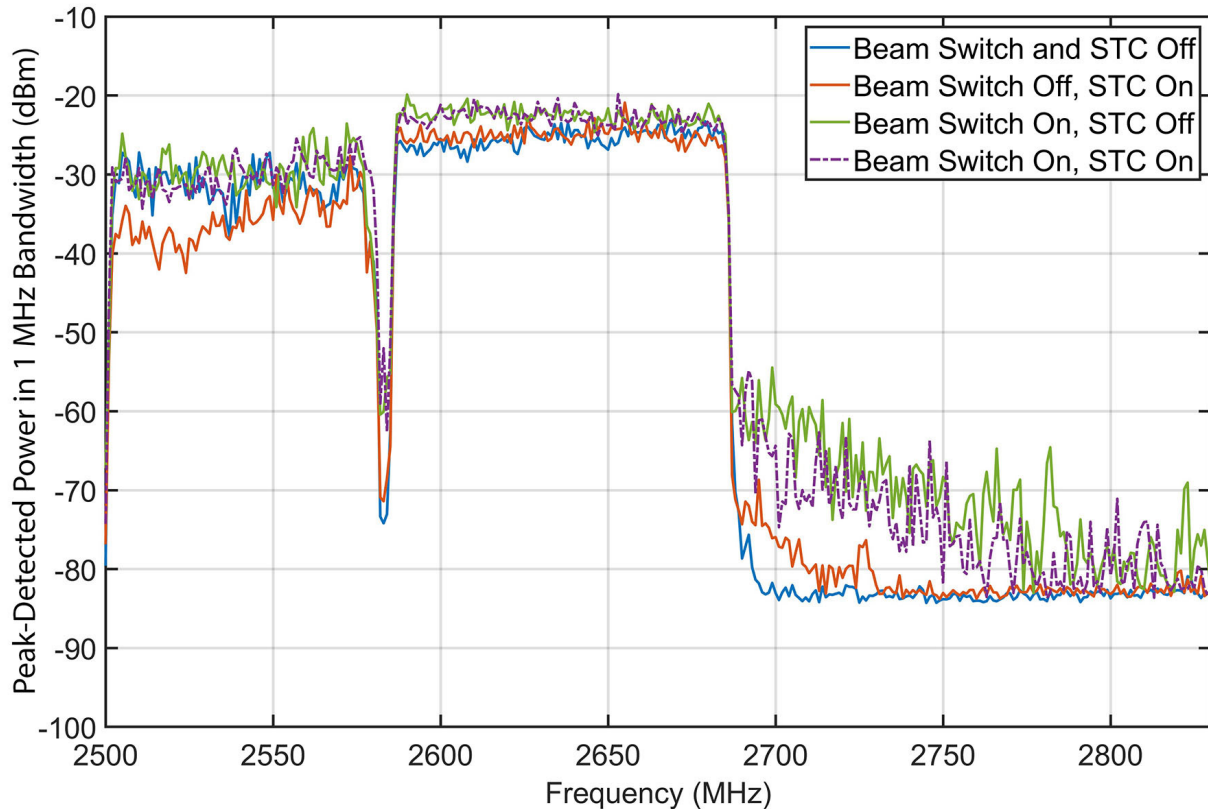


Figure 14. Fourier spreading into the radar band of a live, local B41 5G base station signal at the FAA Technical Center, through a work bench-mounted beam switch; STC stage; and in-series combination of beam switch and STC stage.

The 5G input signals in Figure 14 were 26 dB to 30 dB below the power-overload point for the beam switch. The figure's curves demonstrate that the spectrum spreading of the B41 5G signal into the radar receiver's frequency band is due to the beam switch; that the STC stage's contribution is comparatively small; and that therefore the coexistence issue reduces to keeping the Fourier spreading of the beam switch down to output power levels that do not interfere with the radar receiver's operations.

We note here, and will discuss further below, that the radar receiver utilizes multiple RF beam switches in a variety of locations and signal paths, with *all of them being positioned ahead of the RF bandpass filter*, as shown in Figure 5. While the particular beam switch position on which we initially focused was the one directly in front of the STC stage, which alternately feeds the STC and the weather processor, *all of the beam switches in the radar receiver's RF front end can, and should, generate the Fourier spreading effect*. This means that, given that the receiver's first RF beam switch is located at the radar's antenna feed, installing supplemental RF bandpass filtering into the radar receiver ahead of all of its beam switches would be technically challenging. The local 5G signals may need to be isolated from the beam switches through other, non-filter, physical approaches or means. The degrees of freedom for such isolation are

frequency separation; distance separation; antenna directionality and power reduction. Table 2 summarizes the ASR-9 receiver interference-effects test results for this study.

Table 2. Interference-effects test results for ASR-9 receiver components.

Receiver Component	Average-Detected Total-Power Input Overload Threshold (dBm)	Observed Interference Mechanism
RF Beam Switch	0 dBm specified minimum +6 dBm measured	Linear Fourier spectrum spreading, not RF power overload
STC Stage	0 dBm specified minimum +6 dBm measured	Linear Fourier spectrum spreading, not RF power overload
RF Beam Switch plus STC	0 dBm specified minimum +6 dBm measured	Linear Fourier spectrum spreading, not RF power overload

Our topic therefore segues at this point to the B41 5G base station emission spectra, and associated, available base station EMC features that are candidates for improved coexistence with adjacent-band radar receivers.

Radar RF bandpass filters tuned at the radar central frequencies could also play a significant role in mitigating the Fourier spreading effects. For instance, in testing performed by the FAA in an ASR-9 with WSP, operating with $\Delta f_1 = 65$ MHz away from 5G carrier central frequency and $\Delta f_2 = 130$ MHz away from 5G carrier central frequency, different levels of power attenuation were required to remove the interference. For Δf_1 , reduction of 20 dB (from 2W/MHz to 0.02 W/MHz) was needed from the 5G fundamental to achieve compatibility, while a power reduction of 10 dB (from 2W/MHz to 0.02 W/MHz) was required to achieve compatibility with Δf_2 .

This additional contribution from the ASR receiver to mitigate the interference due to its filter frequency response will vary case by case because it will depend on the geometry (antenna heights, antenna coupling, and distance between the radar and 5G base station, as well as operational environment conditions such as terrain and human-made obstructions).

3. CONTROLLED-CONDITION MEASUREMENTS OF RADIATED 5G BASE STATION EMISSION SPECTRA

Referencing Figure 4, the emission spectra of the two widely deployed B41 5G base station models, 5G Radio-A and 5G Radio-B, needed to be measured, including a variety of spectrum coexistence-enhancement features that they potentially offer. The emission spectra would quantify, finally, exactly what the 5G unwanted-emission power levels were at frequencies above 2700 MHz, in the radar band. Beyond the emission spectra, additional measurements and observations needed to be performed on these 5G base station coexistence-enhancement features:

- 5G base station antenna-beam muting
- 5G base station antenna-beam elevation control (i.e., antenna-beam downtilting)
- 5G base station channel physical resource block (PRB) muting
- Steering 5G base station antenna radiation beams away from selected azimuths

Table 3 summarizes the radiated measurements and tests that were performed on each of the Radio-A and Radio-B base station CoWs at Table Mountain.

Table 3. Outcome status (yes or no) of radiated measurements performed with OEM support on 5G Radio-A and Radio-B base station transmitter CoWs at Table Mountain.

5G Base Station CoW Parameter	5G Radio-A Base Station CoW Test Status	5G Radio-B Base Station CoW Test Status
Emission Spectrum in 100 MHz B41 Channel	Yes	Yes
Emission Spectrum in 90 MHz B41 Channel	Yes	No
Emission Spectrum in 80 MHz B41 Channel	Yes	No
Emission Spectrum in 60 MHz B41 Channel	Yes	No
Emission Spectrum in 20 MHz B41 Channel	Yes	No
Beam-Muting Effective Radiated Power Reduction Test	Yes	No
Antenna Beam Elevation Control (Extra Downtilting)	No	Yes
Antenna Beam Off-Axis Azimuthal Rotation	No	Yes
5G Channel Physical Resource Block (PRB) blanking	No	No

The CoWs were operated by engineering staff from the base stations’ respective OEMs. We note that these technical staff were well-trained and proficient, and provided excellent support for the fieldwork. Where “No’s” occur in Table 3, it was not due to any fault of the OEM support engineers.

Even with such knowledgeable people involved, it was in some cases difficult or impossible to access and implement particular features in these radio transmitters. This situation is reflected in the “No” entries of Table 3. We have experienced similar difficulties ourselves, with our ITS-owned 5G base stations in slightly higher frequency 3-GHz spectrum bands. Difficulties in accessing special, or at least uncommonly implemented, 5G features appear to be inherent in 5G base station designs, which seem not to countenance human intervention in their operations.

Based on our first-hand experiences with our own 5G base stations, and our experiences with OEM personnel in this and other projects at ITS, 5G base stations are designed to be set up and operated as plug-and-play in standard (which is to say, ordinarily expected) formats. Their designs seem to not necessarily be intended to be custom-configured or operated. The result being that, although some 5G coexistence features are optimistically touted³⁶ as being available for use, per the published 3GPP standard [9],³⁷ they are not necessarily (a) easily accessible or programmable; or else (b) are not included as part of a given 5G base station design, at all. In this case study, we will explore this situation with our experience with 5G Radio-A and Radio-B CoWs during Table Mountain radiated-emission measurements.

3.1 Adequacy of Base Station Spectrum Certification Emission Spectra

In Appendix E, we discuss at length the Spectrum Certification Test Report data for the two models of 5G base station that were examined in this case study. As described there, the certification data lacked the dynamic range (DR) that we needed for our EMC and coexistence analyses, as the maximum DR of the certification data sets was 60 dB. The certification data also lacked resolution (measurement) bandwidths for the 5G transmitter spectra, and did not provide the power levels of the unwanted emissions relative to the power at the 5G fundamental (in-channel, licensed) emissions, at least as far as we were able to understand the data presentations.

To determine the power levels of the 5G Radio-A and Radio-B transmitters in the 2700–2900 MHz radar band with at least 100 dB of dynamic range, and to gather information about the effectiveness of additional 5G coexistence features (as noted above), we needed to measure the radiated 5G base station emissions under controlled conditions, with dedicated 5G base stations set up as CoWs for the measurements.

3.2 5G CoW Base Station Radiated-Emission Setup at Table Mountain

3.2.1 Physical Radiated Measurement Location and Geometry

Wireless carrier T-Mobile procured and made available 5G base stations, as previously noted, from two OEMs. To measure the radiated emission spectra of these base stations along with their respective spectrum-coexistence features, the wireless carrier worked with the OEMs to get each of the base station models, 5G Radio-A and 5G Radio-B, to the Department of Commerce Radio Quiet Zone north of Boulder, Colorado, as CoWs, along with OEM personnel who could configure and operate them. Figure 15 shows an overview of the Table Mountain facility.

³⁶ Based on the authors' experiences in industry-government spectrum coexistence meetings and fora.

³⁷ Some features are provided in the standard as being allowed, or optional, but are not necessarily required to be available in any given radio.

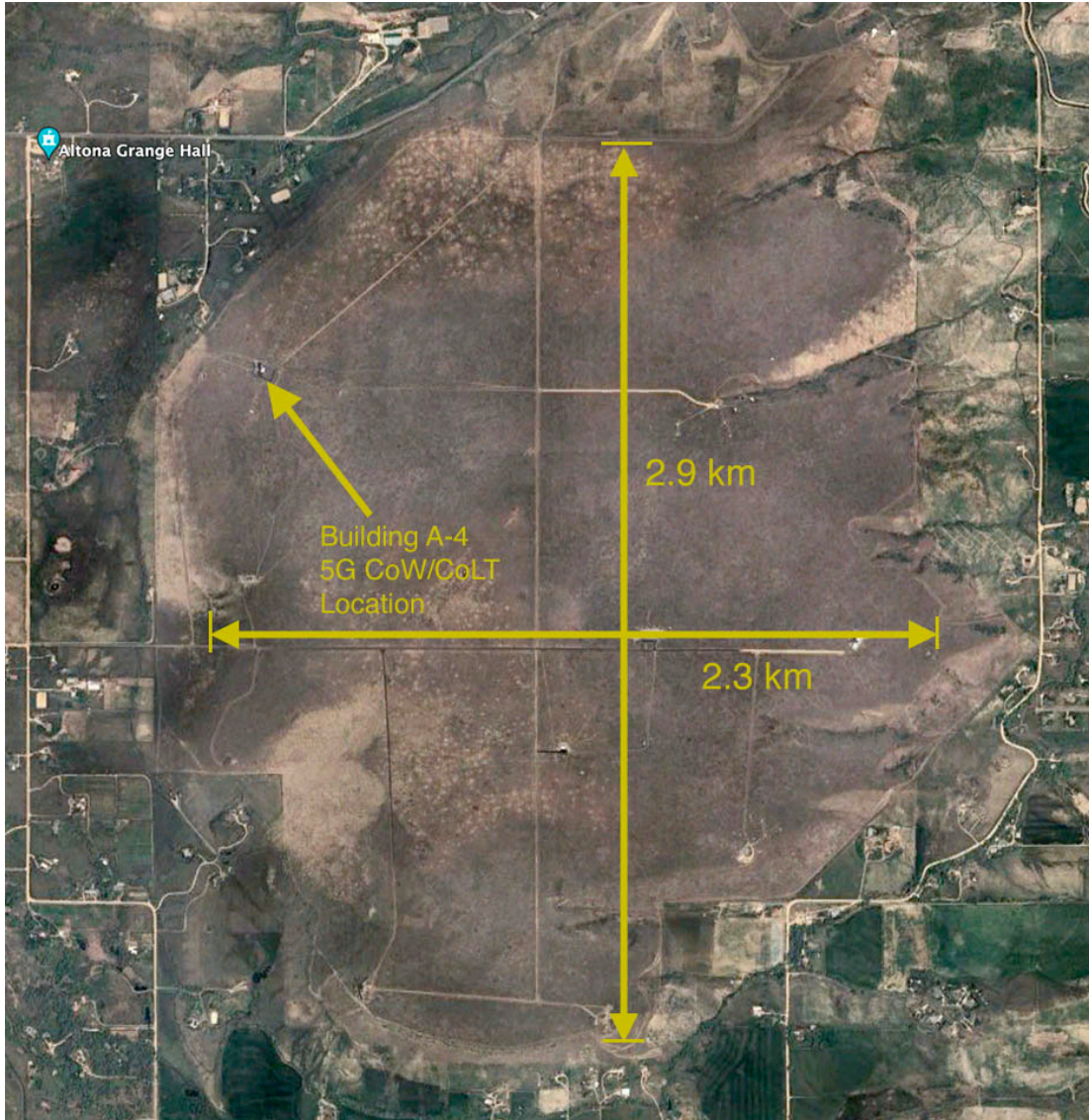


Figure 15. Overview of the Department of Commerce Table Mountain field site. The Pliocene-Pleistocene alluvial-outwash mesa is flat and level, with short-grass vegetation. The mesa center is $40^{\circ}07'50.3''$ N, $105^{\circ}14'40.6''$ W. Elevation is 1701 m (5574 ft) MSL.

The CoWs (transported to Table Mountain and set up and measured separately, weeks apart) were erected in the yard area of a Table Mountain building called A-4, with the mobile NTIA Radio Spectrum Measurement System (RSMS) set up at a distance of 100 m, as shown in Figure 16. Respective on-the-ground CoW and RSMS views are shown in Figures 17 and 18.



Figure 16. 5G base station CoW and RSMS geometry at Table Mountain.



Figure 17. View of 5G Radio-A base station CoW during radiated emission measurements at Table Mountain, looking westward.



Figure 18. View of the NTIA mobile, self-contained RSMS during radiated emission measurements at Table Mountain, looking eastward.

The A-4 yard surface was crushed gravel; other ground between the CoW and the RSMS was coarse Pleistocene alluvial-fan outwash with sparse short-grass vegetation. Measurement site coordinates were $40^{\circ}08'18.6''$ N, $105^{\circ}15'16.8''$ W. The true-north azimuth from the 5G CoWs to the RSMS was 105° . CoW antenna heights were 10 m above ground level (AGL); RSMS antenna height was 3.9 m AGL. The downtilt angle from the CoW antennas to the RSMS antenna was -3.5° . Other than for CoW beam-downtilting and beam azimuth-rotation measurements where the CoW beams were intentionally decoupled from the RSMS, all measurements were performed with main-beam-to-main-beam coupling between the CoWs and the RSMS antenna.³⁸

The 5G base station 64T64R MIMO-technology antennas faced eastward, center-boresighted on the RSMS. The RSMS was positioned 100 m from the base stations, with its measurement antenna (a 1-m diameter parabolic dish with a vertically-polarized linear feed) aligned westward on them. The transmitter and measurement-receiver antennas were boresighted on each other. This geometry kept local ASR-9 stations³⁹ in the backlobes and sidelobes of the measurement antenna. (See below for further discussion of local ambient ASR-9 and 5G signals.)

³⁸ The CoW antenna beams were manually adjusted by the OEM crews to illuminate the RSMS measurement position. The RSMS 1-m diameter parabolic dish antenna was boresighted on the CoW antennas with a standard manually controlled box-search technique.

³⁹ At Denver International Airport (DIA), eastward; and at Platteville, Colorado, northeastward.

3.2.2 RSMS Measurement System Hardware

The RSMS measurement system is shown in the block diagram of Figure 19.

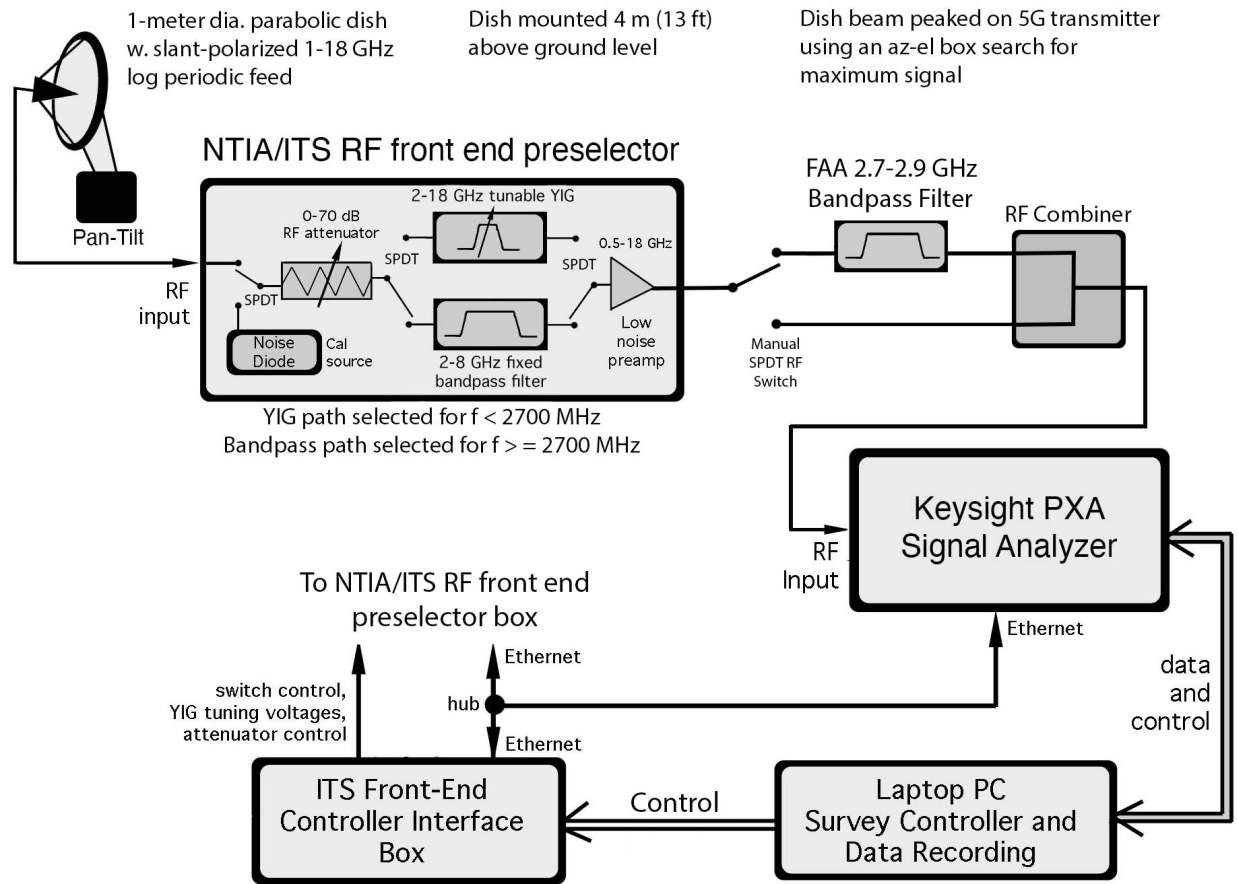


Figure 19. Block diagram schematic of the RSMS measurement system used to measure radiated emissions from the 5G Radio-A and Radio-B base stations at Table Mountain.

The RSMS, a self-powered, self-contained mobile radio spectrum measurement system, was configured as follows for these measurements. A 1-m diameter parabolic dish antenna with a linearly (slant) polarized feed was mounted on a pan-and-tilt directional controller and was manually boresighted on the 5G transmitted signals with a manually controlled box-search approach.

The measurement antenna fed into a custom-built RF front-end box, as diagrammed in Figure 19.⁴⁰ The box features four major sections: A noise diode for standard Y-factor gain and noise figure calibrations; a 0-70 dB RF attenuator, controllable in 10-dB step increments; yttrium-iron-

⁴⁰ The RF preselector box components have been reduced and simplified in Figure 19, to show only those that are pertinent to the 5G measurement.

garnet (YIG) tunable and fixed-frequency bandpass front-end filters; and low-noise preamplification designed to overdrive the noise figure of the rest of the measurement system.

For these measurements and based on the results of the observations of the 5G signals at the Technical Center and an *ad hoc* 5G base station emission spectrum measurement of January 2024, the RF filtering was handled as follows.

For spectrum measurement data collected at and below 2700 MHz, the YIG filter was used. (The YIG frequencies are tuned via a feedback loop that keeps them tracking on the tuned frequency of the systems' signal analyzer.) At the point that each measurement transitioned to frequencies above 2700 MHz, the NTIA box's internal filter path was switched from the YIG to a fixed, 2-4 GHz bandpass filter. Simultaneously, an external, manually operated switch (see Figure 19) was flipped from a straight-through path to a path that ran through the same high-performance FAA 2700-2900 MHz fixed-bandpass filter that had been used for the Atlantic City Technical Center measurements and observations. This approach ensured that all 5G emissions measured above on frequencies 2700 MHz were definitively originating as 5G base station transmitter unwanted emissions within the radar band.

Downstream from the manual RF switch, the paths ran through an RF power combiner and then into a Keysight PXA signal analyzer. The signal analyzer outputs were recorded digitally for later retrieval, analysis and graphing.

3.2.3 RSMS Measurement System Calibration

Prior to performing any measurement, a noise diode in the box is switched to the RF input in lieu of the measurement antenna. The diode is alternately turned on and off while the power flowing through the measurement system is measured across the frequency range that will be used for the planned measurement (e.g., across 2500–2800 MHz for these spectrum measurements).

Using the measured decibel difference between power observed in the diode ON versus OFF conditions, along with the known, pre-calibrated excess noise ratio (ENR) of the noise diode, the custom-written computer software computes the gain and noise figure of the measurement system as a function of frequency. The noise figure data are stored for future use. The gain data are used to later correct the indicated power level in the measurement system to the true power level that the antenna is putting into the front end of the measurement system. All of this is performed under automated control, the operator only inputting the desired frequency range for each calibration. The uncertainty in the calibration is about ± 0.5 dB.

3.2.4 RSMS Measurement System Software

As noted above, although the instantaneous dynamic range of the system's signal analyzer or spectrum analyzer is about 60 dB, we extend that dynamic range using the variable, stepped-level RF attenuator of Figure 19Figure 16. This attenuator has levels of 0 dB to 70 dB of attenuation, available in 10 dB steps. Adding the 70 dB of the attenuator to the instantaneous

60 dB of the down-stream analyzer gives a maximum measurement dynamic range of 130 dB (non-instantaneous).

This extension of dynamic range depends on two additional factors: the use of a stepped-frequency instead of a conventional swept-frequency spectrum-coverage algorithm (described below); and having enough power available from a transmitter to illuminate its emission spectrum that far down.

In practice, our dynamic range may be limited by not always being able to get sufficiently close to a transmitter's antenna, while still remaining in its main antenna beam and not being in its far field, to obtain the maximum possible 130 dB.

For multi-gigawatt (sometimes 45 to 60 GW) EIRP radars, we routinely obtain 110–120 dB of dynamic range, and sometimes the maximum possible 130 dB. For the relatively low-powered (only about 56 kW EIRP) 5G base station transmitters that we have examined in this case study, the maximum dynamic range that we could obtain was about 100 dB to 110 dB.

Although manual control of the front-end level-stepping RF attenuator is possible, we have programmed our measurement-control software to automatically detect where the received signal's power level is located relative to the signal analyzer's DR window as a measurement progresses; and to add, reduce or keep constant the setting of the RF stepped-attenuator as the measurement system progresses itself across each measured emission spectrum. This feedback-and-control of the RF attenuator setting is made possible by the custom-designed frequency-stepping algorithm that controls our spectrum measurements, as described below.

Given the amount of 5G base station antenna downtilt that was available, we could realistically obtain a physical distance of 100 meters from the 5G transmitters to the RSMS measurement antenna, while retaining mainbeam coupling between these systems. With 25 dBi of gain in our 1-meter diameter measurement system antenna at 2590 MHz and a radiated 5G power-per-megahertz of +65 dBm, we predicted a power level of +9 dBm/MHz in our measurement system front end.⁴¹

Our Y-factor noise-diode calibrated system noise figure was 14 dB and our measurement bandwidth was 1 MHz to match the ASR-9 IF-stage bandwidth. Thus, we expected a noise floor of $(-174 \text{ dBm/Hz } kT + 60 \text{ dB/MHz measurement bandwidth} + 14 \text{ dB noise figure} = -100 \text{ dBm/MHz}$. This was 109 dB below the expected incident 5G power level of +9 dBm/MHz, from above. Thus, we expected to achieve 109 dB of dynamic range in the 5G radiated emission spectrum measurements.⁴²

⁴¹ We actually obtained +10 dBm/MHz when we finally ran the measurements.

⁴² We obtained 110 dB of DR when we finally ran the measurements.

3.2.5 RSMS-5G Measurement Software Including Stepped-Frequency Algorithm

3.2.5.1 Frequency-Stepped Algorithm Measurements

The RSMS operates via custom-written fifth-generation software.⁴³ The software allows automatically controlled noise diode calibrations; custom-programmed spectrum and time-domain measurements; real-time display of results; and storage of the results for later retrieval and analysis.

The key to the 5G spectrum measurement capability, adapted from earlier applications in radar emission spectrum measurements, is the stepped-frequency algorithm. With this algorithm, a spectrum is measured a single frequency at a time. *The algorithm steps across the spectrum in discrete frequency points, instead of sweeping as is conventionally done.*

At the outset of a spectrum measurement, the operator selects a set of measurement parameters: start frequency; stop frequency; detector; IF (resolution) bandwidth; video bandwidth; the number of frequency steps that will be taken across the specified frequency range; and the time interval (“dwell”) that will be used for each step.

The measurement then runs under computer control. The measurement system tunes to the start frequency. A zero-span (time domain) sweep is performed on the frequency for the specified dwell period with the selected detector and IF bandwidth. The measurement system stores the time domain sweep at that frequency. It also extracts the maximum power point that occurred within that sweep, corrects it for the gain-calibration factor that was stored earlier from the noise diode calibration, and displays that point on an evolving spectrum graph for the operator.

Next, the measurement system tunes to the second frequency to be measured. This stepped-frequency interval is equal to the frequency range of the measurement divided by the number of data points that were originally specified. For example, if the specified frequency range is 2500 MHz to 2800 MHz and the number of data points had been specified as 301, then the frequencies of the spectrum data points would be 2500 MHz, 2501 MHz, 2502 MHz, and so on until the 301st data point would be measured at 2800 MHz.

3.2.5.2 Resolution Bandwidth and Frequency Step Size

Ordinarily, the number of frequency-measurement steps (data points) taken across a spectrum is driven by the resolution bandwidth. This is because there are no spectra without measurement bandwidths; *all spectra exist only in conjunction with their specified measurement (also known as resolution or convolution) bandwidths.* The resolution bandwidth is selected first, based on any of a number of possible criteria. Then the number of steps to take across the spectrum is usually driven by that bandwidth choice.

⁴³ Largely written by one of the authors, G. Sanders.

If a spectrum is to be measured in, for instance, 1 MHz, then the most logical and straightforward frequency step size is the same: 1 MHz.⁴⁴ That way, the convolution size just equals the step-size between the measured points.

Our emission spectra measured for 5G base station transmitters have in fact been measured in 1 MHz for three reasons: (a) because the FCC's regulatory transmitter power limit is defined in terms of power per megahertz spectrum power density; (b) because interference effects on ASR-9 receivers are often assessed on a per megahertz basis, the same bandwidth as the radar's IF stage; and (c) because many EMC assessments for many systems are in general performed on a per megahertz basis, making our spectra potentially usable in other work at later dates.

3.2.5.3 Dwell Time per Frequency Step

The dwell time per step is important because it needs to be long enough to capture whatever time-domain behavior in the measured signal waveform might be important, while not being overly long to the point of needlessly extending the total time required to complete the spectrum measurement. The operative concept behind the dwell interval is to ensure that it is long enough to "see" the entire periodicity of the waveform to ensure that the waveform's maximum possible power is captured at each frequency during each step. For radars with rotating or electronically scanned antenna beams that may take anywhere from a few seconds to a minute to return to the same frequency and antenna beam direction, the step interval is set from perhaps 3 seconds for a rotating short-range navigation radar or a sector-scanned airborne fire-control radar; to 5 seconds for a short-range ATC radar; to 12 seconds for a long-range air search and surveillance radar; to 20 or 30 seconds for a long-range weather radar; to perhaps 60 seconds or more for a super long range, frequency-hopping phased-array space-search and tracking radar.

For the 5G base station transmitter spectrum measurements in this case study, with a TDD cycle of 5 milliseconds (ms),⁴⁵ the dwell per step was set to 500 ms. This gave us 20 TDD 5G cycles that were observed and recorded at each measurement frequency step. This ensured that we saw the maximum possible power transmitted by the 5G base station transmitters at every measured frequency across the selected spectrum-measurement frequency range of, say, 2500 to 2800 MHz in 301 steps of 1 MHz.

3.2.5.4 Dwelling and Stepping versus Sweeping or High-Speed Digitizing

In the dwell-and-step approach to measuring a radar or 5G spectrum, we operate our measurement system like an ambush predator. Rather than chasing the targeted signal as it moves in the time, space, and frequency domains, our measurement algorithm waits patiently for the transmitter being measured to *come to us* on each measured frequency in time and space. The dwell-and-step approach only needs to make the dwell interval long enough to accommodate any transmitter's combined behaviors of antenna beam-pointing; frequency hopping or sweeping; and waveform time-behavior (e.g., pulsing or time division duplexing) to ensure that, within

⁴⁴ There are some cases, not considered here, where the step size needs to be larger than the resolution bandwidth.

⁴⁵ The typical 5G TDD time-cycle is: 3.5 ms for the base station downlink (DL) transmissions while its attached UEs listen; and then 1.5 ms for UE uplink (UL) transmissions while the base station listens.

each dwell interval, all those factors will eventually align and give us a maximum-power “hit” on the frequency being measured.

In addition to allowing us to control our dynamic range this way (see below), another advantage of our wait-for-lunch-to-come-to-us strategy is that we know unequivocally (and can prove with our recorded time-domain sweeps at each measured frequency) that a maximum-power hit has definitely occurred on each measured frequency. There is no equivocation about whether we have indeed captured the spectrum in its entirety, at full available power on all frequencies.

This is in contrast to conventional frequency-sweeping and high-speed digitizing approaches, where the intersection between the digitization of the input time-varying waveform and the antenna beam-pointing and frequency-hopping or sweeping behavior of the transmitter being measured may combine so as to cause difficulty in entirely understanding or characterizing the results. Moreover, in experimental side-by-side measurements using the two approaches we have documented that the dwell-and-step approach ends up finishing the spectrum faster than high-speed digitization, for radars and other complexly designed transmitters such as 5G.

The dwell-and-step approach turns out to be well pre-adapted to measuring the 5G base station transmitter signals. We merely set the dwell to 500 ms (about 100 TDD cycles) and treat the rest of the measurement as if we are looking at a radar signal.

3.2.6 Stored Emission Spectra and Supporting Associated Data

At the conclusion of every stepped emission spectrum measurement, the spectra are automatically stored in MATLAB[®] formatted (.mat) electronic data files. The final, stored data for each spectrum include: the spectrum measurement parameter settings including start and stop frequencies, the measurement bandwidth, the dwell interval and the detector selection; the time domain scan that was taken in each dwell interval at each measured frequency; the raw (uncorrected) maximum power that was obtained (sorted) from each dwell cycle; that same power level, but calibration-corrected for each data point; the RF attenuation level that was invoked at each measured frequency; and any operator notes for the measurement, including the given name of the transmitter, and so forth. We can, if needed, reconstruct the entire spectrum measurement from the data stored in each spectrum file.

3.2.7 Local ASR-9 Signals at Table Mountain

There are two local ASRs, one toward the east-southeast at DIA (called Irondale Station) and another to the northeast called Platteville Station. As with all ASR-9s, these stations have two klystrons for two frequency channels, only one of which is operated at a time. The stations alternate between their available pair of channels on something like a weekly basis. We consulted with the FAA to determine which channels the respective local ASR-9s would be using when we performed our measurements on the 5G base stations. The FAA avoided using

local channels in the lower part of the radar frequency band during our measurements at Table Mountain.⁴⁶

We nevertheless expected, however, to see some ASR-9 signal power within the OoB emission measurement of the 5G base stations. How did we cope with that?

This was another point where the stepped-frequency spectrum measurement approach was helpful. Because we could see the time domain characteristic of each measurement point in our spectra, we could visually see, easily, the ASR-9 signals, as opposed to the 5G signals as our OoB measurements progressed. Any time that we saw a measurement point where the ASR-9 signal exceeded the 5G OoB signal power, we noted it. When we completed the spectrum across the range where we saw any ambient ASR-9 signals in our data, we performed re-measurements of the contaminated data points. As we re-measured each point, we looked at the ASR-9 signal again. Every time we re-measured when the ASR-9 was *not pointing at us* and therefore not contaminating our data, we kept the new point.

We continued that process until all our measurement points were uncontaminated by ASR-9 signal power. A further assistance in keeping ASR-9 signals from contaminating our measurement results was that we had main-beam coupling between the 5G CoWs and our 1-meter dish antenna. The ambient ASR-9 signals were kept in our measurement antenna backlobes and sidelobes, limiting the extent to which the local, ambient ASR-9 signals could interfere with our measurement results. This was why, in fact, we had the 5G CoW base station signals radiating eastward from Building A-4 while we had our measurement antenna pointing westward, away from the local ASR-9 stations.

The sum-total result being that we could see the ASR-9 signals when they contaminated any of our initial data points, and we re-measured them out of those data points before we completed our OoB measurements on each 5G base station radio transmitter.

3.2.8 Local B41 5G Signals

There were some local, ambient B41 5G signals visible at our measurement location at Table Mountain. They belonged to the wireless carrier with whom we were doing our measurements. Prior to commencement of the 5G base station emission measurements, we worked with the carrier's engineering staff to isolate and identify any ambient B41 signals that could interfere with the measurement. To the extent that local communication network conditions and configurations permitted, the carrier turned those signals down or off to eliminate them as contaminating factors in our data collections.

Just as with the ASR-9 signals, the fact that we had main-beam coupling between the 5G CoWs and our 1-meter dish antenna, with the ambient B41 5G signals in our measurement antenna

⁴⁶ Coordinating FAA personnel were present during the Table Mountain 5G emission spectrum measurements, along with wireless carrier company personnel and OEM personnel.

backlobes and sidelobes, further assisted us in ensuring that the local, ambient 5G signals did not interfere with our measurement results.

As will be described below, we took baseline spectrum data to identify and quantify local ASR and 5G signals, further assisting us later, in our post-measurement analyses.

3.3 5G Base Station Transmitters

3.3.1 64T64R MIMO Array Designs, Briefly

One of the distinguishing characteristics of 5G base stations is the use, in these transmitters, of Multiple Input Multiple Output (MIMO) arrays that can form directed, individual antenna radiation beams. This selectable beam directionality is beneficial in allowing 5G base stations to maximize RF power with desired UEs while nulling (to an extent) against non-desired UEs. Figure 20 shows a diagram of the RF-level architecture of one of these MIMO arrays.

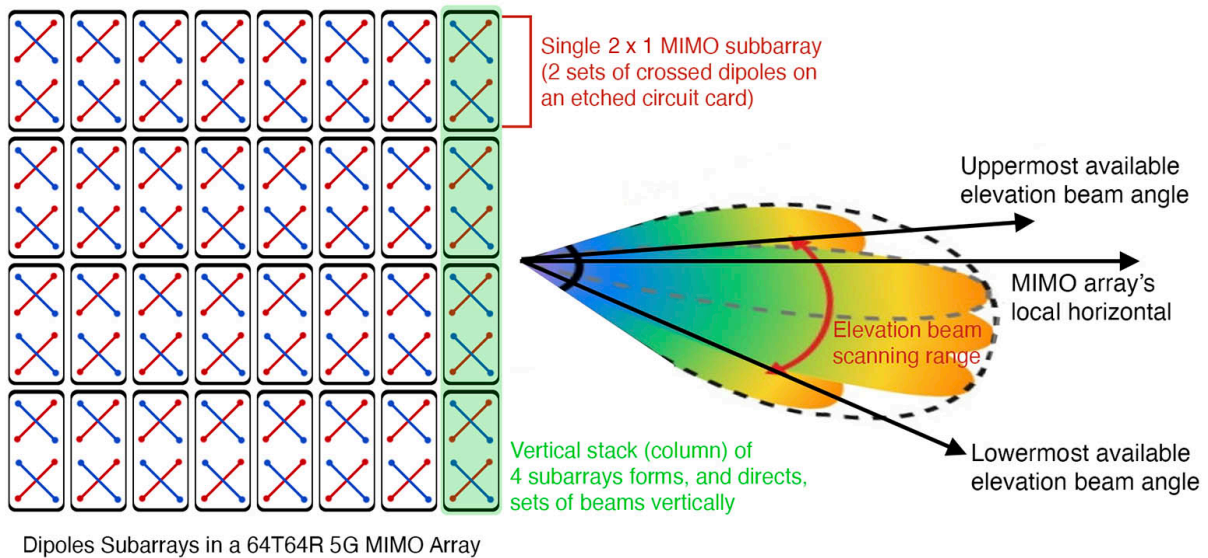


Figure 20. Diagram of 64T64R MIMO array architecture and beam-directing capability.

The 5G radios in this case study use a MIMO transmitter design designated 64T64R, for 64 transmit and 64 receive sections. Each such MIMO box (see Figures 20 and 21 for examples) contains 64 pairs of crossed dipole antenna elements. The pairs are laid out in an 8×8 circuit-card planar array. Pairs of these crossed dipoles are grouped into subarrays. Figures 22 and 23 show representative narrow-beam 5G antenna patterns in azimuth and elevation planes.



Figure 21. A MIMO 64T64R transmitter-receiver box for 5G base station. It is an integrated, weather-sealed unit with connectors on the lower edge for power and data.

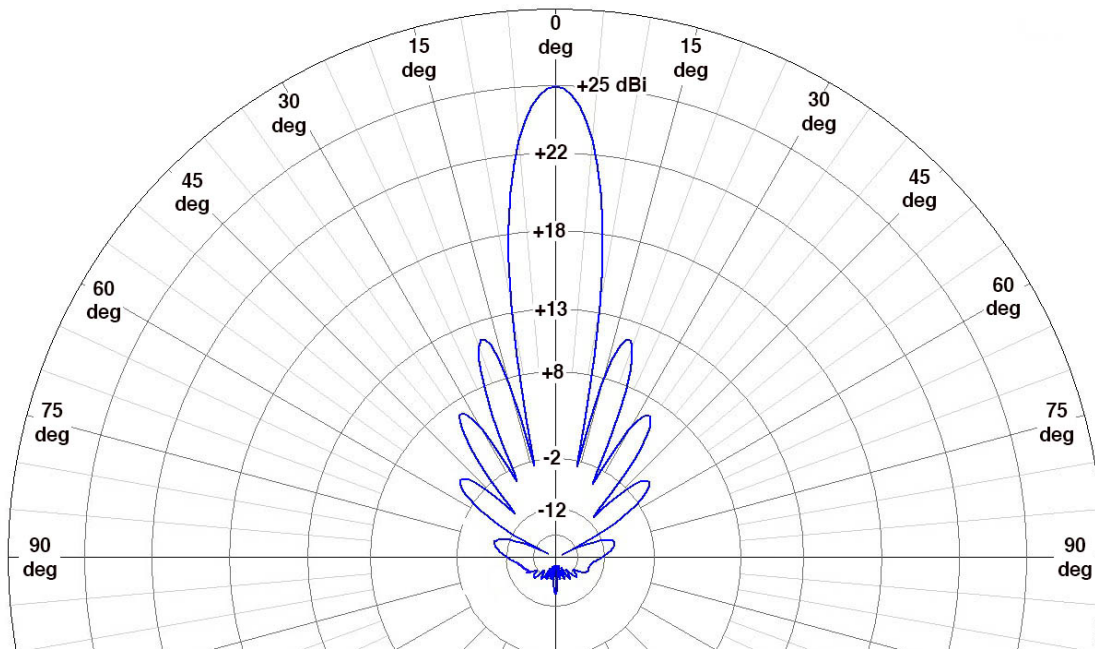


Figure 22. Azimuthal computed radiation pattern for a 3 GHz band MIMO array antenna in narrow-beam mode. Courtesy and permission of MITRE.

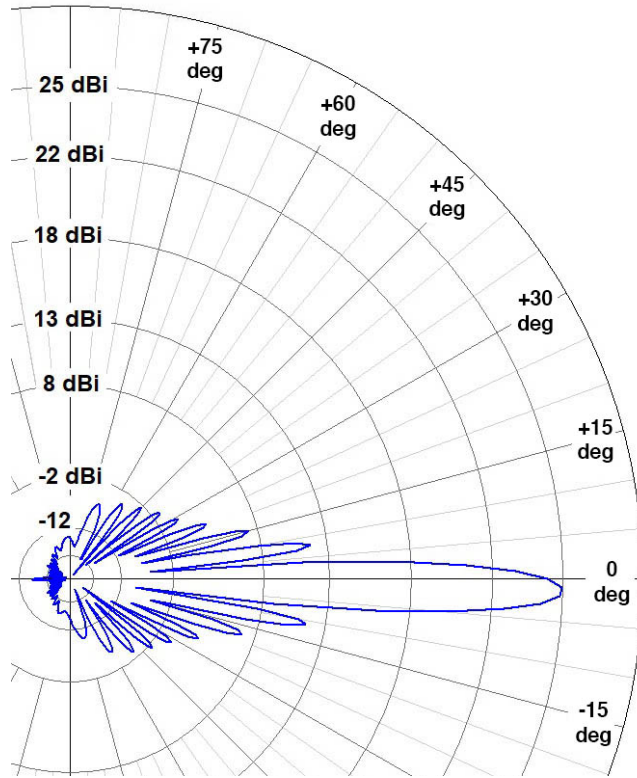


Figure 23. Elevation computed radiation pattern for a 3 GHz band MIMO array antenna in narrow-beam mode. Note the -1.5 degree downtilt. Courtesy and permission of MITRE.

3.3.2 5G MIMO Beam Elevation Angle Range and Control

3.3.2.1 Beam Elevation Angle Range for 5G MIMO Arrays

Vertically arranged groups of MIMO subarrays, as shown for example in Figure 20Figure 19, use phase control to form beams at various elevation angles relative to the array's broadside axis.⁴⁷ Table 4 lists manufacturer's stated limits of electronic elevation beam scanning for the three OEMs of 5G base station MIMO arrays deployed in the U.S.

Although 5G elevation angles can go above the broadside axis for these base stations, as shown in the table, the 5G technical literature seems to focus mostly on how to tilt 5G beams downward rather than upward. This is consistent with customers' UEs ordinarily being located at downtilt elevation angles, below tower-mounted or rooftop-mounted 5G base station transmitter boxes.

⁴⁷ MIMO arrays can be mounted with varying but limited amounts of mechanical elevation tilt.

Table 4. Manufacturer-specified electronic elevation beam scanning limits for 5G MIMO Arrays, relative to the MIMO broadside axis.

Manufacturer⁴⁸	Lowermost Elevation Below MIMO Array Broadside	Uppermost Elevation Above MIMO Array Broadside
A	-19 degrees	+7 degrees
B	-3 degrees	+3 degrees
C	-10 degrees	+3 degrees

3.3.2.2 5G Beam Elevation Angle Control

Regarding control of the 5G antenna beam elevation angles through time, as the external UE locations shift, the beams are not computed on the fly. Instead, large catalogs or codebooks of 5G antenna beams are ordinarily pre-computed and stored in what amount to look-up tables in 5G antenna-beam control software systems. These pre-computed beams are loaded and formed one after another in the 64T64R MIMO arrays as UEs move through each base station’s coverage.

UEs are therefore not tracked, *per se*, by the base station MIMO beams. Rather, optimal beam selections are taken from the codebooks for time-evolving DL-UL links to desired UEs, and for nulling to some extent against non-desired UEs. These individual selections are made on a discretely stepped time-domain basis. The pre-computed beams are repeatedly located in the codebooks and formed one after another to maintain this desired UE coverage and nulling as the UE environment evolves in time. Beams that might theoretically be formable, but that have not actually been pre-computed and loaded into the codebooks are not (cannot be) formed by the MIMO arrays.

3.3.3 Table Mountain 5G CoW Configurations

3.3.3.1 5G MIMO Antenna Beam-Aiming

5G beam elevation angles were manually set, by on-site OEM support engineering staff, to boresight the RSMS at Table Mountain, for the full-power spectrum measurements. Antenna beam angles were further manually muted, downtilted or rotated azimuthally for special, separate measurements, as described below.

3.3.3.2 5G Traffic and RF Channel Loading for Radiated Measurements

5G communications include two types of loading: traffic loading, which is binary-information data streams at baseband; and RF channel loading, which is the series of individual, narrowband PRBs that together make up the full width of an RF channel (itself set somewhere between 20 MHz to 100 MHz).

⁴⁸ There are three OEMs whose 5G MIMO radio base station transmitters are being procured and deployed by wireless carriers in the U.S. These manufacturers are called A, B and C in this table.

At Table Mountain, the OEM staff used a software-based load generator to load the B41 5G channels at baseband during the emission measurements. The next layer upward is the RF channel, consisting of a series of adjacent-frequency, narrowband (e.g., 180-kHz wide) PRBs. To assure that all 5G RF channel PRBs are in radiation, an air interface load generator (AILG) is used. AILG arbitrarily populates the narrowband PRB RF-channel slots, to fill in the channel's full (total available) RF bandwidth of 20 MHz to 100 MHz. Between baseband loading, plus built-in 5G encryption, and then RF loading, the 5G CoWs at Table Mountain were always operated with as much information-loading and RF channel-loading as 5G can support.⁴⁹

The CoWs at Table Mountain were not operated with any paired UEs for these measurements. Forcing the transmitters to operate with maximal baseband traffic (OCNS or iPerf) and RF-channel loading (AILG) was sufficient to assure maximal loading. Likewise for full-power output, on-site OEM staff who operated the CoWs commanded the transmitters into full available output power.

3.4 5G Radiated Emission Data from Table Mountain

3.4.1 Baseline (Background) Spectrum Environment

As noted above, there are some measurable ASR and 5G background signals in the Table Mountain environment. As noted above, to minimize the effects of these signals the FAA coordinated operation of its two nearest radars, at Denver International Airport and at Platteville, to not radiate on channels in the lowest part of the radar band. T-Mobile, likewise, coordinated its local 5G operations to avoid use of B41 as much as possible. Further, the measurement geometry had the RSMS receiving antenna directed westward from Table Mountain, keeping local ASRs and 5G base stations in its backlobes and sidelobes. Figure 24 shows baseline (background) emissions at Table Mountain relative to one of the 5G base stations (foreground) that was subject to measurement in this case study.

⁴⁹ We do not, however, refer to these loading levels as 100 percent. There is no such thing *per se* in 5G technology. Any input bit string at baseband, even if it is all 1s or all 0s, is built into a maximal-entropy output string. Built-in encryption in the 5G standard subsequently re-mixes that first level of entropy, resulting in another maximal-entropy output string to RF. Running "loading" data at baseband may be redundant; the 5G baseband always ends up "loaded," no matter what anyone does with it. As for the RF channel loading, TDD only allows up to 70 percent base station DL talk-time, and up to 30 percent UE UL talk-time. So, 70 percent and 30 percent are, respectively for the DL and UL, 100 percent. These facts have been a persistent source of confusion in 5G link testing.

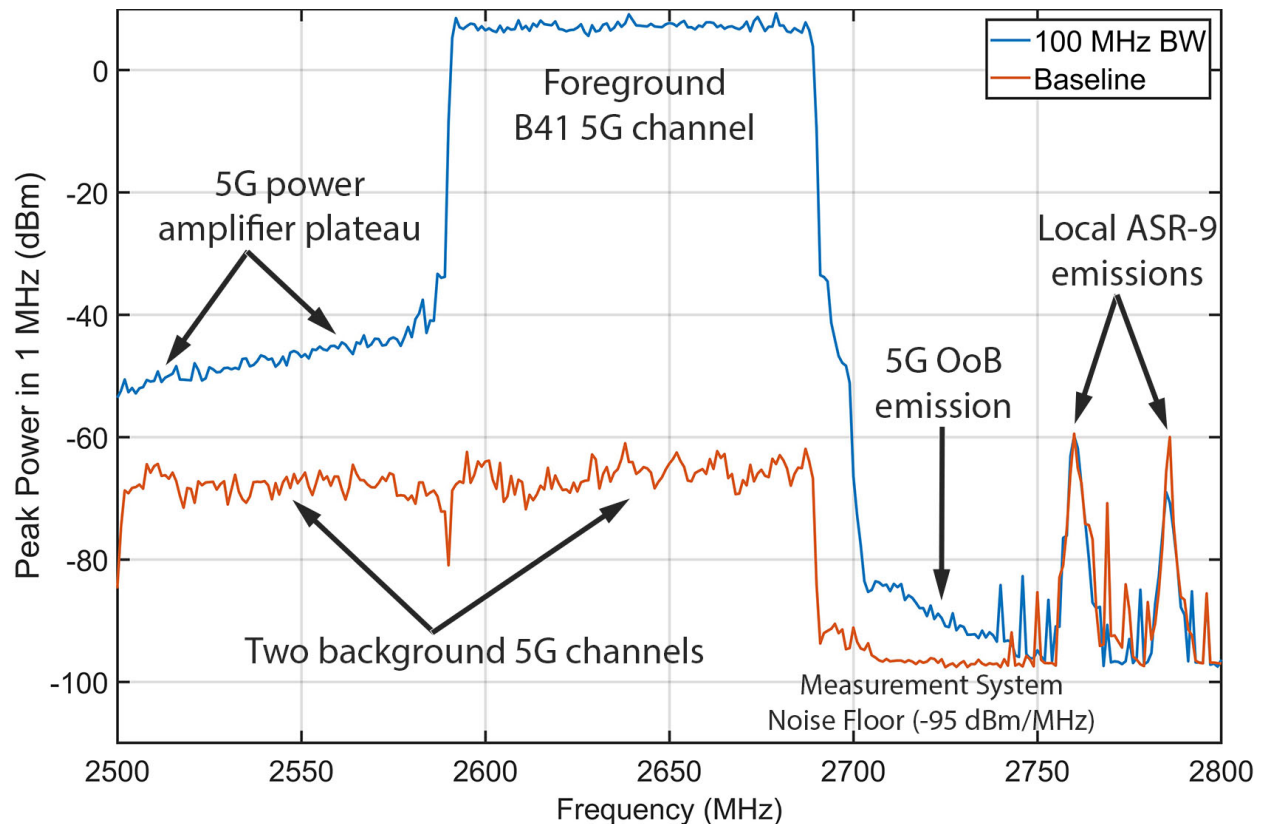


Figure 24. Baseline (background) ASR-9 and 5G environmental emissions at Table Mountain relative to a foreground B41 5G base station being measured in this case study.

In the figure, background ASR-9 station emissions are seen at 2760 and 2785 MHz. Background 5G emissions in lower and upper segments of B41 (2500–2590 MHz and 2590–2690 MHz) are seen as well. None of these background emissions are coupled into the RSMS measurement system at high enough power levels to affect the foreground, peak-detected B41 5G base station emission measurement. Not only is there no additive-power effect for peak detection, but the background 5G emissions are always at least 10 dB lower in power than the foreground 5G emission power. Furthermore, all measurable 5G emissions above 2700 MHz are lost in the -95 dBm RSMS measurement noise at frequencies that are below the frequencies of the local background ASR-9 signals.

Note too, that in Figure 24 the predicted measured 5G power level of +9 dBm has been matched nearly to the decibel by the actual measured power. The total DR of the 5G emission measurement is 105 dB, exceeding the original DR goal of 100 dB. This measurement demonstrates that this sort of DR is needed, as these 5G unwanted emissions do not even begin to appear until the measurement reaches about 92 dB below the 5G intentional-emission power level.

3.4.2 5G Base Station Emission Spectra as a Function of Channel Bandwidth

Figures 25 through 30 show radiated, measured emission spectra of 5G Radio-A and Radio-B as a function of selected 5G channel bandwidth, between 20 MHz to 100 MHz.

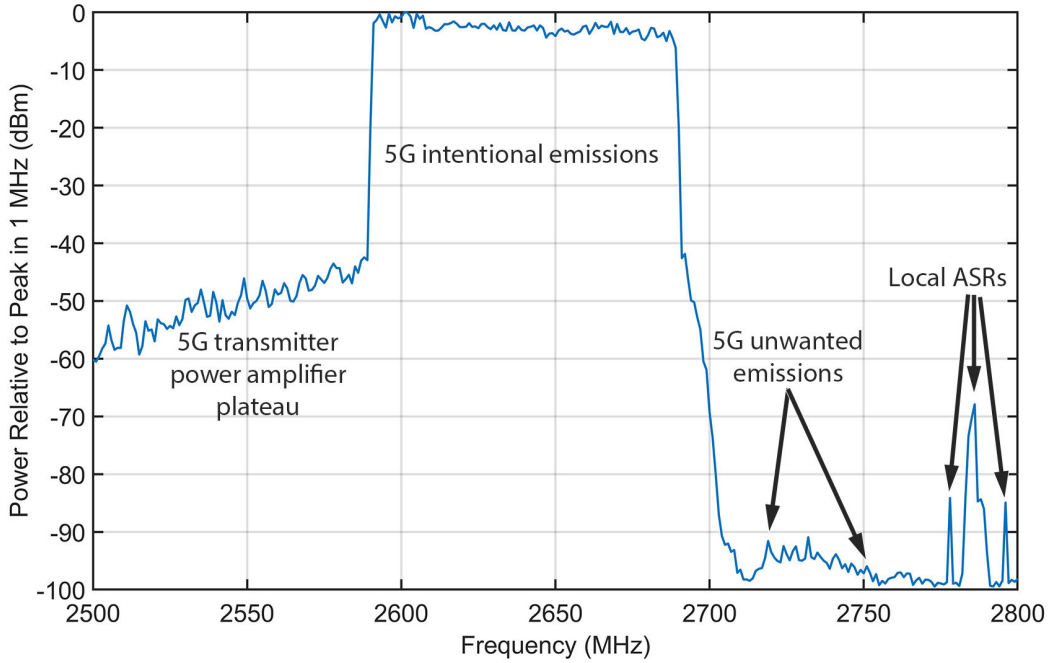


Figure 25. 5G base station Radio-A radiated emission spectrum, 100 MHz channel bandwidth.

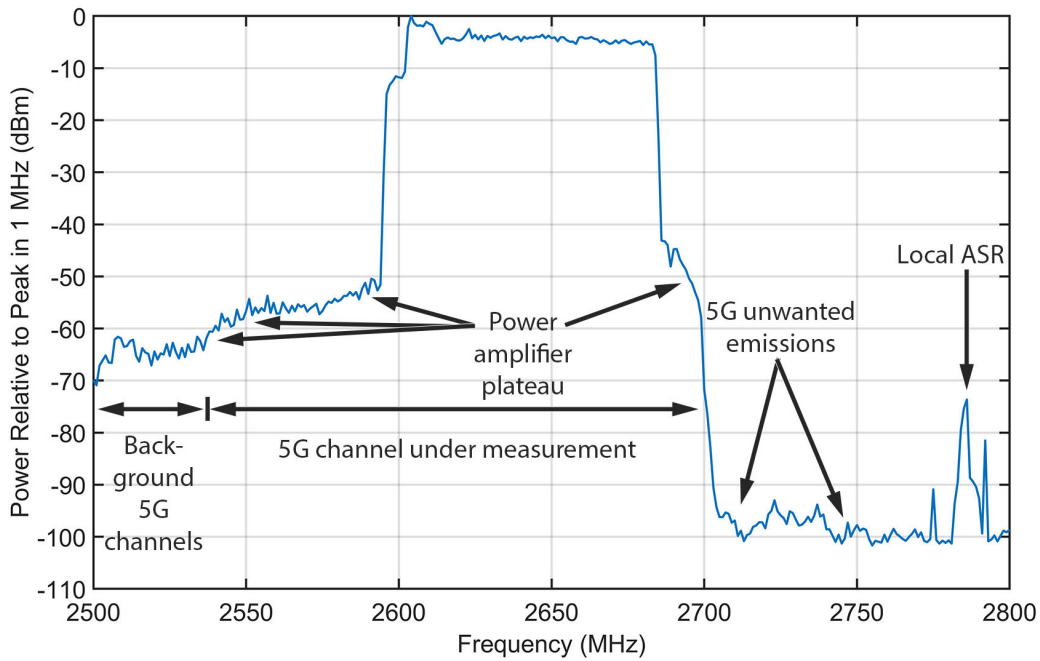


Figure 26. 5G base station Radio-A radiated emission spectrum, 90 MHz channel bandwidth.

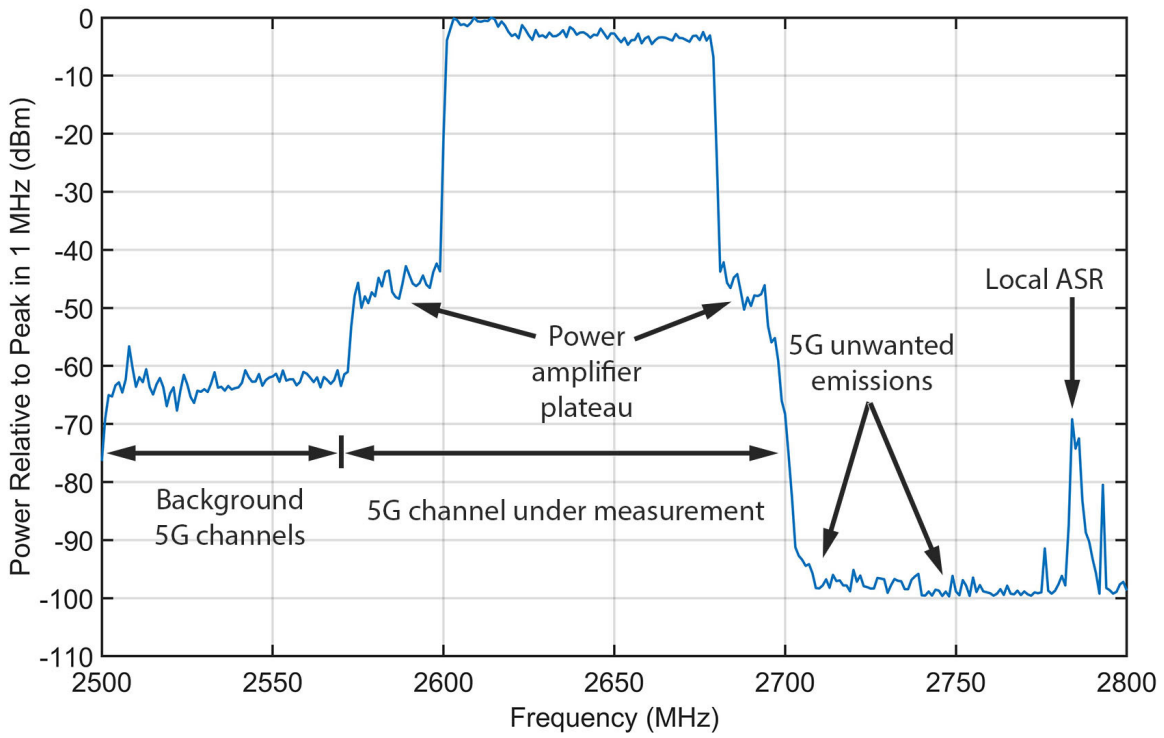


Figure 27. 5G base station Radio-A radiated emission spectrum, 80 MHz channel bandwidth.

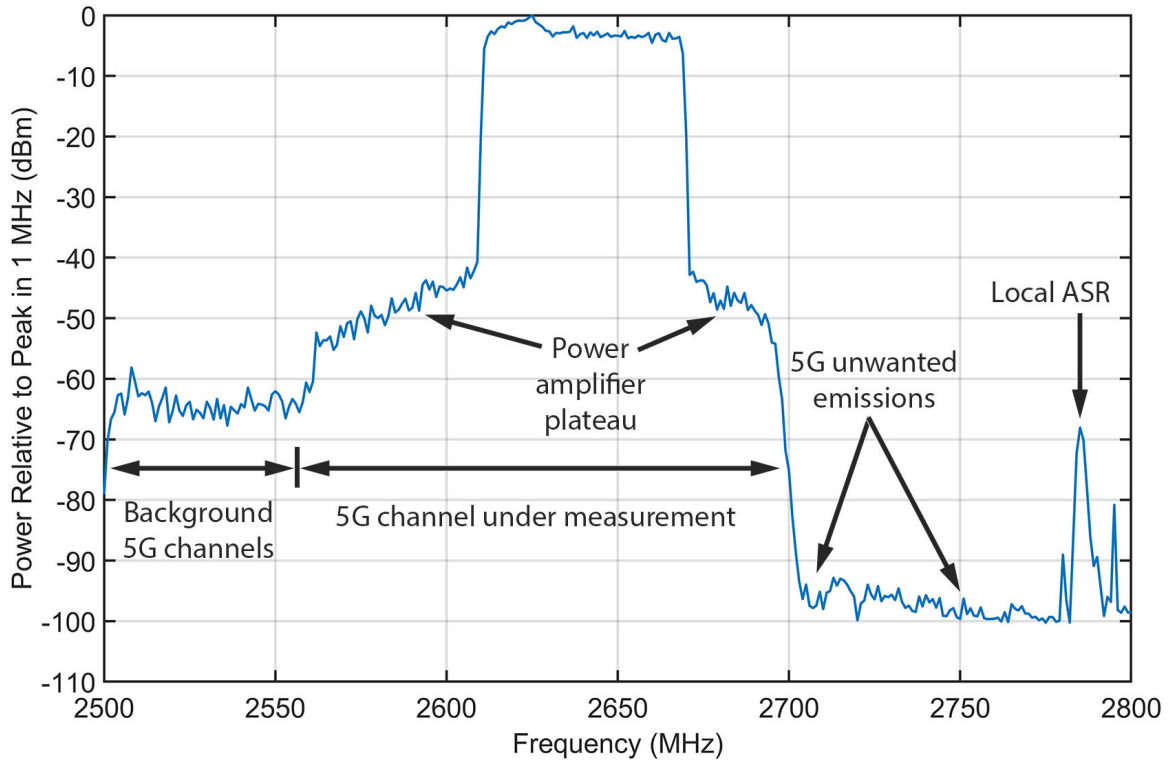


Figure 28. 5G base station Radio-A radiated emission spectrum, 60 MHz channel bandwidth.

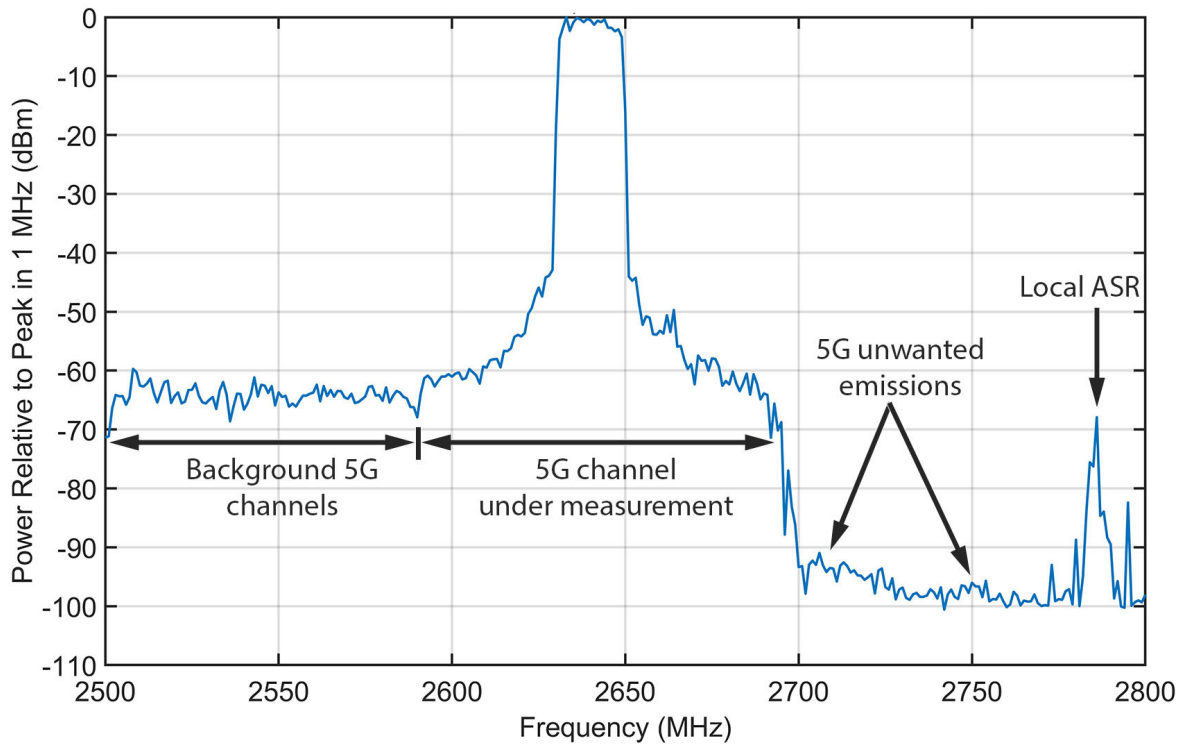


Figure 29. 5G base station Radio-A radiated emission spectrum, 20 MHz channel bandwidth.

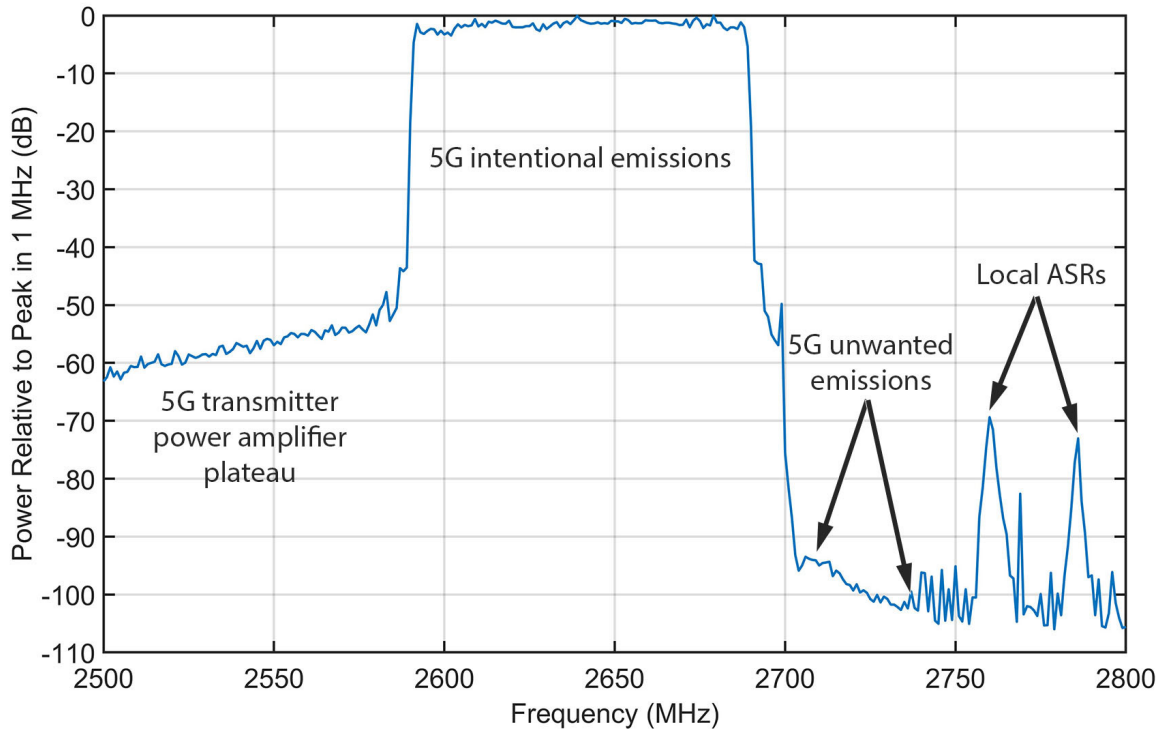


Figure 30. 5G base station Radio-B radiated emission spectrum, 100 MHz channel bandwidth.

3.4.3 5G Base Station Emission Spectrum Channel-Width Discussion

Recognizing the interference mechanism of 5G in the ASR-9 receivers as Fourier spreading of the 5G intentional-emission signal into the radar band by the receiver RF front-end switches, we further note that the spreading begins from the uppermost frequency-edge of the 5G channel. This is shown in Figure 14 and also in the figures of Appendix D. Therefore, bringing the upper-edge frequency of the B41 5G channel downward may reduce the 5G signal power that Fourier-spreads into the radar receiver. We now examine the measured 5G emission spectra to see how much this reduction in frequency can be done, and how much it can improve spectrum coexistence for 5G and the ASR-9 radars.

In Figures 25 through 30, our emission spectra show the power levels of unwanted 5G emissions from Radio-A and Radio-B as a function of selected 5G transmitter channel bandwidths, ranging from a minimum of 20 MHz to a maximum of 100 MHz.⁵⁰ In all cases, the incident 5G peak-detected power in 1 MHz measurement bandwidth (approximating the bandwidth of the radar receivers) was +10 dBm at the measurement signal analyzer's detector.⁵¹ This absolute power is graphed in Figure 30. In the remaining emission-spectrum graphs (Figures Figure 32 and Figure

⁵⁰ The 5G Radio-B emission spectrum was only measured for a 100 MHz channel, as the radio recalcitrantly resisted all attempts to force it into narrower channel bandwidths. This behavior was consistent with other work we have done with other 5G transmitter base stations.

⁵¹ Received with a 25-dBi measurement antenna gain at a distance of 100 m from the 5G CoW base station antenna.

33), the power is graphed relative to the 5G intentional, in-channel maximum power, again in a spectrum power density of 1 MHz. The unwanted levels above 2700 MHz, relative to the intentional-emission power levels, are thus read directly off the figures. In all cases, the unwanted levels range from -92 to -95 dB below the 5G intentional-emission levels. The unwanted levels are more than 100 dB down, in all cases, by the time the measurement frequency reaches 2750 MHz.

Addressing the problematic Fourier spreading, which commences at the upper edge of the 5G intentional channel emissions, reducing 5G channel bandwidths brings the channel upper-edges downward in frequency, which may improve adjacent-band spectrum coexistence. The 5G base stations PAs do continue to generate their own wideband power plateaus irrespective of the output-channel widths, but the PA emission-spectrum plateaus are reduced in power by 45 dB to 60 dB, as shown in Figures 25 through 30.

Additional isolation (power decoupling) between 5G base station transmitters and ASR-9 radar receivers may be achieved by narrowing the 5G channel bandwidth to less than 100 MHz (e.g., to perhaps 60 MHz) and the ASR-9 receivers might be protected from the Fourier-spreading effect.

Note that, in the Table Mountain measurements, the 5G transmitter channel bandwidths were reduced while maintaining the 5G channel center frequencies at a constant frequency of 2640 MHz; the channel reductions were performed symmetrically around the nominal center frequency of 2640 MHz. This meant that, for example, when the 5G channel bandwidth was 60 MHz, the upper edge of the 5G channel was brought down to $(100 - 60)/2 = 20$ MHz below 2690 MHz, to 2670 MHz.

But if the entire 5G channel at 60 MHz bandwidth had been simultaneously down-shifted to a new center frequency of 2620 MHz, then the channel's upper edge in the 60 MHz bandwidth would have been brought lower in frequency by a full $(100 - 60) = 40$ MHz, for a new upper-edge frequency of 2650 MHz.

Doing that 5G transmitter total-channel downshift in frequency, with a 60 MHz 5G channel bandwidth, would provide a gap of $(2705 \text{ MHz} - 2650 \text{ MHz}) =$ a total 55 MHz gap between the new 5G channel upper edge and the lowest ASR-9 spectrum band frequency.

With the PA plateau at a power level of -45 to -60 dB down from the 5G intentional emission level, ASR-9 receivers might be protected from the Fourier spreading problem for even closer physical separation distances than existed for the FAA Technical Center measurements.⁵²

3.4.4 5G Base Station Antenna Beam-Muting Experiment

A second sometimes-proposed 5G-to-radar power decoupling method is to turn off selected 5G antenna beams in selected directions. This is called beam-muting. An example theoretical-

⁵² Recall from above that, at the FAA Technical Center, we assessed a -35 dB power reduction (decoupling) of the 5G signal to be enough to protect that radar receiver from the interference phenomenon.

simulation computation for beam muting in a B41 5G transmitter base station 64T64R MIMO array is shown in Figure 31.

Beam muting is not the same as beam nulling. In phased-array nulling, antenna radiating elements are programmed to destructively interfere with themselves on a given azimuth, to actively suppress radiation on that azimuth. In muting, otherwise-active beams in an array are switched off, but the *sidelobes of adjacent beams are still present*, radiating in the same direction as the one or two beams that have had their main lobes turned off. The result being a definitively limited amount of power reduction in the direction of the muted beam, for example -15 dB.

Figures 32 and 33 show the results of an antenna beam-muting experiment conducted with 5G Radio-A at Table Mountain.⁵³ The baseline condition for the radio was six beams running, none muted. In Figure 32, we see the result of muting beams designated 2 and 5. In Figure 33, we see the result of muting beams designated 2 and 3.

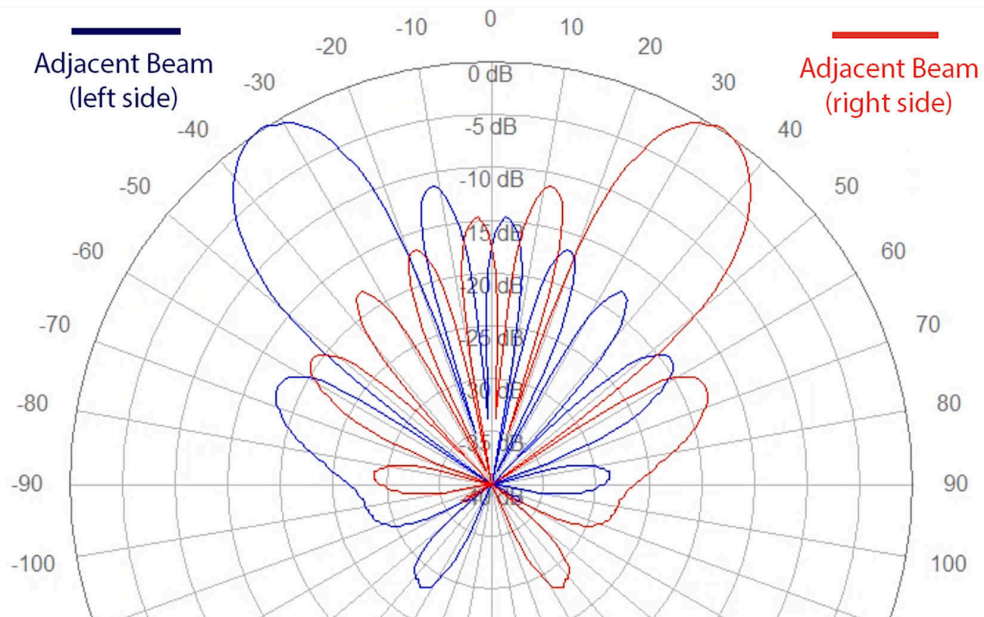


Figure 31. Example of a 5G antenna beam-muting simulation prediction. Maximum decoupling in the muted-beam direction is -15 dB, due to sidelobe contributions from adjacent beams.

⁵³ It was not possible to get 5G Radio-B to do antenna beam-muting.

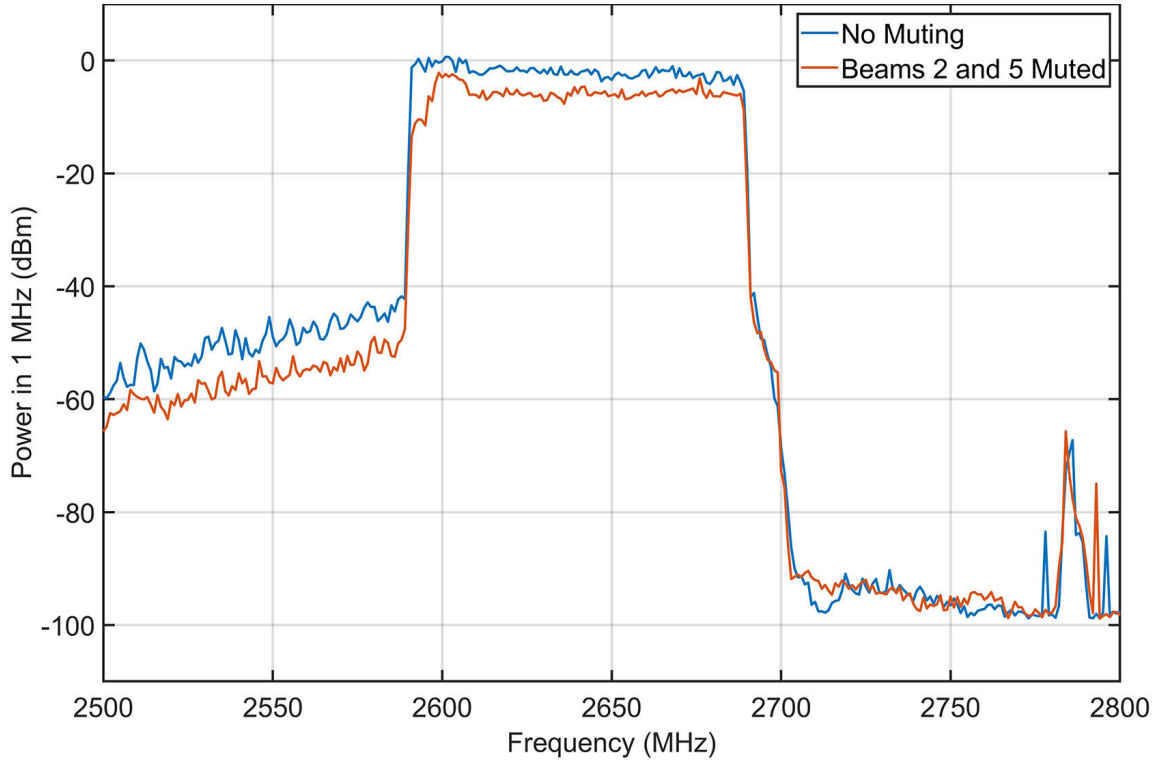


Figure 32. 5G Radio-A array Beams 2 and 5 muted.

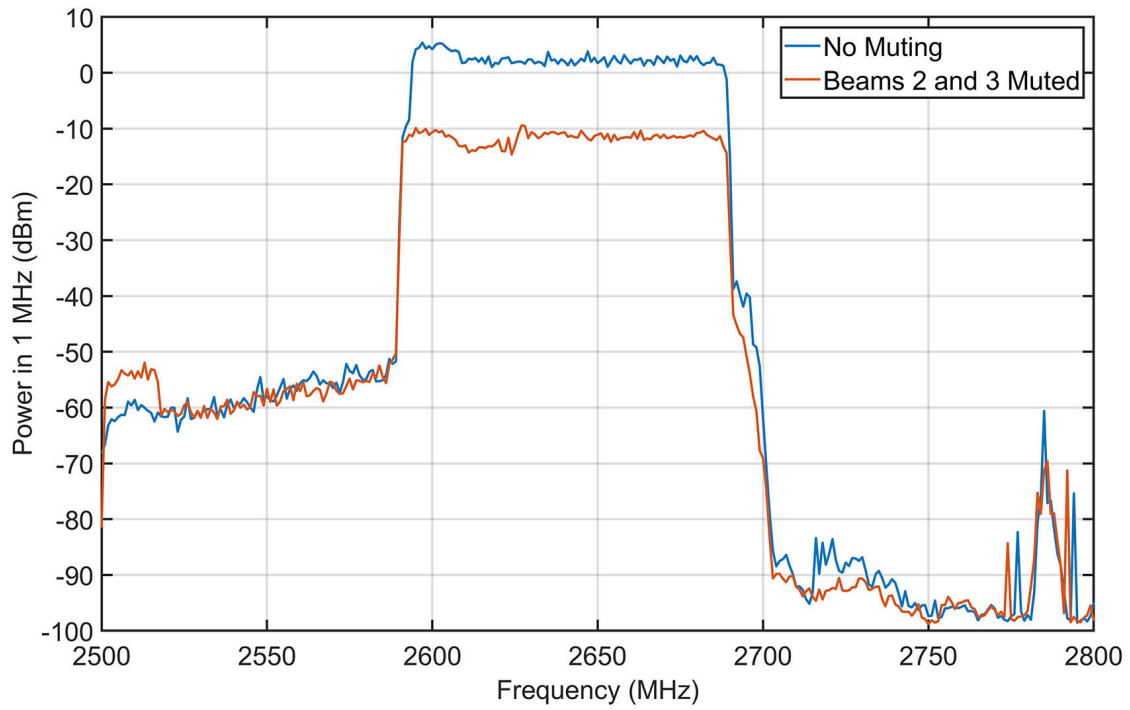


Figure 33. 5G Radio-A array Beams 2 and 3 muted.

3.4.5 5G Base Station Antenna Beam-Muting Discussion

The beam-muting figures show distinct effects, or lack thereof, in three spectrum regions. In the 5G intentional-radiation channel chimneys, the decoupling, power-reduction effect ranges from as little as about -3 or -4 dB to as much as -11 dB. These channel-power reductions are not as good as theoretical prior predictions, although the -11 dB reduction is at least in the vicinity of the maximum 15 dB that had been predicted (Figure 31).

Consider now the 5G intentional-radiation overload power reduction that would be needed at an ASR-9 site (such as the one where we evaluated the problem at the Atlantic City Technical Center), which has been observed to have been on the order of -35 dB to alleviate the problem. The observed beam-muting power reduction of -11 dB in our experiment would fall about 24 dB short (that is, deficient by two and a half magnitudes in linear power) of what would be required in terms of power decoupling between the transmitter and the receiver.

The second region is the PA plateau. Muting beams 2 and 5 produced *more offset* in decoupled power than in the intentional-emission channel. Conversely, muting beams 2 and 3 produced *no* change at all in the PA plateau. We believe that these results are consistent with the PA spectrum-plateau power having many contributions from various combinations of the 64T64R MIMO array elements, in various directions in space, our measurement system's direction from the array being idiosyncratic to our measurement. We believe the same measurement made from other locations on the ground would have yielded varying results, just as we see in the two measurements we performed at a particular location. In any event, these results indicate that the effects of beam muting in spectrum not contained in a transmission-channel bandwidth would need to be separately modeled from the in-channel part of the spectrum.

The third spectrum region is the unwanted-emission spectrum emission power in the adjacent frequency band, at frequencies above 2700 MHz. In this region, beam muting had no effect on radiated power. Similarly to the PA plateau results, we believe this outcome is due to 5G beam-muting effects being frequency-dependent, as the 64T64R MIMO arrays are built out of relatively phased elements. Although beam muting can turn off radiation in a given direction in the desired-frequency part of the spectrum, there is no guarantee that the same power-muting effect will translate into the adjacent spectrum. Furthermore, the unwanted emissions in the adjacent spectrum may be generated partially or mostly from contributions from adjacent, non-muted antenna beams.

The conclusion is that beam muting has not been demonstrated as an effective method to decouple unwanted emission spectrum power from receivers in the adjacent band. Only in cases where the power-decoupling margin would need to be about -10 dB, or less, would beam muting potentially resolve the adjacent-band receiver-power overload problem. If co-channel interference to a radar receiver were ever to occur, beam muting would apparently be ineffective as a mitigation option.

3.4.6 5G Base Station Antenna Beam Downtilting Experiment

For 5G Radio-B, antenna beam downtilting was performed to observe how much decoupling was achievable with this mitigation option. The result is shown in Figure 34. The power decoupling was only about -3 dB when the antenna beam was downtilted by -10 degrees from zero degrees. As an approach to relieve overload levels in a radar receiver, this experiment did not demonstrate much benefit.

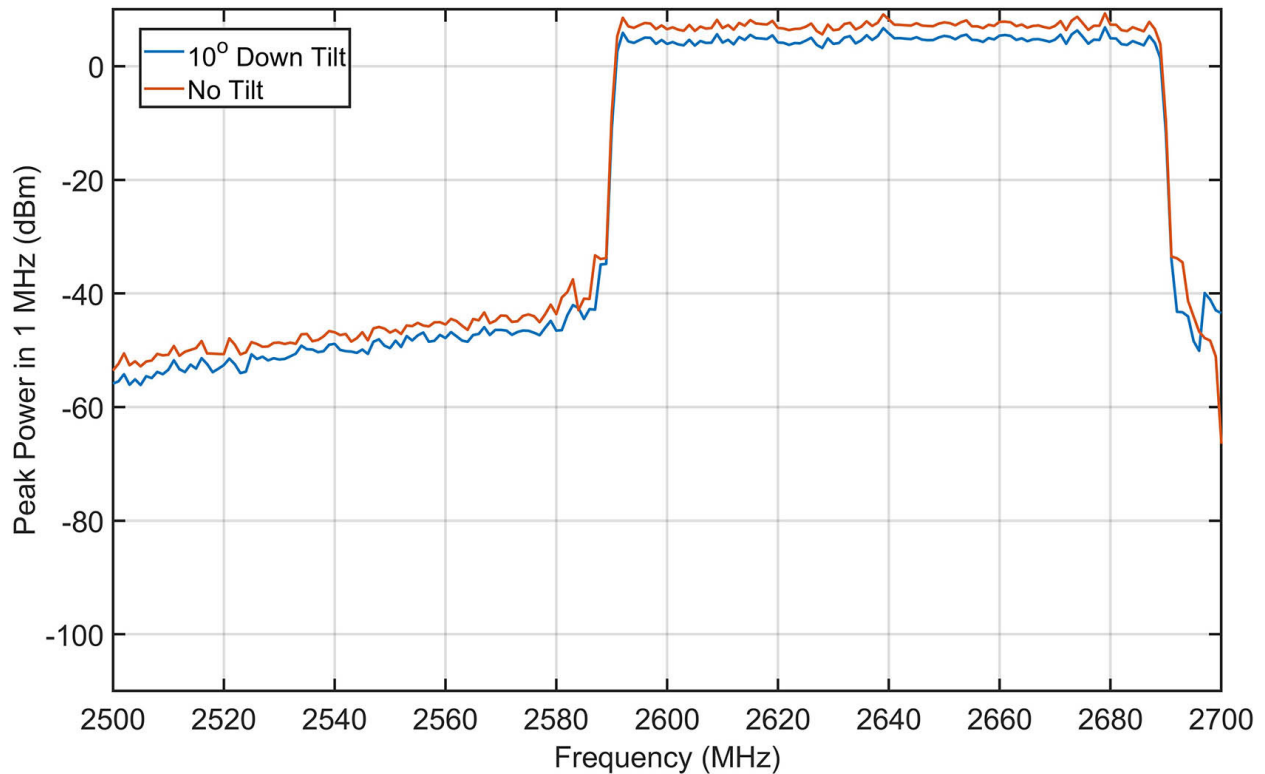


Figure 34. 5G antenna beam downtilt experiment, -10° versus no downtilt.

3.4.7 5G Base Station Antenna Beam Azimuth-Rotation Experiment

Another decoupling approach that has been considered is to rotate the 5G antenna array away from a coexistence azimuth with a radar station. At Table Mountain, we performed this experiment with 5G Radio-B.⁵⁴ The result is shown in Figure 35.

With a 70-degree azimuthal rotation of the array (mechanical rotation, not electrical), the decoupling was -70 dB. This would have more than accommodated the -35 dB of decoupling that was observed as being needed during the Atlantic City Technical Center work. The downside

⁵⁴ The entire CoW tower was pivoted horizontally, to ground level; the array was re-set by 70 degrees of azimuthal rotation; and the tower was re-erected to vertical.

being, of course, that 5G customer coverage would have been lost in much of the (nominally 120-degree azimuth coverage for 5G MIMO arrays) off-rotated sector.

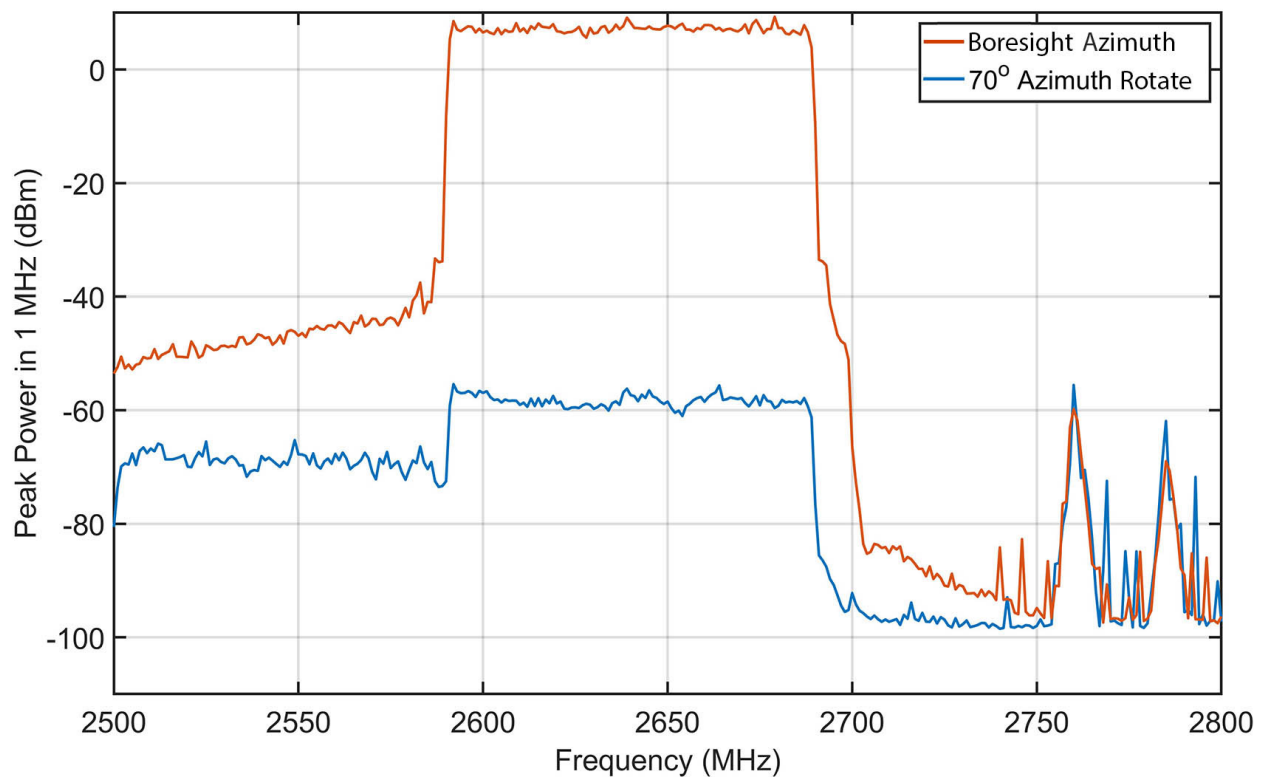


Figure 35. Power-decoupling effect of mechanically off-rotating the 5G Radio-B MIMO array in azimuth by 70 degrees.

3.4.8 5G Transmitter Base Station Channel PRB Blanking

PRB blanking is often suggested as a method of coexistence improvement between 5G transmitters and other radio-system (e.g., radar) receivers. In this interference case study, PRB blanking could offer a coexistence solution, as the fundamental EMC problem is to bring the upper edges of the 5G channel intentional emissions downward, to lower frequencies.

In the measurements at Table Mountain, we encountered the same problem with trying to run the CoWs with PRB blanking as has occurred in other, unrelated 5G testing we have done: It is difficult to activate PRB blanking in operational 5G transmitter base stations, even with dedicated OEM support.⁵⁵ But we do encourage 5G channel-edge PRB blanking to be considered as a coexistence option for adjacent-band operations with ASR-9 radar stations.

⁵⁵ The only PRB blanking we have ever seen implemented is in our own 5G CoWs at Table Mountain, implemented, with difficulty, by ourselves.

4. COEXISTENCE ANALYSIS

4.1 Power-Decoupling Approaches

The coexistence-limiting factor that we have identified is Fourier spectrum spreading of the upper-frequency edge of 5G intentional-emission channel power by one or more (probably all) of the radar ASR-9 radar receiver RF beam switches. The radar receivers need to be decoupled from the adjacent-band B41 5G channel emissions at full-channel widths that go as high in frequency as 2690 MHz.

One approach would be to re-design the radar receiver RF front ends bandpass or highpass filtering in front of the first beam switch, cutting off at 2700 MHz, and then retrofit or re-build the radar station receivers with this filtering. Unfortunately, the first such switch in the radar receivers is located at the antenna feed (see Figure 5). Installing an RF bandpass filter at that point could be mechanically difficult and impractical, if not impossible. In any event, such an engineering modification would promise to be time-consuming and costly to design, test and implement.

Another approach, which we discuss here, is to decouple the ASR-9 receivers from adjacent-band B41 5G base station transmitters through 5G channel bandwidth reduction and center-frequency readjustment; increased physical distance separation; integration of terrain factors in power-coupling predictions; and adjusting antenna beam-coupling geometries.

4.2 Desirability of Proactive Power-Decoupling Coordination

The base station-radar coordination approach, outlined below, requires analytical numerical inputs for such factors as: the power level coupled into the radar receivers at the B41 5G channel frequency upper-edges; radar-receiver gains and losses in front of the waveguide beam switch; radar antenna gain toward a B41 5G base station transmitter; propagation loss between the radar and the 5G station; 5G antenna beam gain toward the radar; and 5G transmitter total-channel power delivered to the transmitter antenna.⁵⁶

4.3 Wireless Carriers Need to Know Where to Power-Decouple

As discussed below, wireless carriers need to be informed by the government of the physical zones where power decoupling from 5G channel frequency upper edges is needed, and how much decoupling is needed as a function of location of 5G base stations. The wireless carriers will need to know directions to individual radar stations for antenna coordination and beam muting (if implemented). Unless the government does, at least, inform the wireless carriers of physical coordination zones, needed decoupling factors within those zones, and directions for

⁵⁶ Aggregate-station emissions in the radar-adjacent spectrum band on a given communication tower are thought to not be problematic, as the key parameter is the frequency separation between any given radar's tuned frequency and the frequency of the upper-edge of the adjacent-band B41 5G channel.

antenna coordination, the carriers cannot assist the government with coexistence of their 5G base stations with government radar receivers.

4.4 Computation Approach for Spectrum Coexistence Coordination-Zone Development

We provide here an approach for how spectrum coexistence coordination zones can be developed for 5G base station transmitters and adjacent-band radar receivers, based on the interference mechanism that we have identified.

The 5G base station parameters that can be varied are channel center frequency; channel bandwidth; antenna gain directed toward the radar; and transmitter power. There are technical limits to how much each of these parameters can be varied. At each site where radar receivers are impacted by local 5G base stations, site-specific work will need to be performed to determine which of these parameter variations is effective in mitigating interference effects. For example, just prior to this report's publication, such work was performed jointly at a 5G/ASR-9 site near Tucson, with engineers from the FAA, T-Mobile and NTIA performing the effort.

In the case of the 5G base station power that coupled into the ASR-9 at the Atlantic City Technical Center, for example, the 5G power in the receiver's RF waveguide at the pre-STC beam switch was -20 dBm/MHz peak power (= -30 dBm/MHz RMS average power); the frequency separation was $(2725 - 2690) = 35$ MHz; the needed reduction in 5G power to eliminate the observed interference tics in the receiver's circuitry was empirically observed to be 35 dB, as described in Section 2.4.

This amount of decoupling could be achieved through combinations of: reducing the B41 5G channel frequency upper-edge (itself a combination of possibly reduced channel bandwidth and readjustment of the channel's center frequency, as discussed in Section 3); deactivating selected PRBs in the 5G channel's upper-frequency portion; and readjusting the antenna beam-coupling geometry between the 5G base station and the ASR-9 antenna.

Other power-decoupling values will be indicated for other 5G-to-radar site geometries. We emphasize that a site-by-site analyses will be required. These analyses will need to take into account the frequency separations between the radar receivers and the 5G transmitter channel upper edges; the physical separation distances and terrain factors; and the antenna beam coupling geometries between the 5G transmitters and the radar receivers.

The coordination-zone or coordination-distance challenge can be approached as follows:

- Specify distance-radii around selected ASR-9 sites for simulation
- Define a grid spacing of 5G base stations within the simulation radius
- Run the Irregular Terrain Propagation Model (ITM) in point-to-point (P2P) mode for each link with these model inputs:
 - Input antenna-beam coupling between transmitter and receiver stations⁵⁷

⁵⁷ This could be mainbeam-to-mainbeam coupling, but lower coupling factors should be considered as, for instance, the lower-angle (reduced-gain) edges of the radar antenna beams.

- Run multiple candidate power-mitigation levels (e.g., 0, to 60 dB in 10-dB increments)
- Create KML contours
- Implement the frequency roll-off rate for the Fourier spectrum spreading.
- Run these computations for all candidate ASR-9s
 - Run $P_R = \text{EIRP}_{5\text{GBase Station}} + G_R - P_L - \text{System Loss}$
 - Logic: IF $P_R > \text{Beam Switch Level}$, THEN $P_R - \text{Beam Switch Level} = \text{Margin [dB]}$.
- If unwanted (out-of-band emission) coupling were to be considered, then use:
 - $P_R = \text{EIRP}_{5\text{GBase Station}} + G_R - \text{FDR} - P_L - \text{System Loss}$
 - $P_T = \text{Radar Noise Floor} + I/N$
 - If $P_R > P_T$, $P_R - P_T = \text{Margin [dB]}$

4.5 Example Coordination Outputs

Here we provide examples of what the computational outputs might look like. *These examples and the Table 5 entries are provided for illustrative purposes only.*

Table 5. Dummy coexistence numerical inputs (for illustrative purposes only)

Parameter	Dummy Input
B5G transmitter base station EIRP (dBm)	+75 dBm/100 MHz
Radar receive-antenna gain toward 5G station (dBi)	+33
Beam switch overload level (dBm/100 MHz)	-45
Radar receiver <i>I/N</i> threshold for interference (dB)	-10
Radar receiver noise floor (dBm)	-112.8
5G base station transmitter height AGL (m)	30
Radar antenna height AGL (m)	10
Simulation radius (km)	80
5G grid spacing (km)	1
ITM propagation input (percent time)	10
ITM propagation input (percent location)	50
ITM propagation input (percent confidence)	50

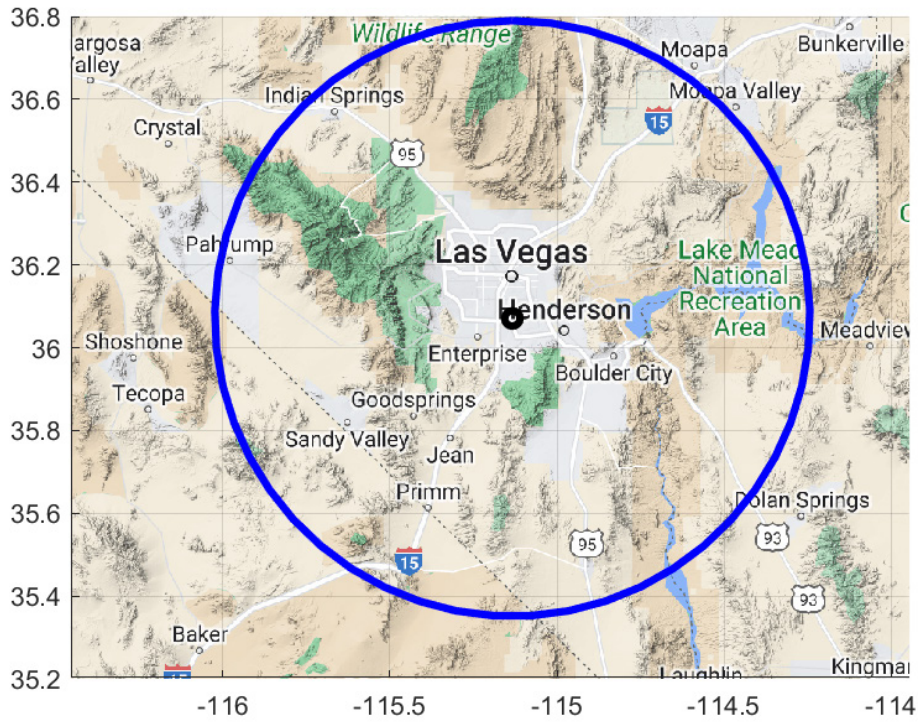


Figure 36. First step: Define a coexistence radar station with a simulation radius.

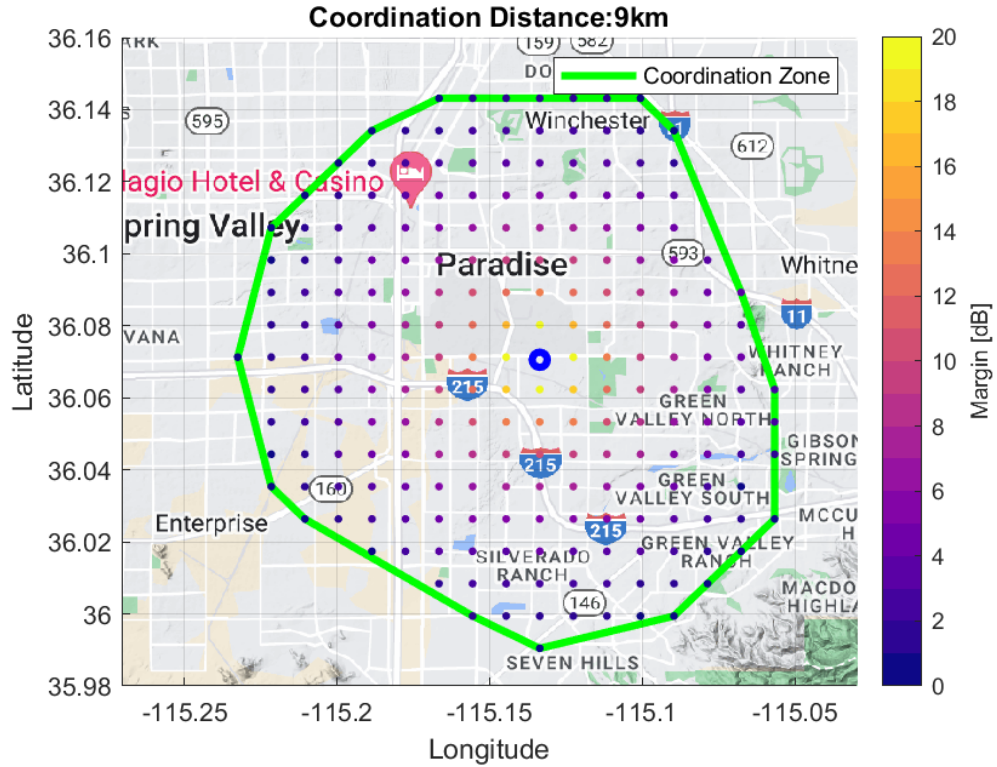


Figure 37. Second step: Define a 5G base station grid spacing within the simulation zone.

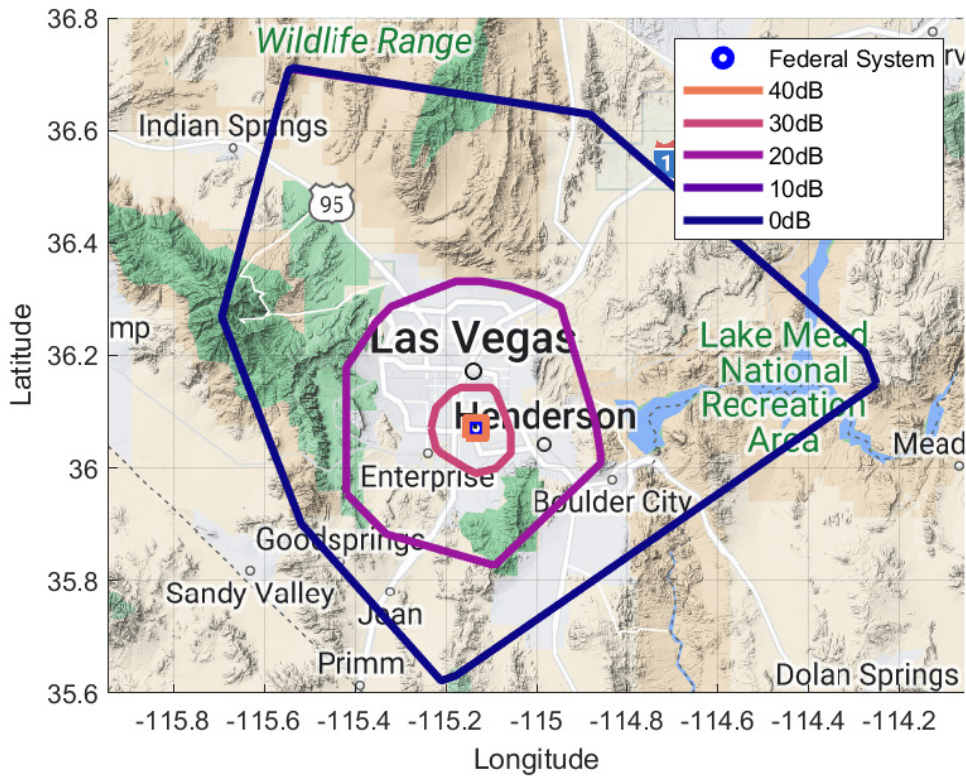


Figure 38. Third step: Compute KML contours for multiple power-mitigation levels.

Figure 39 shows example outputs spread across a map of the U.S. Again, we emphasize that these are not real analyses. These outputs are only intended to provide an idea of what the overall coexistence coordination might look like. Within the coordination zones, B41 5G transmitter base stations might still be deployable. But these are the zones within which the individual deployments would need to be considered individually by engineers.

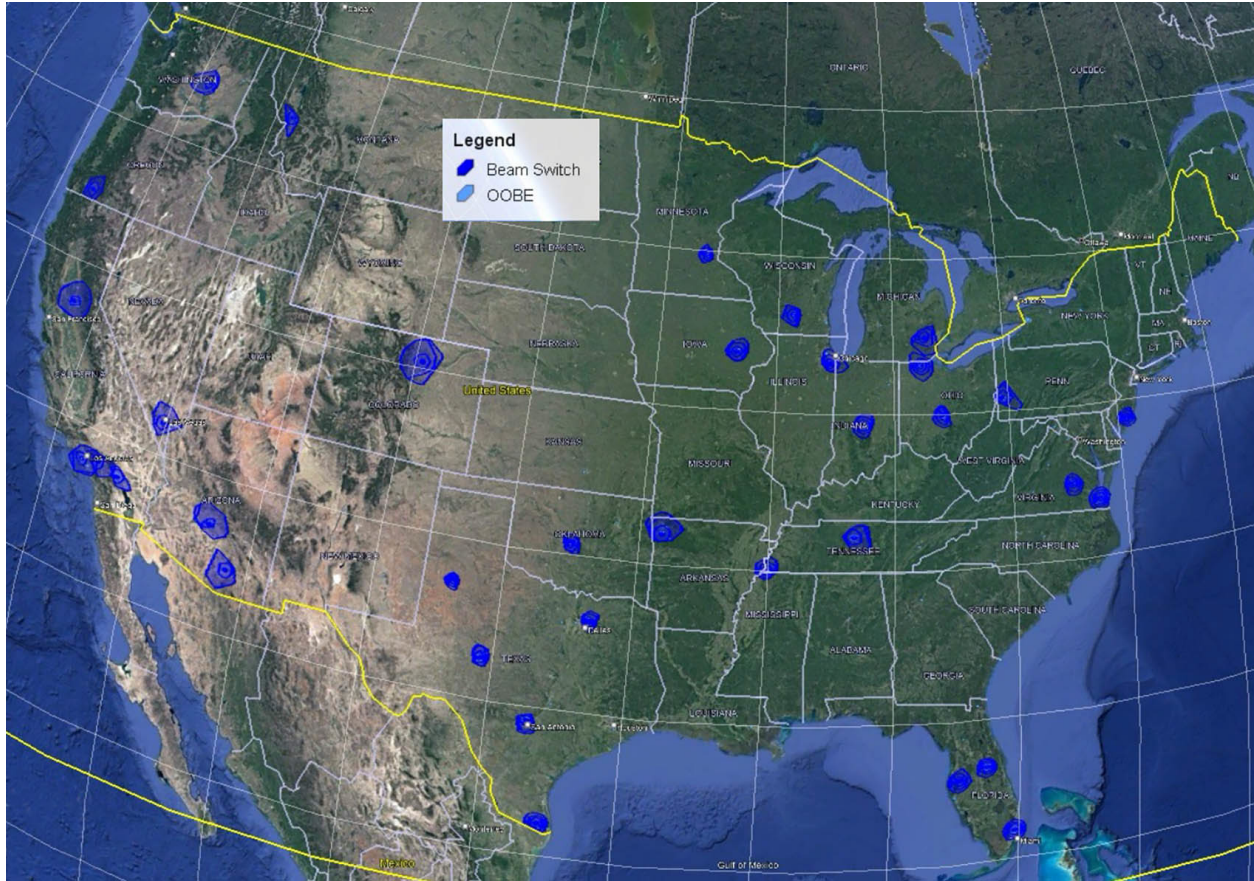


Figure 39. Illustrative dummy example of coexistence contours for B41 5G base station transmitters and ASR-9 radar receivers across the U.S.

5. CONCLUSIONS AND RECOMMENDATIONS

Following a systematic scientific-engineering method, we disproved our initial hypotheses for the causative factor of interference from B41 base station transmitter base stations to ASR-9 receivers. We ultimately discovered a never previously seen⁵⁸ interference mechanism.

Our conclusions are:

- 1) B41 5G base station transmitters, when located sufficiently physically close to ASR-9 stations, and with sufficiently strong antenna-to-antenna coupling and sufficiently small frequency separations between the 5G channel uppermost frequency edges and the ASR-9 station operational frequencies, interact with radar receiver RF beam switches, ahead of the receivers' RF bandpass filters, to spectrum-spread the licensed 5G channel power across the radar spectrum band, producing co-channel interference on the radars' tuned frequencies. (Radar receiver STC stages can also be affected in this way, but they show less of the effect than the beam switches. Protection of the beam switches will preclude problems with the receivers' STC stages.)
- 2) The physical mechanism of the beam-switch spectrum spreading across the radar spectrum band is the ordinary, non-exotic Fourier wave-mechanics effect of chopping a power waveform in the time domain, into pulses, and thus concomitantly and (physically inevitably) forcing the input signal power to spread in the frequency domain. This Fourier spectrum spreading effect is linear; no non-linear phenomena are involved.
- 3) While it is possible for the radar receiver beam switches, which are based on solid-state PIN diode technology, to experience power overload from adjacent-band B41 5G base station transmitters and behave non-linearly, the beam-switch power-input threshold of +6 dBm (or higher) total power is only reached well after the Fourier spectrum effect has already been activated and is causing its own interference effects in the radar target and weather processors. Protection from the power levels that cause Fourier spectrum-spreading interference effects will therefore protect the radar receiver, collaterally, from non-linear power overload effects in the beam switches.
- 4) The 5G base station parameters that can be varied are: channel center frequency; channel bandwidth; antenna gain directed toward the radar; and transmitter power. There are technical limits to how much each of these parameters can be varied. At each site where radar receivers are impacted by local 5G base stations, site-specific engineering work will need to be performed to determine which of these parameter variations is effective in mitigating interference effects.
- 5) Due to radar receiver beam multiple radar receiver RF front end beam switches being located ahead of the radar receiver's RF bandpass filter, and because the first such switch is at the radar antenna feed, re-engineering the radar receivers to incorporate an additional RF bandpass filter in front of the first beam switch will/would be technically challenging. The long term solution of re-engineering the radar receiver is complex and impractical, given the

⁵⁸ Never previously seen by the authors, at any rate, in four and a half decades of such EMC coexistence work.

age of the original design and the resources that would be required to retrofit a radar that is approaching obsolescence.

- 6) We describe, in this report, using readjustment of B41 5G channel bandwidths and center frequencies, at candidate interference locations, to bring the channel upper-frequency edges substantially lower in frequency and thus mitigate interference effects. Further mitigation may be achieved by turning-off (deactivating) high-frequency PRBs in 5G channels. Adjustment of antenna-to-antenna coupling between 5G base stations and ASR-9 antennas can also be implemented; this may include beam muting and beam re-direction.
- 7) Since the radar receiver beam switches are not being power-overloaded, the total aggregate of transmitted power on base station towers, from multiple communication transmitters, is not a factor in this coexistence challenge.

Our recommendations are:

- 1) U.S. Government agencies (FAA, NTIA, FCC) should work together to analyze ASR-9 radar stations and surrounding B41 5G base station deployments to determine where coordination zones are needed.
- 2) Wireless carriers need to be informed of these zones, and of the amounts of 5G-to-radar channel upper-frequency edge power decoupling that are needed in each zone.
- 3) The government and wireless carriers should use this report's technical information to formulate technical plans for preventing or mitigating this interference.
- 4) If any FCC licensee winners in B41 desire assistance with mitigation of possible interference into the FAA radar receivers *before* their 5G networks are deployed, NTIA can use simulation and modeling to develop physical separation and/or frequency separation plans if the licensees provide specific geographical locations of their proposed 5G base station transmitters and associated antenna heights and coverage directions.

6. LESSONS LEARNED

This study's lessons learned are:

- 1) More technical work needs to be performed, in advance of new-system field deployments, to understand possible coexistence challenges between new radio systems being introduced into a given spectrum band and legacy radio systems in the same, as well as in the adjacent, bands. This case study and [4] both serve as recent examples where this work has been needed. Ideally, this work should be done well in advance of new-system field deployments.
- 2) Paper studies may be inadequate for this purpose. The coexistence interference mechanism and challenge highlighted in this report would surely never have been identified, short of performing laboratory-grade system-to-system coexistence measurements and observations at a field or laboratory facility.

7. REFERENCES

- [1] Federal Communications Commission Report and Order: “Transforming the 2.5 GHz Band,” WT Docket No. 18-120, July 11, 2019; Doc. FCC-19-62A1.pdf <https://docs.fcc.gov/public/attachments/FCC-19-62A1.pdf>
- [2] Sanders, F., R. Sole, B. Bedford, D. Franc, and T. Pawlowitz, “Effects of RF Interference on Radar Receivers, Technical Report NTIA TR-06-444, U.S. Department of Commerce, National Telecommunications and Information Administration, Institute for Telecommunication Sciences, September 2006. <https://its.ntia.gov/publications/2481.aspx>
- [3] Achatz, R., “Examination of Radar Interference Protection Criteria Power Threshold Measurement Methods,” [Publication pending in Proc. of the 2025 National Radio Science Meeting, January 7–10, 2025, Boulder, Colorado].
- [4] Sanders, F. H., K. R. Calahan, G. A. Sanders, and S. M. Tran, “Measurements of 5G New Radio Spectral and Spatial Power Emissions for Radar Altimeter Interference Analysis,” Technical Report NTIA TR-22-562, U.S. Department of Commerce, National Telecommunications and Information Administration, Institute for Telecommunication Sciences, October 2022. <https://its.ntia.gov/publications/3289.aspx>
- [5] Sanders, F. and V. S. Lawrence, “Broadband Spectrum Survey at Denver, Colorado,” Technical Report NTIA TR-95-321, U.S. Department of Commerce, National Telecommunications and Information Administration, Institute for Telecommunication Sciences, September 1995. <https://its.ntia.gov/publications/2353.aspx>
- [6] Sanders, F., B. Ramsey, and V. S. Lawrence, “Broadband Spectrum Survey at San Diego, California,” Technical Report NTIA TR-97-334, U.S. Department of Commerce, National Telecommunications and Information Administration, Institute for Telecommunication Sciences, December 1996. <https://its.ntia.gov/publications/2366.aspx>
- [7] Sanders, F., B. Ramsey and V. S. Lawrence, “Broadband Spectrum Survey at Los Angeles, California,” Technical Report NTIA TR-97-336, U.S. Department of Commerce, National Telecommunications and Information Administration, Institute for Telecommunication Sciences, May 1997. <https://its.ntia.gov/publications/2368.aspx>
- [8] Sanders, F., B. Ramsey, and V. S. Lawrence, “Broadband Spectrum Survey at San Francisco, California May–June 1995,” Technical Report NTIA TR-99-367, U.S. Department of Commerce, National Telecommunications and Information Administration, Institute for Telecommunication Sciences, July 1999. <https://its.ntia.gov/publications/2398.aspx>
- [9] European Telecommunications Standards Institute (ETSI), Technical Specification for 5G NR Base Station (BS) Radio Transmission and Reception, 3GPP TS 38.104, Version 16.4.0, Release 16, August 2020, ETSI Reference RTS/TSGR-0438104vG40. https://www.etsi.org/deliver/etsi_ts/138100_138199/138104/16.04.00_60/ts_138104v160400p.pdf

ACKNOWLEDGEMENTS

The work described in this report has required intensive ongoing support from several organizations and many individuals. Here we recognize these organizations and people, and their significant contributions.

This work was funded by two ITS projects, Salaries and Entitlements (S&E) RSMS Operations (for assessment and analysis of the overall coexistence problem); and 5G FACTS (for measurements and analysis of the 5G base station emission spectra). Both projects pre-dated this effort's advent. That circumstance allowed us to respond swiftly and effectively to this problem when we were first connected to it by the FAA in November 2023. Setting up a new project, with new funding, solely for this effort would likely have taken about a year (based on previous experience), while the problem itself would have festered and gone unresolved. This effort's timeliness exemplifies the advantages of having such projects in place on an ongoing basis, to accommodate high-priority problems and contingencies on a fast-reaction timeline when they arise.

Furthermore, the ITS physical resources that were critically important to moving this work forward, including the RSMS vehicle and hardware, the RSMS software, our analysis software, and all of the equipment (plus custom data-collection and analysis software) that was shipped to, and used at, the FAA Atlantic City Technical Center, were procured and developed with RSMS Development Project funding. No such system could have been developed on an ad hoc basis on some newly implemented, special-purpose project. Reinforcing the fact that the only way these sorts of efforts can be funded, implemented and completed is with such pre-existing, in-house, long-term sustainability projects.

This entire effort depended on a close working relationship between the U.S. Government (specifically the FAA and NTIA) with the wireless carrier, T-Mobile US Inc. As was the case for having pre-existing government projects that has already laid the physical groundwork and that could fund the work of NTIA and FAA, the value of having an engineer-to-engineer relationship with T-Mobile people cannot be over-stated. The timeline alone that would have been required for setting up a formal project with T-Mobile, never mind the possible additional costs of such a project, would likely have crippled any response in any reasonable timeframe.

T-Mobile in turn leveraged a strong working relationship with their two 5G OEM radio manufacturers and vendors to get CoWs deployed and operating at the TMRQZ for controlled-condition emission spectrum measurements. The cost of making those assets available, transporting them, setting them up, operating them, and then taking them down again, was significant. We deeply appreciate that expenditure of resources, in terms of coordination, staffing and funding, with T-Mobile. The TMRQZ measurements were critically important, as described in this report. But they would not have happened if T-Mobile had not supported them.

We especially wish to thank Mr. Dan Wilson and Mr. Gary Cook of T-Mobile for all of the hard work that they did on this project. This included, but was not limited to, participating as full partners in the initial diagnosis of the likely problem; developing the test plans for the Atlantic City work and the Table Mountain work; consulting on data analysis and interpretation; and pre-

publication review of this report. It is difficult to imagine any comparable situation with any other private sector wireless carrier that could have worked out better.

Within the FAA, we deeply thank all of the technical staff who participated in development of the work and test plans; who participated in the measurements in Atlantic City and at Table Mountain; who diagnosed the performance of the waveguide beam switch and the STC section in the lab at Atlantic City; and who participated in writing this report and reviewing it, pre-publication, for technical accuracy and completeness.

Specifically, this work could not have been completed without the crucial contributions of the following FAA staffers. Mr. Oscar Valle-Colon provided extensive administrative and technical support and cover for us, within the FAA and with T-Mobile. Mr. David Harris partnered with us in all of the Atlantic City work; and at the Table Mountain measurements (including coordinating with the local ASR-9 stations); and doggedly undertook to help convince us of the issues with the beam switch and the STC section; and brought his deep and insightful, in-the-field understanding of interference problems at ASR-9 locations such as Richmond and Charlotte into the project, augmenting our overall understanding and prodding us to work harder to understand exactly what was happening in the reported interference cases. Mr. Sampson Afuape provided important technical and administrative support for our work. Last but not least, Mr. Aatman Nandi provided key technical support and administrative coordination for our Atlantic City work; was the first to exclaim, “it looks like Fourier spreading of a carrier wave,” when we ran our first bench test; and oversaw the subsequent bench tests of the beam switch and STC components at the Atlantic City facility.

The authors would also like to acknowledge Mr. Nickolas LaSorte and Mr. James Yoe with NTIA. Nick developed the coordination zone software used to perform the analysis presented in Section 4. James assisted with the September testing at the Atlantic City FAA facility.

APPENDIX A: ASR-9 RECEIVER CHARACTERISTICS MEASUREMENTS

As part of this case study, we here provide measurements of key receiver EMC characteristics of the ASR-9. These sorts of measurements are fundamental in EMC and coexistence studies. These measurements were performed by NTIA engineers at FAA engineering facilities in years prior to the immediate interference issues of 2023. They were retained and catalogued for future support of these sorts of projects.

Figure A-1 shows the radar's measured receiver RF bandpass filter response. It was performed by sweeping a carrier wave through the filter. This particular filter was tuned to 2700 MHz center frequency; in operational ASR-9s, these filters are individually tuned for the radars' frequencies. As noted in the main body of the report, these filters decouple the receiver LNAs from strong off-channel signals, but they are located downstream in the receivers from the waveguide beam-switch and STC stages.

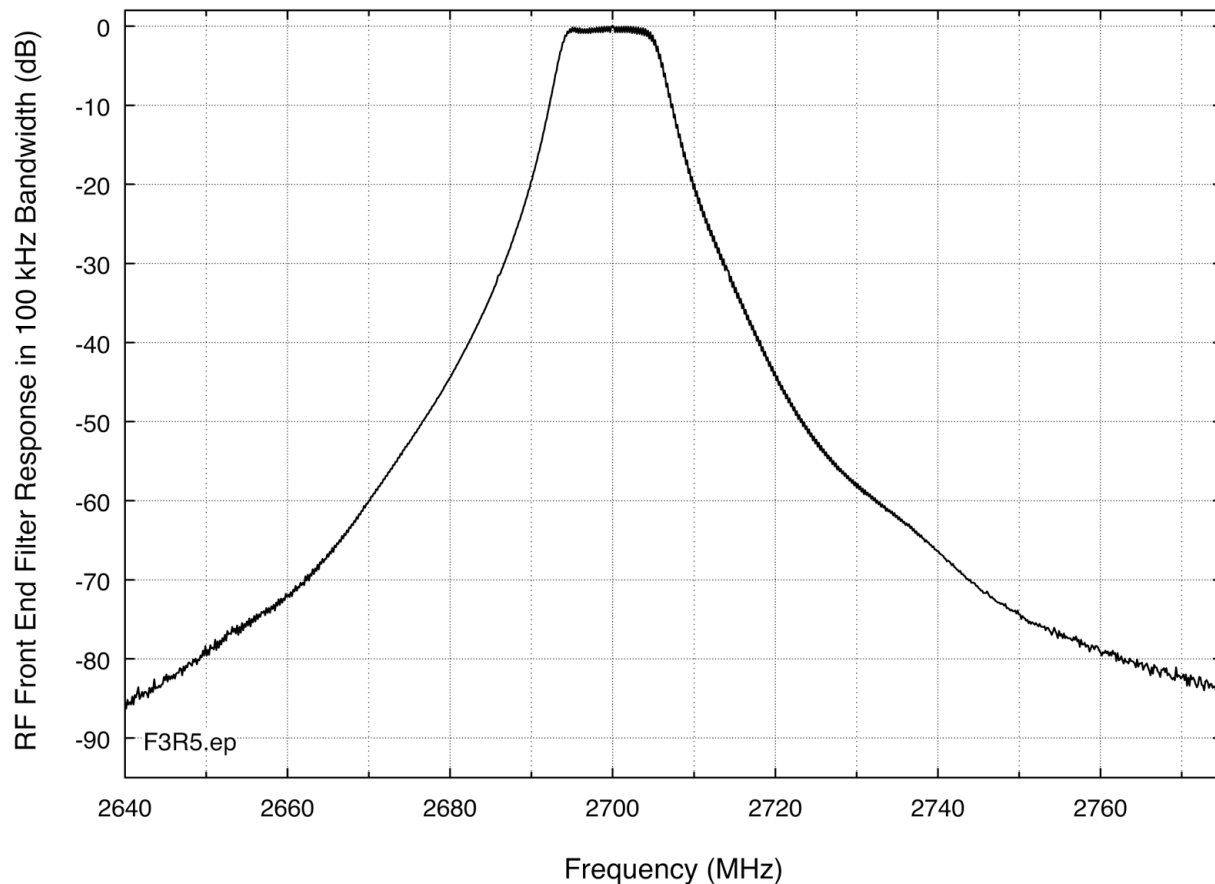


Figure A-1. Measured bandpass filter response for the ASR-9 receiver.

Figure A-2 shows the measured frequency-domain response curve for the ASR-9 receiver IF stage.

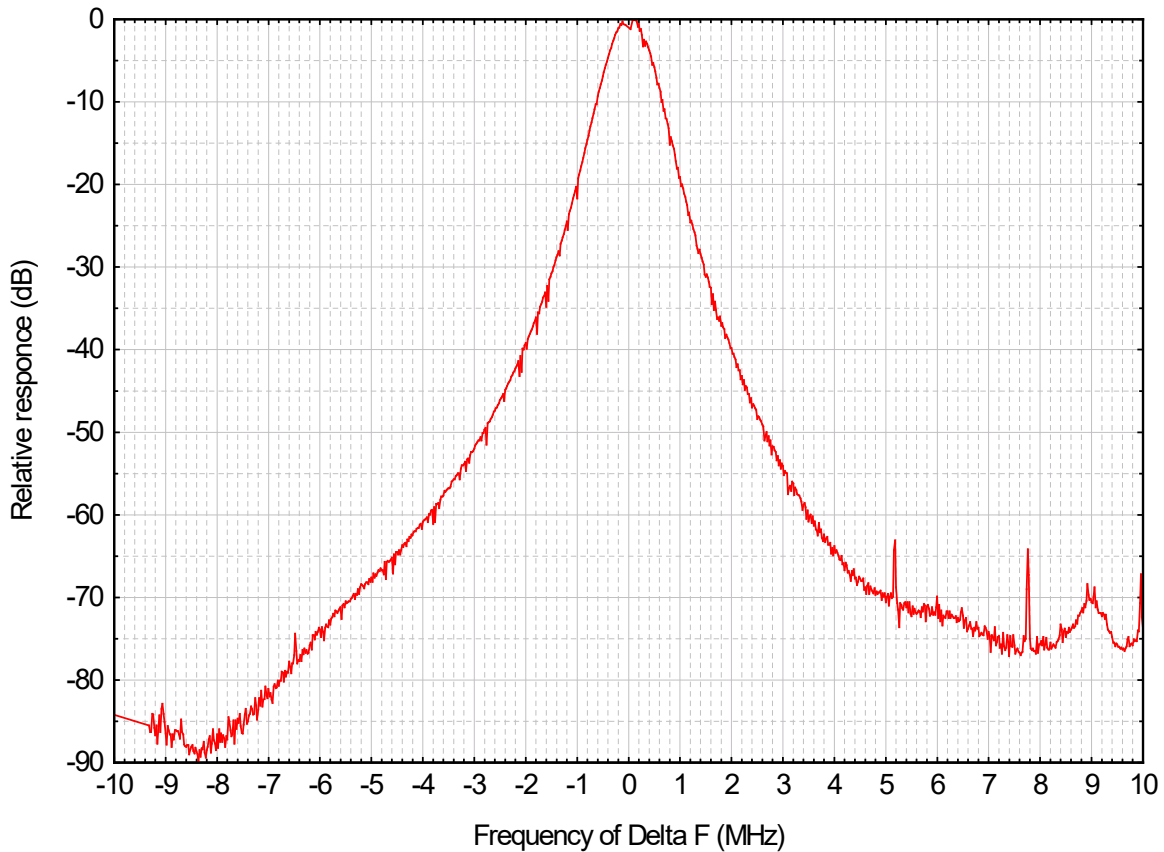


Figure A-2. Measured frequency-domain response of the ASR-9 receiver IF stage. The IF is about 720 kHz wide at its 3-dB points.

Figure A-3 shows the ASR-9 antenna beam patterns, although not measured by NTIA. The reflector is illuminated by two horns, one placed above the other, to produce paired (upper and lower) coverage beams in space.

The radar rotates mechanically 360 degrees every 4.75 seconds in the horizontal plane, with a 3 dB angular beamwidth of about 1 degree.

In the vertical plane, the radar's beam coverage has a standard cosecant-squared (CSC^2) pattern. The vertical beamwidth is broad for maximal air surveillance. The radar sites sometimes employ a slight uptilt to raise the vertical beam's lower edge above local ground clutter.

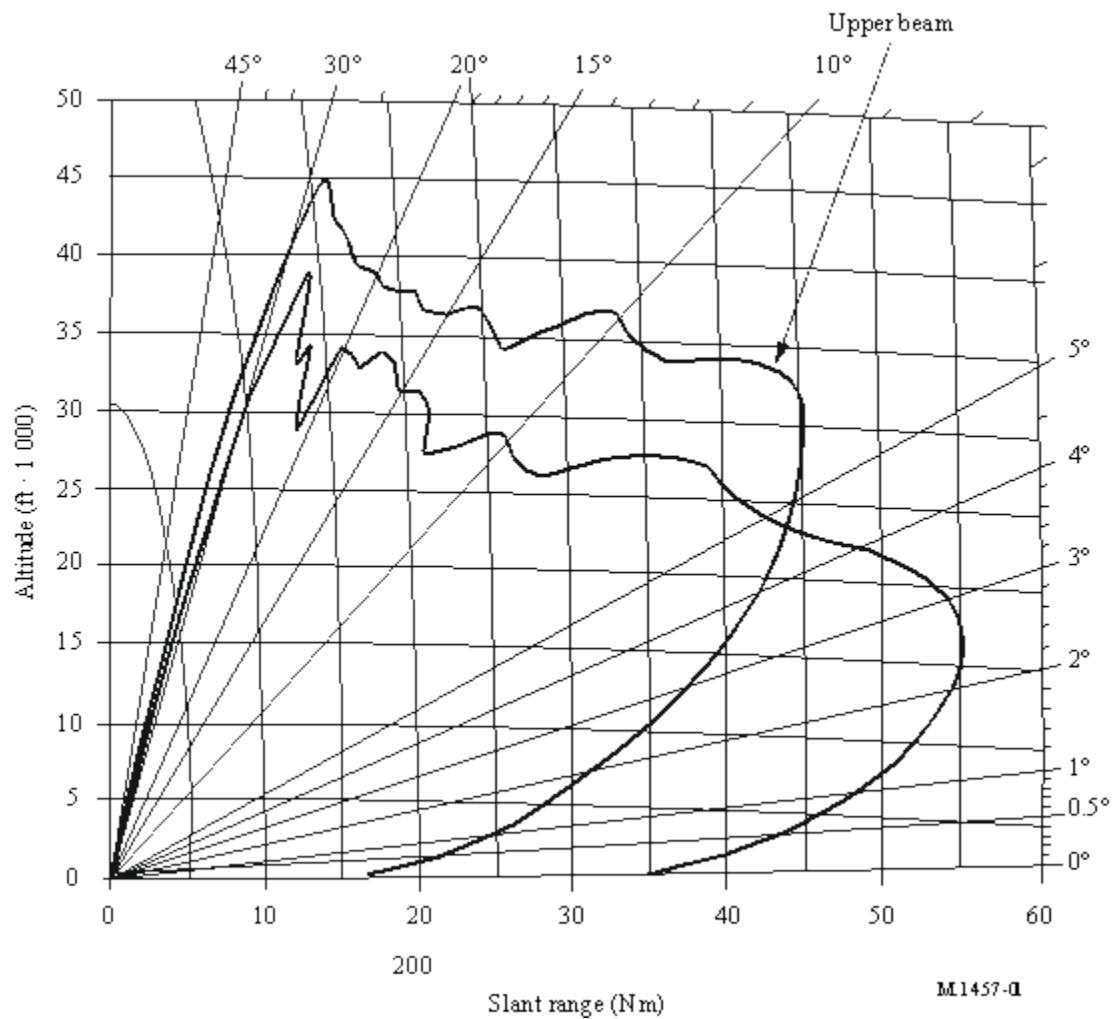


Figure A-3. ASR-9 vertical-plane antenna patterns and beam coverage.

APPENDIX B: TEST PLAN FOR ASR-9 RECEIVER-RESPONSE CHARACTERIZATION MEASUREMENTS AT THE FAA TECHNICAL CENTER

Finalized March 25, 2024, prior to measurements of April 2-4, 2024.

B.1 Background

Airport surveillance radars, model 9 (ASR-9) operated by the FAA in the 2700–2900 MHz band are experiencing interference effects at 10-30 locations around the U.S. The wedge-shaped interference effects in the radar stations’ receivers, called strobes, include individual drop-out zones on plan position indicator (PPI) scopes; multiple strobes (“rising sun” patterns); and ring-around interference, depending on the individual station.

At least some of the interference is associated with Band 41 Channels (2590–2690 MHz) transmissions from 4G and 5G Massive MIMO Radio (here called simply “Band 41” or “B41”) base stations. The wireless carrier that operates these base stations uses two models, one built by Original Equipment Manufacturer (OEM) A and the other built by OEM B. 5G Radio-A model’s emissions were measured in an ad hoc effort, with wide dynamic range across the 2700–2900 MHz band, at a field location in Boulder on January 9, 2024. Controlled-condition measurements of 5G Radio Model A and B spectra, with wide dynamic range, are planned for completion with cells on wheels (CoWs) at the Table Mountain Radio Quiet Zone north of Boulder in late April and early May.

Based on preliminary technical analysis, the interference mechanism of the B41 5G transmitters to the ASR receiver is thought to more likely be coupling of unwanted 5G base station emissions on frequencies above 2700 MHz, co-channel to ASR-9 receivers. However, this is not yet definitive; we need to complete the work in this plan to obtain certainty about the mechanism.

This Test Plan describes proposed tasking for work at the FAA’s Atlantic City Technical Center. The needs are:

- 1) Determine whether the B41 5G base station transmitter interference is due to co-channel power from 5G base station unwanted emissions above 2700 MHz on ASR-9 tuned frequencies
- 2) Further confirm that either:
 - a) RF front end overload of the radar receiver’s beam switches, STC stage, and LNAs is *not* occurring
 - b) Or, if such overload is occurring, determine in which radar receiver components and at what 5G signal-input overload-power threshold levels
- 3) Gather additional, needed data on the interference (I) to receiver internal noise (N) ratio (I/N) in the ASR-9 receivers

Accomplishment of this tasking will allow the conversation about B41 5G base station transmitter interference mechanisms and levels in ASR-9 receivers, between the government and

the wireless carrier, to move forward into agreement of the mechanism and levels of the interference. This will in turn allow mitigation options to be explored among the FAA; the wireless carrier; NTIA; and the FCC.

Note that similar measurements and analyses were performed on a National Weather Service NEXRAD weather radar receiver in 2011 when it was found that some WiMAX transmitter unwanted emissions were causing co-channel interference to NEXRAD weather radars in the 2700–2900 MHz band. The results were published in NTIA Technical Report TR-13-490, “Analysis and Resolution of RF Interference to Radars Operating in the Band 2700–2900 MHz from Broadband Communication Transmitters,” Oct. 2012.

<https://its.ntia.gov/publications/2684.aspx>

B.2 Objectives

- 1) Identify and measure licensed (intentionally radiated) B41 5G base station transmitter spectrum emissions through the RF path at locations within the radar receiver that are ahead of the radar receiver’s bandpass filter. Obtain the 5G spectrum across the B41 2590–2690 MHz intentional-radiation frequency range.
- 2) Using a supplemental measurement bandpass or bandstop RF filter that rejects power at frequencies below 2700 MHz, continue the measurement of that same 5G transmitter emission in the radar receiver, as far as possible into the frequency range above 2700 MHz.
- 3) Measure those same B41 5G unwanted emissions (above 2700 MHz) in the ASR-9 receiver at a location in the receiver chain after the LNA output (but still at the radar receiver’s RF, not IF, frequencies).
 - a) Show that the radar receiver’s built-in RF bandpass filter (ahead of the receiver’s LNA stage) is in fact blocking the 5G wireless intentionally radiated emissions at frequencies below 2700 MHz.
 - b) Show that RF front end overload characteristics, as described below in this Test Plan, are absent from the LNA’s time domain output.
- 4) Measure the 5G unwanted emissions in the ASR-9 receiver’s IF stage.
 - a) Identify the 5G unwanted emissions’ I/N power levels within the radar receiver’s IF stage, on the radar’s tuned frequency.

B.3 Approach

B.3.1 Data Collection

The data will be collected from a spectrum analyzer or signal analyzer, such as an E4440A, PXA or EXA model, on a laptop computer for subsequent distribution and analysis. NTIA/ITS can do this with a laptop brought from Boulder, Colorado.

Both frequency-domain (spectrum) and time domain data will be collected from the analyzer. NTIA/ITS will ship an appropriate analyzer (probably an Agilent E4440A) from Boulder to the Technical Center.

B.3.2 FAA, NTIA/ITS, and NTIA/OSM Participation

The FAA is in charge of the measurement at the Technical Center. NTIA/ITS and NTIA/OSM will provide additional subject matter expertise as deemed appropriate by the FAA. Some NTIA engineers will attend the measurement in person.

FAA Technical Center staff engineers and technicians will be requested to make access available to the ASR-9 radar receiver per descriptions provided below. Access will be needed at five points (minimum) within the ASR-9 receiver, as described below.

One of these access points within the radar receiver will be a tap point where the radar receiver's IF stage can be monitored and recorded.⁵⁹

B.3.3 Classification of the Work

The measurement data/results will be Controlled Unclassified Information (CUI) unless otherwise designated. The work outputs (collected data) will be shared between the FAA and NTIA. Further distribution will be considered to the FCC; the Department of Defense (DoD); and in possible future technical reports describing the work and its results.

B.4 Data Collection Measurements

B.4.1 Measurement Location

As noted above, the measurements will be performed at the FAA Atlantic City Technical Center's ASR-9 facility. Figure B-1 shows the locations of the ASR-9 radar and two locations of B41 5G base station transmitters in the 2.5 GHz band that are known to be causing strobes on the ppi of the radar.

⁵⁹ Based on past experience, a solder connection needs to be made on a radar receiver circuit card to accomplish this. NTIA/ITS and NTIA/OSM have done this before, and the FAA's Technical Center personnel are likewise conversant with this temporary modification. A spare (swap-out) card will likely be modified at the Technical Center.

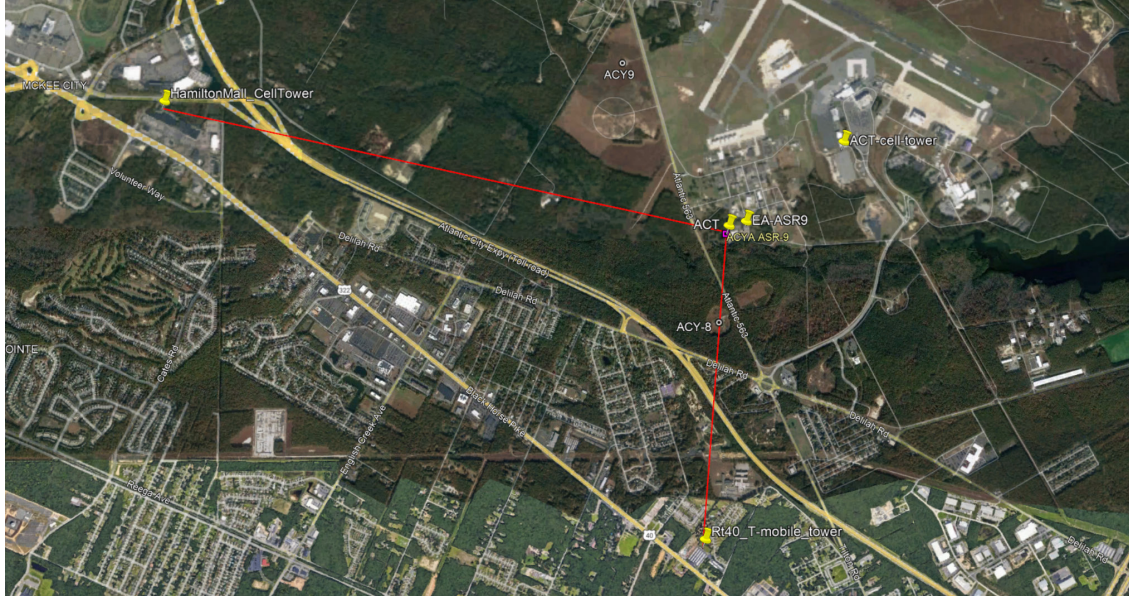


Figure B-1. Locations of the ASR-9 and two local 5G base station transmitters.

B.4.2 Measurement Procedures

Successful completion of the measurements hinges on accomplishing the following goals:

- 1) Identification and acquisition of a B41 (2590-2690 MHz) 5G base station signal by the radar receiver.⁶⁰
- 2) Measurement of that 5G base station's emissions at about five points (discussed in more detail below) within the ASR-9 receiver.
- 3) Both the radar's weather path and target-processing path will be examined. Behaviors of sensitivity time control (STC) and beam-control switches will be evaluated.

For reference, a simplified block diagram schematic of the ASR-9 radar receiver is shown in Figure B-2.

⁶⁰ At the Technical Center (Atlantic City) ASR-9, the 5G signal of interest is about 30 dB lower than in the ASR-9 at Richmond, Virginia. We will work with the wireless carrier to try to get even more power directed toward the Technical Center ASR-9, for these measurements.

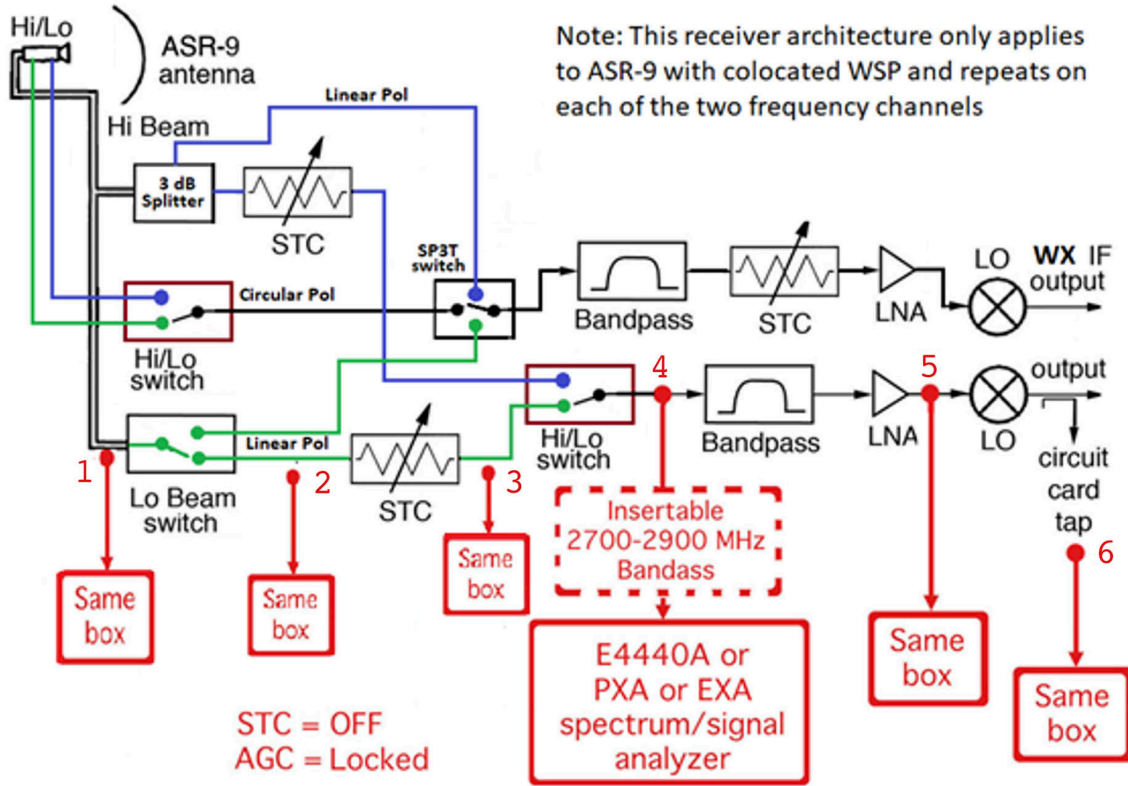


Figure B-2. Simplified block diagram schematic of the ASR-9/WSP receiver.

Requested access points (APs) within the radar receiver are as indicated in Figure B-2. The measurements will be performed in the order shown in the flow diagram of Figure B-3.

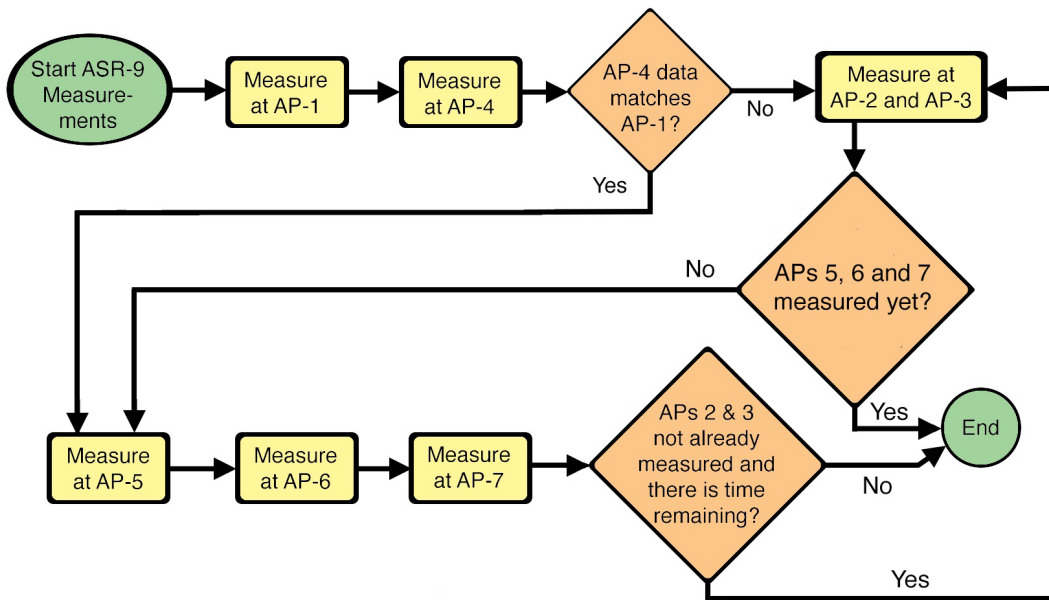


Figure B-3. Flow diagram for the order in which the measurements will be performed.

B.4.3 Note on Controlling the 5G Signal Input-Power to the Radar Receiver.

For all measurements, the power level of the 5G input signal to the radar receiver will be controlled by moving the radar antenna from on-axis to the 5G base station azimuth (where maximum 5G power will couple into the ASR-9 receiver) to the radar's antenna sidelobes/backlobes (likely at least as much as 20 dB of achievable reduction and perhaps as much as 30 dB of reduction in the 5G signal power level).

B.4.4 Note on Determining ASR-9 Receiver Overload-Power Thresholds, If Overload is Observed

If we do see any non-linear behaviors in the ASR-9 receiver chain (i.e., in antenna beam switches; the STC stage; or the LNA), then we will pivot the ASR-9 antenna sideways (off-axis from the 5G base station) enough to eliminate the effect. We will note the exact level of reduced 5G signal input power at the antenna, where the behavior ceases. That input-power reduction step will show us exactly what the 5G signal overload input-power threshold is, for whatever receiver component(s) might show overload behavior.

B.5 ASR-9 Receiver Measurements

B.5.1 Measurement 1: Locating and Documenting a Receivable Band-B41 (2590–2690 MHz) 5G Base Station Coupling into the ASR-9 at Highest Available Power (AP-1 tap point)⁶¹

Note that if the data from test points AP-1 and AP-4 are equivalent and the traces overlap with little or NO differences, then data collections at point AP-2 and AP-3 are not needed.

Goal: In this first-step measurement, we identify, and lock the ASR-9 antenna onto, a (or the) local, high-power 5G base station transmitted signal (Figure B-4).

⁶¹ As mentioned above, the identified 5G tower at the Technical Center (TC) transmits 60 MHz bandwidth; based on data provided by the wireless carrier, the ASR-9 is located in the null between two of its sectors (outside of the 3-dB point of each sector). Nevertheless, the sensor still reflects the strobe, which may indicate the out-of-band emission (OOBE) issue. Even when the ASR-9 center frequency is 65 MHz away from 5G fundamental, and the ASR-9 is outside the 3-dB azimuthal point of the undesired 5G signal, the sensor still reflects strobe on the tower direction. This might also explain why the fundamental 5G signal was captured at the TC ASR-9 with a power level of -45 dBm/244KHz, around 30 dB less than the Richmond (RIC) ASR-9, (-15 dBm/293 KHz) at a similar distance (1.0 nm and 1.25 nm). Differences in path losses due to distance should be around 2dB. Our contact at the wireless carrier states that they can configure the antenna to point directly to our sensor. We are unsure if they can increase the BW due to license limitations, but this is conditioned to presence at the ASR-9 site.

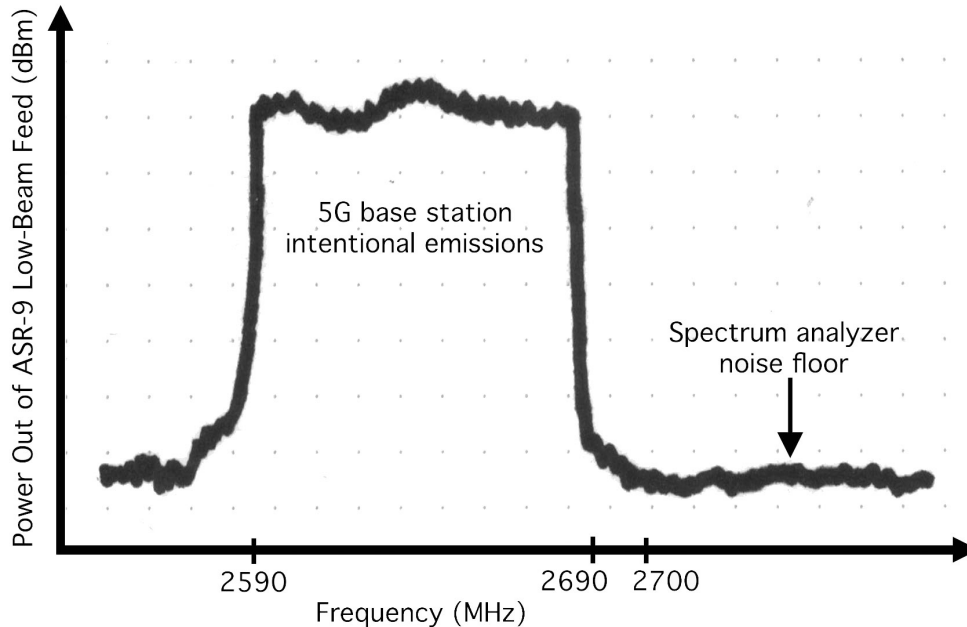


Figure B-4. Sketch of what we expect to see in the first measurement.

B.5.1.1 Measurement 1: Test Equipment and Radar Settings Needed

- **Spectrum analyzer** (E4440A planned).
- **Laptop computer** to record spectrum analyzer data traces (or at least a way to image the analyzer's datB-display screen).
- **Handie-Talkies** (best option) or cell phones (if needed) to talk between the ASR-9 antenna and the ASR-9 receiver room downstairs.
- **Connection of analyzer to Access Point 1 in Figure B-3** (see above)
- **Radar Transmitter = OFF** on both channels (Both Channels A & B into dummy load).
- **ASR-9 antenna beam selection = Lower Beam**
- **ASR-9 Receiver STC = OFF** (although for this one it shouldn't matter if STC is ON)
- **ASR-9 Receiver AGC = Locked to a fixed value** (although for this one it shouldn't matter if AGC floats)

B.5.1.2 Measurement 1: Test Procedure:

Step 01.

With the spectrum analyzer connected at AP-1, let the radar's antenna rotate repeatedly while the spectrum analyzer (or signal analyzer) operates as follows:

- $f_{\text{start}} = 2500 \text{ MHz}$
- $f_{\text{stop}} = 2700 \text{ MHz}$
- Resolution Bandwidth = 1 MHz

- Video Bandwidth = 3 MHz
- Points per Trace = 401
- Sweep Time = Analyzer's self-selecting default for the above settings
- Detector = Positive Peak
- First Trace Display Mode = Maximum Hold on Data Trace 01 (like, yellow)
- Second Trace Display Mode = Clear-Write on Data Trace 02 (like, blue or whatever)
- RF attenuation = 0 dB
- RF preamplifier = OFF
- Reference Level = Default with 0 dB attenuation running and no preamp

If there is any appropriate B41 Band (2590–2690 MHz) 5G base station being received, it will fill in on the spectrum analyzer's screen display as the radar repeatedly rotates past the station's azimuth. It will look like a spectrum chunk filled-in across 2590–2690 MHz.

We'd like to get the 5G signal at something like 40 dB to 60 dB above the analyzer's noise floor.⁶² This is because the more 5G signal we get in its licensed, intentional-emission B41 Band Channel, the higher its unwanted emissions will be at frequencies above 2700 MHz, interfering with the radar on the radar's lower tuned frequency.

IF the 5G signal is saturating the analyzer (the analyzer's built-in OVLD warning comes on, for instance), then invoke 10 dB of RF attenuation to get out of saturation/overload. Keep adding attenuation (20 dB of RF attenuation, etc.) until overload condition stops.

Step 02. Get the Approximate 5G Base Station Azimuth

Note the approximate azimuth where the 5G station is hitting at maximum power. Do this by watching the Clear-Write analyzer Trace 02 against the maximum-hold Trace 01 as the radar antenna rotates through the 5G station's azimuth.

Step 03. Align the ASR-9 Antenna on the Exact 5G Azimuth

Stop the ASR-9 antenna rotation. Go up on top, to the antenna, free it to move manually, and rotate the radar antenna by hand through the 5G station.

Communicate on the handie-talkies between the roof and the downstairs to establish the exact azimuth where the 5G base station's signal maximizes. (Clear-write Trace 02 hits on maximum-hold Trace 01.)⁶³

Note that exact ASR-9 antenna azimuth relative to true north,⁶⁴ for the record.

⁶² With a 10 dB noise figure, the spectrum analyzer's noise floor will be -94 dBm in a 1 MHz bandwidth, with positive peak detection selected.

⁶³ Or, connect directly to the low-beam H port on the roof.

⁶⁴ The antenna's reference might be to magnetic north; we'll correct for that if needed.

Lock down or stabilize the ASR-9 antenna’s pointing azimuth so that it doesn’t (can’t) drift or windsock off that azimuth. (That one can really get you, if it drifts later and you didn’t know it. ☹)

Verify one more time that, with the ASR-9 antenna locked down, the Clear-Write Trace 02 is hitting the same level as maximum-hold Trace 01.

Step 04. Record the Analyzer’s Maximum-Hold Trace 01 with the laptop (or whatever you have available).

This recording documents the peak-detected power/megahertz that is coupling into the radar’s bandpass filter and LNA on its front end, through the radar antenna on the low-beam selection. This is super-important for later data analysis.

B.5.2 Measurement 2: Measure and Document the 5G Unwanted Emission Power Levels in the Spectrum Above 2700 MHz (AP-1 tap point)

Goal: We measure and document how much 5G base station unwanted-emission power is hitting the radar receiver on frequencies *within* the radar’s operational band, *above 2700 MHz*, at the input to the beam switch (see Figure B-5).

This measurement picks up the 5G base station emission spectrum where the previous measurement left off. The measurement is performed at the input to the radar’s tuned-channel bandpass filter.

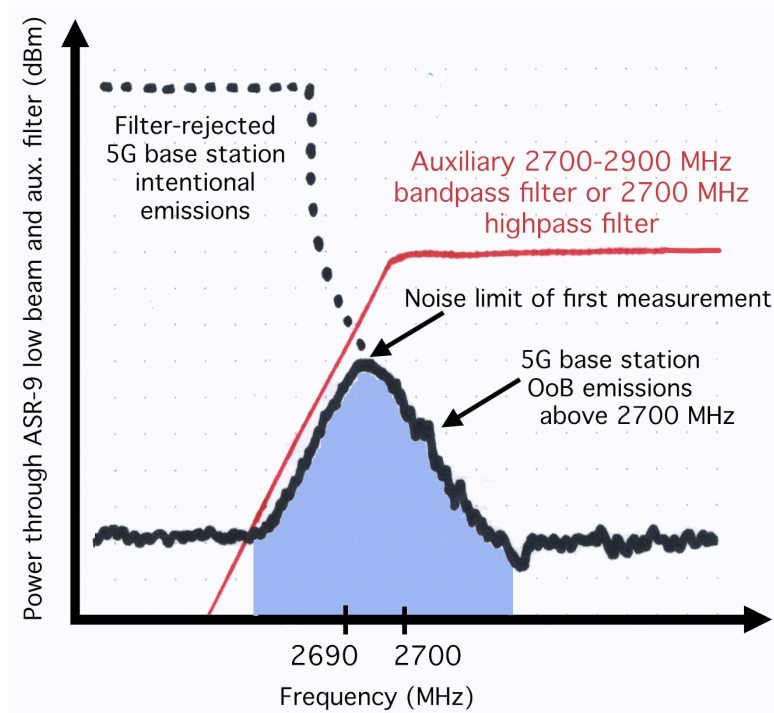


Figure B-5. Sketch of what we expect to see in the second measurement (at AP-1).

The trick here is to reject the 5G base station's intentional (on-tuned) power as much as possible, with a band-stop or band-reject filter, so that the preamp in the signal analyzer can be used.

B.5.2.1 Measurement 2: Test Equipment and Radar Settings Needed

- **Spectrum analyzer** (E4440A planned).
- **Laptop computer** to record spectrum analyzer data traces (or at least a way to image the analyzer's datB-display screen).
- **Connection of analyzer to Access Point 1 in Figure B-3** (see above)
- **New Item⁶⁵** = 2700–2900 MHz bandpass filter
 - or a 2700 MHz highpass filter
 - or a 2500–2700 MHz band-stop filter
 - or a tunable bandpass filter adjusted (tuned) to reduce (cut off) power below 2700 MHz
- **Radar Transmitter = OFF** on both channels (Both Channels A & B into dummy load).
- **ASR-9 Antenna Beam Selection** = Lower Beam
- **ASR-9 Antenna Azimuth** = Pointing to 5G base station on the locked-down azimuth from the previous tasking.
- **ASR-9 Receiver STC** = OFF (although for this one it shouldn't matter if STC is ON)
- **ASR-9 Receiver AGC** = Locked to a fixed value (although for this one it shouldn't matter if AGC floats)

B.5.2.2 Measurement 2: Test Procedure

Step 01. Insert the auxiliary RF filter into the line between Access Point 1 (see Figure B-3) and the analyzer.

Tip: You might want to either screw the filter directly onto AP-1 on the radar receiver, or else screw it onto the analyzer's input port, to avoid adding another RF cable to your setup.

Step 02. Configure the spectrum/signal analyzer:

With the spectrum analyzer connected at AP-1; the auxiliary RF filter installed in front of the analyzer's input; and the ASR-9 antenna locked on the 5G base station; configure the spectrum analyzer (or signal analyzer) as follows:

- $f_{\text{start}} = 2680$ MHz
- $f_{\text{stop}} = 2880$ MHz
- Resolution Bandwidth = 1 MHz
- Video Bandwidth = 3 MHz
- Points per Trace = 401
- Sweep Time = Analyzer's self-selecting default for the above settings

⁶⁵ The FAA has 2700–2900 MHz bandpass and 2500–2700 MHz bandstop filters. ITS used a tunable bandpass with 150 MHz bandwidth, tuned to reject input power below 2700 MHz.

- Detector = Positive Peak
- First Trace Display Mode = Maximum Hold on Data Trace 01 (like, yellow)
- Second Trace Display Mode = Clear-Write on Data Trace 02 (like, blue or whatever)
- RF attenuation = 0 dB
- **RF preamplifier = ON**
- Reference Level = Default with 0 dB attenuation running and analyzer preamp = ON.
- **Step 03.** Let the 5G signal fill-in on the analyzer's maximum-hold Trace 01 while you watch it in real-time on the analyzer's Clear-Write Trace 02.

Be patient while it fills in on the maximum-hold trace.

IF the signal above 2700 MHz is saturating (OVLN warning comes on, or the data trace hits the top of the analyzer's display, etc.), then **try turning the preamp to OFF**.

IF the overload condition continues, add 10 dB of RF attenuation in the analyzer's input.

Remember, we want to achieve maximum measurement dynamic range here, short of overloading the analyzer.

Step 04. Record the 5G unwanted emissions (above 2700 MHz) that are hitting the radar receiver's own RF front end, ahead of the radar's beam switch input.

This is important, because it will be used to determine whether non-linear behavior is occurring within the beam switch.

B.5.3 Measurement 3: Measure and Document the 5G Unwanted Emission Power Levels in the Spectrum Above 2700 MHz (AP-2 tap point)

Goal: We measure and document how much 5G base station unwanted-emission power is hitting the radar receiver on frequencies *within* the radar's operational band, *above 2700 MHz*, between the beam switch output and the STC input (see Figure B-2).

This measurement picks up the 5G base station emission spectrum where the previous measurement left off: now *after* the beam switch and *before* the STC stage. Comparison to what was measured at the beam switch input indicates whether any non-linear effects have occurred within the beam switch (see Figure B-6).

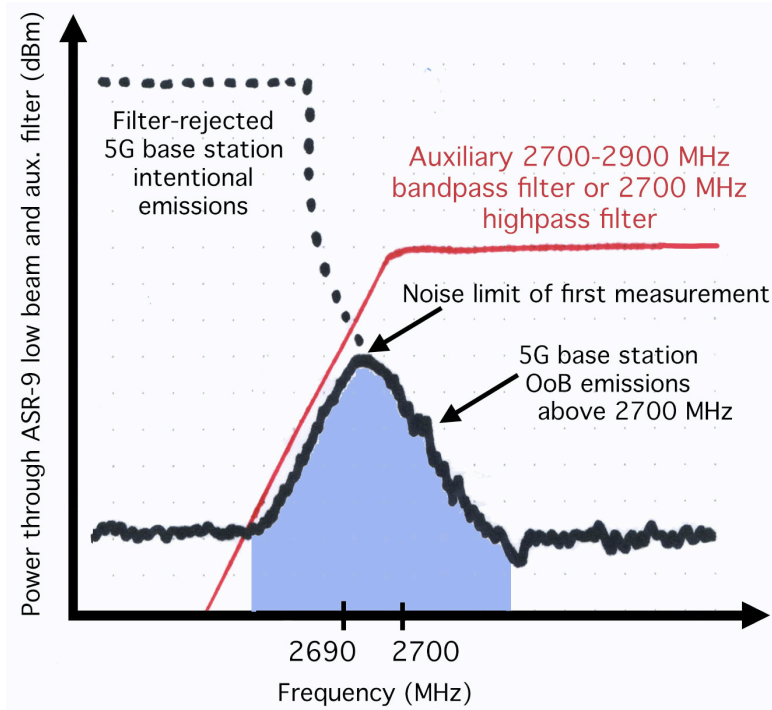


Figure B-6. Sketch of what we expect to see in the measurement at AP-2.

The trick here is to reject the 5G base station's intentional (on-tuned) power as much as possible, with a band-stop or band-reject filter, so that the preamp in the signal analyzer can be used.

B.5.3.1 Measurement 3: Test Equipment and Radar Settings Needed

- **Spectrum analyzer** (E4440A planned).
- **Laptop computer** to record spectrum analyzer data traces (or at least a way to image the analyzer's datB-display screen).
- **Connection of analyzer to Access Point 2 in Figure B-3** (see above).
- **Filter(s) needed:**
 - 2700–2900 MHz bandpass filter
 - or a 2700 MHz highpass filter
 - or a 2500–2700 MHz band-stop filter
 - or a tunable bandpass filter adjusted (tuned) to reduce (cut off) power below 2700 MHz
- **Radar Transmitter = OFF** on both channels (Both Channels A & B into dummy load).
- **ASR-9 Antenna Beam Selection = Lower Beam**
- **ASR-9 Antenna Azimuth = Pointing to 5G base station on the locked-down azimuth from the previous tasking.**
- **ASR-9 Receiver STC = OFF** (although for this one it shouldn't matter if STC is ON)
- **ASR-9 Receiver AGC = Locked to a fixed value** (although for this one it shouldn't matter if AGC floats)

B.5.3.2 Measurement 3: Test Procedure:

Step 01. Insert the auxiliary RF filter into the line between Access Point (AP) 1 (see Figure B-3) and the analyzer.

Tip: You might want to either screw the filter directly onto AP-1 on the radar receiver, or else screw it onto the analyzer's input port, to avoid adding another RF cable to your setup.

Step 02. Configure the spectrum/signal analyzer:

With the spectrum analyzer connected at AP-1; the auxiliary RF filter installed in front of the analyzer's input; and the ASR-9 antenna locked on the 5G base station; configure the spectrum analyzer (or signal analyzer) as follows:

- $f_{\text{start}} = 2680$ MHz
- $f_{\text{stop}} = 2880$ MHz
- Resolution Bandwidth = 1 MHz
- Video Bandwidth = 3 MHz
- Points per Trace = 401
- Sweep Time = Analyzer's self-selecting default for the above settings
- Detector = Positive Peak
- First Trace Display Mode = Maximum Hold on Data Trace 01 (like, yellow)
- Second Trace Display Mode = Clear-Write on Data Trace 02 (like, blue or whatever)
- RF attenuation = 0 dB
- **RF preamplifier = ON**
- Reference Level = Default with 0 dB attenuation running and analyzer preamp = ON.

Step 03. Let the 5G signal fill-in on the analyzer's maximum-hold Trace 01 while you watch it in real-time on the analyzer's Clear-Write Trace 02.

Be patient while it fills in on the maximum-hold trace.

IF the signal above 2700 MHz is saturating (OVLD warning comes on, or the data trace hits the top of the analyzer's display, etc.), then **try turning the preamp to OFF**.

IF the overload condition continues, add 10 dB of RF attenuation in the analyzer's input.

Remember, we want to achieve maximum measurement dynamic range here, short of overloading the analyzer.

Step 04. Record the 5G unwanted emissions (above 2700 MHz) that are hitting the radar receiver's own RF front end, ahead of the radar's beam switch input.

This is important, because it will be used to determine whether non-linear behavior has occurred within the lo-beam switch, via comparison with what was measured at the switch's input.

B.5.4 Measurement 4: Measure and Document the 5G Unwanted Emission Power Levels in the Spectrum Above 2700 MHz (AP-3 tap point)

Goal: We measure and document how much 5G base station unwanted-emission power is hitting the radar receiver on frequencies *within* the radar’s operational band, *above 2700 MHz*, at the STC output (see Figure B-3).

This measurement picks up the 5G base station emission spectrum where the previous measurement left off: now *after* the STC switch. Comparison to what was measured at the STC input indicates whether any non-linear effects have occurred within the STC stage (see Figure B-7).

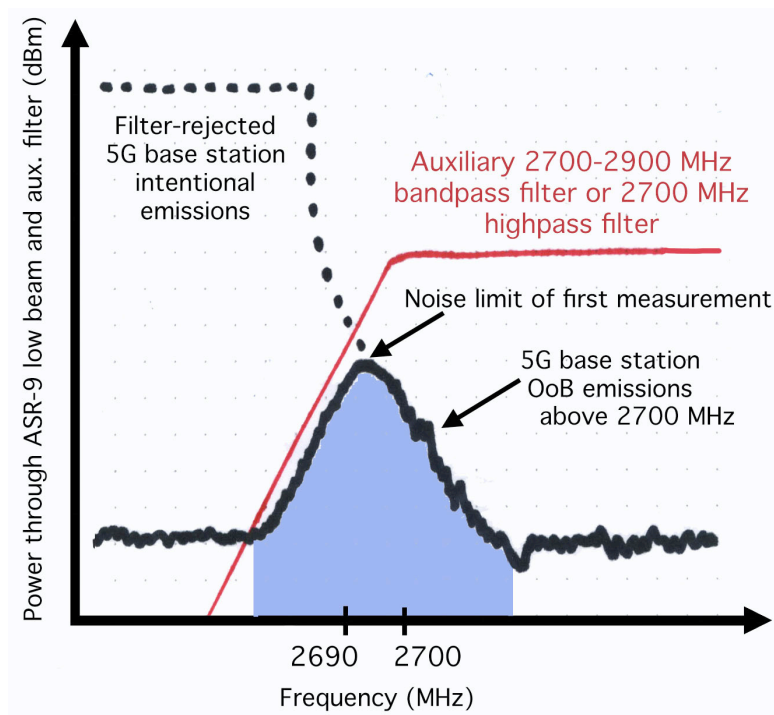


Figure B-7. Sketch of what we expect to see in the measurement at AP-3.

The trick here is to reject the 5G base station’s intentional (on-tuned) power as much as possible, with a band-stop or band-reject filter, so that the preamp in the signal analyzer can be used.

B.5.4.1 Measurement 4: Test Equipment and Radar Settings Needed

- **Spectrum analyzer** (E4440A planned).
- **Laptop computer** to record spectrum analyzer data traces (or at least a way to image the analyzer’s datB-display screen).
- **Connection of analyzer to Access Point 3 in Figure B-3** (see above).
- **Filter(s) needed:**
 - 2700–2900 MHz bandpass filter
 - or a 2700 MHz highpass filter

- or a 2500–2700 MHz band-stop filter
- or a tunable bandpass filter adjusted (tuned) to reduce (cut off) power below 2700 MHz
- **Radar Transmitter = OFF** on both channels (Both Channels A & B into dummy load).
- **ASR-9 Antenna Beam Selection = Lower Beam**
- **ASR-9 Antenna Azimuth = Pointing to 5G base station on the locked-down azimuth from the previous tasking.**
- **ASR-9 Receiver STC = OFF** (although for this one it shouldn't matter if STC is ON)
- **ASR-9 Receiver AGC = Locked to a fixed value** (although for this one it shouldn't matter if AGC floats)

B.5.4.2 Measurement 4: Test Procedure:

Step 01. Insert the auxiliary RF filter into the line between Access Point 1 (see Figure B-3) and the analyzer.

Tip: You might want to either screw the filter directly onto AP-1 on the radar receiver, or else screw it onto the analyzer's input port, to avoid adding another RF cable to your setup.

Step 02. Configure the spectrum/signal analyzer:

With the spectrum analyzer connected at AP-1; the auxiliary RF filter installed in front of the analyzer's input; and the ASR-9 antenna locked on the 5G base station; configure the spectrum analyzer (or signal analyzer) as follows:

- $f_{\text{start}} = 2680$ MHz
- $f_{\text{stop}} = 2880$ MHz
- Resolution Bandwidth = 1 MHz
- Video Bandwidth = 3 MHz
- Points per Trace = 401
- Sweep Time = Analyzer's self-selecting default for the above settings
- Detector = Positive Peak
- First Trace Display Mode = Maximum Hold on Data Trace 01 (like, yellow)
- Second Trace Display Mode = Clear-Write on Data Trace 02 (like, blue or whatever)
- RF attenuation = 0 dB
- **RF preamplifier = ON**
- Reference Level = Default with 0 dB attenuation running and analyzer preamp = ON.

Step 03. Let the 5G signal fill-in on the analyzer's maximum-hold Trace 01 while you watch it in real-time on the analyzer's Clear-Write Trace 02.

Be patient while it fills in on the maximum-hold trace.

IF the signal above 2700 MHz is saturating (OVLD warning comes on, or the data trace hits the top of the analyzer's display, etc.), then **try turning the preamp to OFF**.

IF the overload condition continues, add 10 dB of RF attenuation in the analyzer’s input.

Remember, we want to achieve maximum measurement dynamic range here, short of overloading the analyzer.

Step 04. Record the 5G unwanted emissions (above 2700 MHz) that are hitting the radar receiver’s own RF front end, ahead of the radar’s beam switch input.

This is important, because it will be used to determine whether non-linear behavior has occurred within the STC stage, via comparison with what was measured at the STC-stage input.

B.5.5 Measurement 5: Measure and Document the 5G Unwanted Emission Power Levels in the Spectrum Above 2700 MHz (AP-4 tap point)

Goal: We measure and document how much 5G base station unwanted-emission power is hitting the radar receiver on frequencies *within* the radar’s operational band, *above 2700 MHz*. This measurement picks up the 5G base station emission spectrum where the previous measurement left off. The measurement is performed at the output from the radar’s Hi-Lo beam switch and the input to its bandpass filter (see Figure B-8).

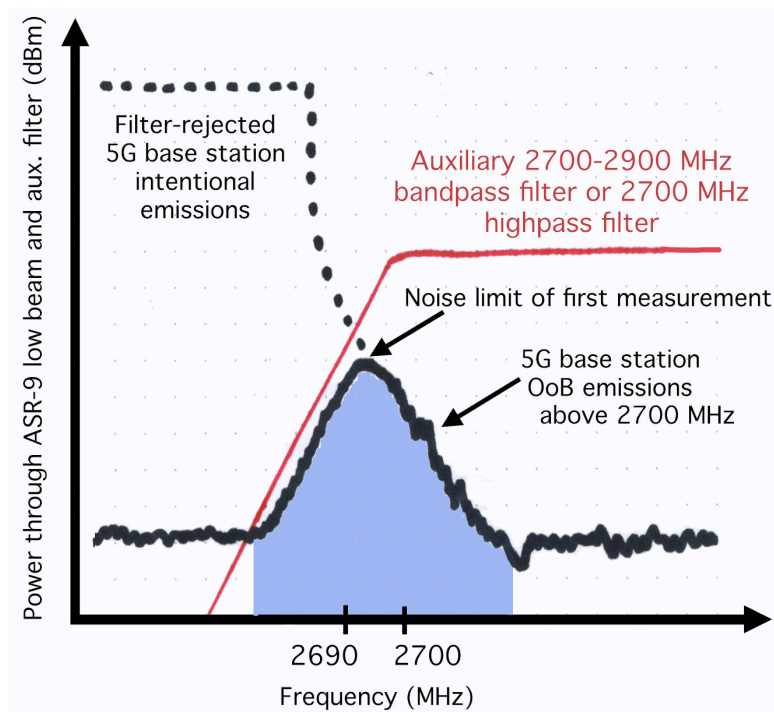


Figure B-8. Sketch of what we expect to see in the measurement at AP-5.

The trick here is to reject the 5G base station’s intentional (on-tuned) power as much as possible, with a band-stop or band-reject filter, so that the preamp in the signal analyzer can be used.

B.5.5.1 Measurement 5: Test Equipment and Radar Settings Needed

- **Spectrum analyzer** (E4440A planned).
- **Laptop computer** to record spectrum analyzer data traces (or at least a way to image the analyzer's datB-display screen).
- **Connection of analyzer to Access Point 4 in Figure B-3** (see above)
 - 2700–2900 MHz bandpass filter
 - or a 2700 MHz highpass filter
 - or a 2500–2700 MHz band-stop filter
 - or a tunable bandpass filter adjusted (tuned) to reduce (cut off) power below 2700 MHz.
- **Radar Transmitter = OFF** on both channels (Both Channels A & B into dummy load).
- **ASR-9 Antenna Beam Selection = Lower Beam**
- **ASR-9 Antenna Azimuth = Pointing to 5G base station on the locked-down azimuth from the previous tasking.**
- **ASR-9 Receiver STC = OFF** (although for this one it shouldn't matter if STC is ON)
- **ASR-9 Receiver AGC = Locked to a fixed value** (although for this one it shouldn't matter if AGC floats)

B.5.5.2 Measurement 5: Test Procedure:

Step 01. Insert the auxiliary RF filter into the line between AP-1 (see Figure B-3) and the analyzer.

Tip: You might want to either screw the filter directly onto AP-1 on the radar receiver, or else screw it onto the analyzer's input port, to avoid adding another RF cable to your setup.

Step 02. Configure the spectrum/signal analyzer:

With the spectrum analyzer connected at AP-1; the auxiliary RF filter installed in front of the analyzer's input; and the ASR-9 antenna locked on the 5G base station; configure the spectrum analyzer (or signal analyzer) as follows:

- $f_{\text{start}} = 2680$ MHz
- $f_{\text{stop}} = 2880$ MHz
- Resolution Bandwidth = 1 MHz
- Video Bandwidth = 3 MHz
- Points per Trace = 401
- Sweep Time = Analyzer's self-selecting default for the above settings
- Detector = Positive Peak
- First Trace Display Mode = Maximum Hold on Data Trace 01 (like, yellow)
- Second Trace Display Mode = Clear-Write on Data Trace 02 (like, blue or whatever)
- RF attenuation = 0 dB
- **RF preamplifier = ON**
- Reference Level = Default with 0 dB attenuation running and analyzer preamp = ON.

Step 03. Let the 5G signal fill-in on the analyzer's maximum-hold Trace 01 while you watch it in real-time on the analyzer's Clear-Write Trace 02.

Be patient while it fills in on the maximum-hold trace.

IF the signal above 2700 MHz is saturating (OVLD warning comes on, or the data trace hits the top of the analyzer's display, etc.), then **try turning the preamp to OFF**.

IF the overload condition continues, add 10 dB of RF attenuation in the analyzer's input.

Remember, we want to achieve maximum measurement dynamic range here, short of overloading the analyzer.

Step 04. Record the 5G unwanted emissions (above 2700 MHz) that are hitting the radar receiver's own RF front end, ahead of the radar's Channel bandpass filter.

This is super-important, because it shows what the radar receiver's bandpass filter needs to be knocking down ahead of the ASR-9 receiver's low noise amplifier (LNA).

B.5.6 Measurement 6: Measure and Document the Radar Receiver's Bandpass Filter plus LNA Output (and Check for Radar Receiver LNA Overload) (AP-5 tap point)

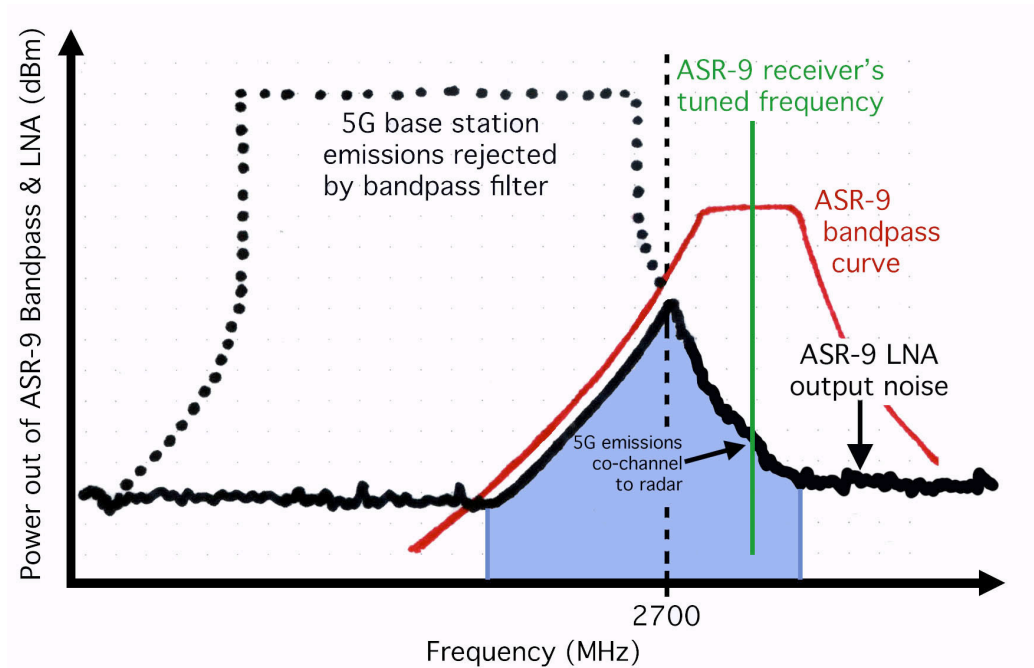


Figure B-9. Sketch of what we expect to see in the measurement at AP-5, frequency domain.

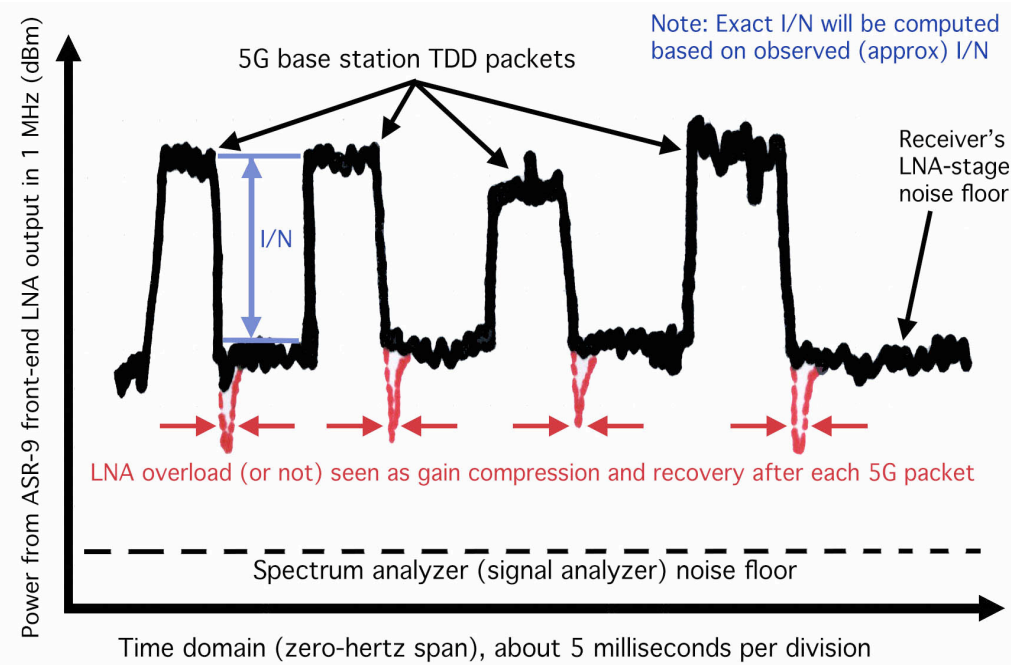


Figure B-10. Sketch of what we expect to see in the measurement at AP-5, time domain.

Goal: a) measure and document how much 5G base station unwanted-emission power is emerging from the radar receiver's LNA output; and b) prove (or disprove) the presence of LNA overload from the 5G base station's TDD data packets (see Figure B-3).

What we expect to see will be the 5G unwanted emission spectrum from the previous measurement, but with a roll-down (roll-off) superimposed on it by the radar receiver's Channel bandpass filter (see Figures B-10 and B-11).

Seeing that feature will verify that the bandpass filter is doing its job of preventing the LNA from seeing the 5G intentional emissions below 2700 MHz, at least not at power levels that would overload the LNA (see Figures B-10 and B-11).

B.5.6.1 Measurement 6: Test Equipment and Radar Settings Needed

Spectrum analyzer (E4440A planned).

- **Laptop computer** to record spectrum analyzer data traces (or at least a way to image the analyzer's datB-display screen).
- **New Item = 50-ohm RF screw-on load, or a screw-on 10-dB or 20-dB RF attenuator.**
- **Connection of analyzer to Access Point 5 (post-LNA) in Figure B-3** (see above)
- **Radar Transmitter = OFF** on both channels (Both Channels A & B into dummy load).
- **ASR-9 Antenna Beam Selection = Lower Beam**
- **ASR-9 Antenna Azimuth = Pointing to 5G base station on the locked-down azimuth from the previous tasking.**

- **ASR-9 Receiver STC** = OFF (although for this one it shouldn't matter if STC is ON)
- **ASR-9 Receiver AGC** = Locked to a fixed value (although for this one it shouldn't matter if AGC floats)

B.5.6.2 Measurement 6: Test Procedure:

Step 01. Connect the spectrum analyzer (signal analyzer) to Access Point 2 (see Figure B-3) and the analyzer. This is the LNA output.

Step 02. Configure the spectrum/signal analyzer:

With the spectrum analyzer connected at AP-2; and the ASR-9 antenna locked on the 5G base station; configure the spectrum analyzer (or signal analyzer) as follows:

- $f_{\text{start}} = 2650 \text{ MHz}$
- $f_{\text{stop}} = 2850 \text{ MHz}$
- Resolution Bandwidth = 1 MHz
- Video Bandwidth = 3 MHz
- Points per Trace = 401
- Sweep Time = Analyzer's self-selecting default for the above settings
- Detector = Positive Peak
- First Trace Display Mode = Maximum Hold on Data Trace 01 (like, yellow)
- Second Trace Display Mode = Clear-Write on Data Trace 02 (like, blue or whatever)
- RF attenuation = 0 dB
- **RF preamplifier = OFF**
- Reference Level = Default with 0 dB attenuation running and analyzer preamp = ON.

Step 03. Make sure the LNA output noise (excess noise) is exceeding the spectrum analyzer's internal noise (!)

This step is super-important. We must KNOW that the noise level being displayed on the spectrum analyzer's display is that of the radar receiver's own LNA, and NOT of the spectrum analyzer itself.

Do this as follows:

- 1) First, disconnect the RF line from the analyzer's input.
- 2) Next, screw on the 50-ohm load (or a 10-dB or 20-dB RF attenuator).
- 3) Look at the analyzer's displayed noise floor. **Record it on Trace 03** (after maximum-holding it for a few moments, enough for the trace to maximize itself.)
- 4) *This is the analyzer's internal noise floor.*

- 5) Next, remove the 50-ohm load (or attenuator) and re-connect the analyzer to the radar receiver's LNA output.

What we want to see here is at least a corresponding 10-dB or 20-dB increase in the displayed noise floor of the analyzer.

When we see that happen, we know that our displayed noise level is that of the radar receiver's LNA, and NOT of the analyzer itself!

The tricky part is, the 5G base station is running through the analyzer's display simultaneously, while we're trying to see the LNA's own noise output.

We may have to improvise a little at this point, to isolate the LNA's noise from the 5G signal. Possible ways forward are:

- 6) Try to read the LNA's noise in-between the 5G base station's TDD packets in the time domain. Downside is, it's a little hard to always know when the 5G TDD is off between packets.
- 7) Try to temporarily disconnect the LNA's input from the radar receiver's signal path, to temporarily knock out the 5G input. Downside is, this might not really be practical with the radar receiver. We don't want to depressurize the waveguide unnecessarily.
- 8) Try switching to High Beam on the radar antenna and see if that reduces the 5G signal enough.
- 9) Temporarily swing the ASR-9's antenna's azimuth off the 5G base station, to get rid of the 5G signal while we're looking at the LNA's baseline noise output.

Our recommendation is, try (3) first.

But if that doesn't give enough isolation, then go to (4): Swing the radar antenna temporarily of the 5G base station. I'm always a little nervous about that, because I hate to lose the 5G signal once it's in the bag. But the best way to definitely see the LNA's output noise and verify that it's exceeding our analyzer's noise by at least 10 dB, is probably to swing the antenna off the 5G.

Anyway, back to the LNA noise: **IF we don't see the LNA output noise at least 10 B above the analyzer's own internal noise, we'll need to turn the analyzer's preamp to ON.** After switching the analyzer's preamp to ON, temporarily disconnect the analyzer again, and verify that the LNA's output noise is now overdriving the analyzer's internal noise by 10 dB or more.

At this point, we should know that the LNA's output is overdriving the analyzer's internal noise by 10 dB or more.

Record the analyzer's displayed noise level showing the LNA noise output.

Step 04. Document the 5G unwanted emission levels above 2700 MHz in the spectrum (frequency) domain.

With the 5G signal coming through the LNA, and knowing that the limiting noise level on the display of the LNA and not of the analyzer, let the maximum-hold trace fill in.

Step 05. Record the 5G output of the radar receiver's LNA with the laptop.

Step 06. Look at the 5G unwanted emissions from the LNA output in the time domain.

Set the spectrum analyzer 's Trace 01 to Clear-Write.

Set the analyzer's other traces to "Blank" so that we don't see them.

Set the analyzer's Trace 01 to "Zero Hertz Span" so that we are running in the time domain.

Set the Zero Span tuned frequency to the radar's lower-frequency Channel Frequency (2725 MHz for the Atlantic City ASR-9).

Set the analyzer trace to the maximum available number of bins (data points). This improves the time resolution of the measurement.

Set the sweep time to, say, 100 milliseconds, so that we can see the 5G signal's TDD behavior, with data packets turning on and off. (Sweep time might need adjustment depending on the 5G signal's TDD behavior.)

Step 07. Look for any signs of LNA overload in the time domain.

The way this works is, overloading LNAs will gain-compress when they are hit (overloaded), and then they relax back to their normal output-noise level when the interference goes away.

With 5G, the overload (if there's any occurring) will gain compress the LNA during the TDD data packets. But when each packet terminates, the LNA will recover.

So, we look for a compressed (reduced) LNA output power level which rapidly recovers (zooms back upward) as soon as each TDD packet ends. In practice, this will/would look like little down vertical spikes at the end of each TDD data packet, followed by fast recovery back to the LNA's nominal noise level.

Step 08. In any event, **record the LNA's output in the time domain**, with the 5G TDD data packets turning on and off. If we see overload signs, so be it.

If we -don't- see the overload compression and recovery in the LNA's output in the time domain, then this confirms that no LNA overload is occurring.

Which confirms that the interference problem is the 5G unwanted emissions that are occurring on the radar receiver's tuned frequency, co-channel with the radar receiver.

B.5.7 Measurement 7: Measure and Document the 5G Signal in the Radar Receiver's IF Stage (AP-6 tap point)

Goal: We measure and document how much 5G base station unwanted-emission power is present in the ASR-9 receiver's IF stage. And we prove (or disprove) the presence of any LNA front end overload in the ASR-9 receiver (see Figure B-11).

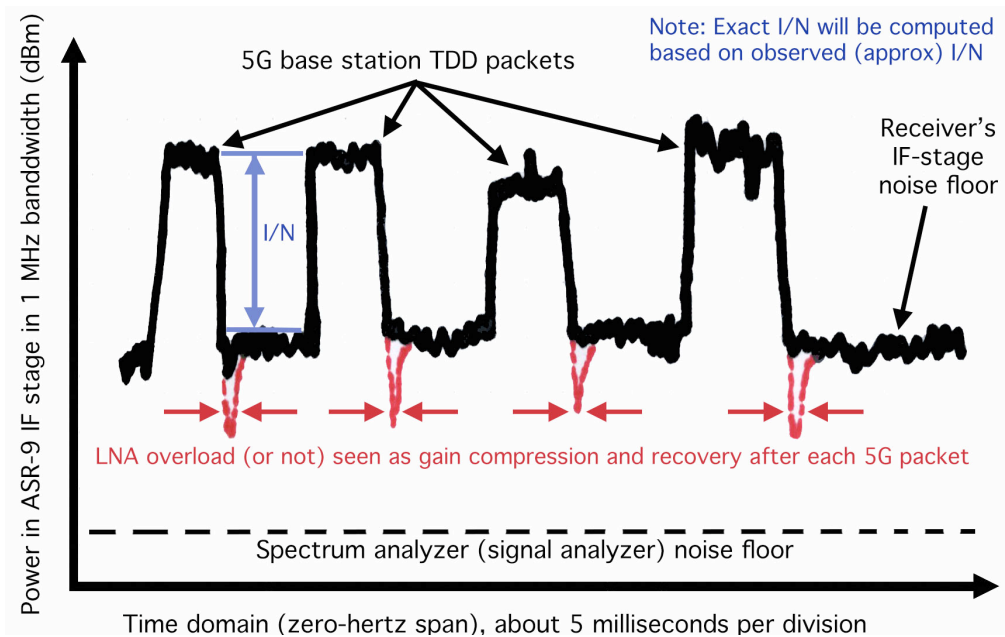


Figure B-11. What we expect to see (or not see) in the final measurement, at AP-6.

This power is measured and documented relative to the IF stage's own noise level. Thus, we get a measurement of the interference-to-noise ratio (I/N) of the 5G unwanted emissions in the receiver's IF stage.

The measured I/N can be compared to the incident power at the RF stages, to confirm analyses. This is important for interference-effects analyses, and it tells us how much more isolation is needed from the 5G power, to get to the FAA's I/N criterion of [e.g., about -10 dB? Or what?].

B.5.7.1 Measurement 7: Test Equipment and Radar Settings Needed:

- **Spectrum analyzer** (E4440A planned).
- **Laptop computer** to record spectrum analyzer data traces (or at least a way to image the analyzer's datB-display screen).
- **Connection of analyzer to Access Point 3, the receiver's IF Stage, in Figure B-3** (see above)
- **Radar Transmitter = OFF** on both channels (Both Channels A & B into dummy load).
- **ASR-9 Antenna Beam Selection = Lower Beam**
- **ASR-9 Antenna Azimuth = Pointing to 5G base station on the locked-down azimuth from the previous tasking.**

- **ASR-9 Receiver STC** = OFF
- **ASR-9 Receiver AGC** = Locked to a fixed value.

Step 01. Connect the spectrum analyzer (signal analyzer) to Access Point 3 (see Figure B-2) and the analyzer. This is the IF stage output.

Sub-Steps for Connecting to the IF Stage Output/Monitoring Access Point:

- The FAA Atlantic City Technical Center ASR-9 technical personnel are already familiar with the method for implementing IF-stage monitoring. TP01 is soldered to TP10 on a designated circuit card. That line is run out of the equipment rack to a BNC connector, with the connector grounded to the rack's TP03 point.
- The FAA Technical Center will endeavor to perform this mod, and verify that it is working, on a spare ASR-9 circuit card prior to commencement of the measurements in mid-March.

Step 02. Configure the spectrum/signal analyzer:

With the spectrum analyzer connected at AP-3 via the modified circuit card; and the ASR-9 antenna locked on the 5G base station; configure the spectrum analyzer (or signal analyzer) as follows:

- $f_{\text{start}} = 28 \text{ MHz}$
- $f_{\text{stop}} = 34 \text{ MHz}$
- Frequency Span = 6 MHz.
- Resolution Bandwidth = 1 MHz (it is IMPORTANT that this bandwidth slightly exceeds the radar receiver's IF bandwidth of about 720 kHz!!)
- Video Bandwidth = 3 MHz
- Points per Trace = 1001
- Sweep Time = Analyzer's self-selecting default for the above settings
- Detector = Positive Peak
- First Trace Display Mode = Maximum Hold on Data Trace 01 (like, yellow)
- Second Trace Display Mode = Clear-Write on Data Trace 02 (like, blue or whatever)
- RF attenuation = 0 dB
- **RF preamplifier = OFF**
- Reference Level = Default with 0 dB attenuation running and analyzer preamp = ON.

Step 03. Record the IF-stage sweep from the spectrum analyzer.

Step 04. Disconnect the IF output from the analyzer. Confirm that we see a 10-dB drop (or more) with the IF stage disconnected. This shows that we are seeing the radar IF-stage noise on the analyzer display, and not the analyzer's own internal noise.

Step 05. Record the noise with the IF disconnected.

Step 06. Re-connect the analyzer to the IF stage output.

Step 07. Center the analyzer on the radar receiver's center-frequency (31.07 MHz, we believe); go to zero-hertz span so we are seeing the IF stage output in the time domain.

Step 08. Record the zero-hertz, time domain sweep of the IF stage output.

Step 08. Go to the maximum number of sweep points available on the analyzer, to maximize time resolution.

Step 09. Adjust the time domain on the analyzer to, like, 100 milliseconds, to allow us to see the 5G data packets running TDD, on and off, every 5 milliseconds or so. But this may need adjustment depending on the 5G signal's time domain behavior.

This step gives us our I/N measurement! Land Ho at Last!

Step 10. Record that trace.

Step 11. Look in detail in the time domain to confirm that we are not seeing any LNA gain compression and recovery at the end of each TDD packet.

Step 12. Record some of those details, to show no gain compression of the LNA.

B.6 Data Analysis

All NTIA/ITS raw data will be collected in .mat formatted electronic files and converted to ascii format.

The collected data will be analyzed and provided to the FAA, the wireless carrier, and OSM by ITS.

Those organizations will be able to use the emission spectrum to establish, for any given amount of frequency separation; physical distance separation; and antenna tilt-angle geometries; the amount of additional unwanted emissions reduction (if any) needed above 2700 MHz to achieve any given target I/N level (e.g., -6 dB; -9 dB; -12 dB) in ASR-9 receivers.

B.7 Timeline

The data collection at the FAA Technical Center, Atlantic City, is scheduled for the week of April 1–5, 2024. ITS and OSM (Geoff Sanders, Frank Sanders, and Brian Nelson) will be at the Technical Center April 2–4, 2024.

APPENDIX C: TEST PLAN FOR ASR-9 RECEIVER-RESPONSE CHARACTERIZATION MEASUREMENTS AT THE FAA TECHNICAL CENTER

The objective of these tests is to characterize the effects of interference on the ASR-9 receiver system. The tests will take place at the FAA Atlantic City Tech Center in Egg Harbor, New Jersey on September 24 and 25, 2024.

C.1 Bench Testing

The purpose of the bench tests is to characterize the effects of interfering waveforms on the waveguide beam switch and sensitivity time control (STC) components of the ASR-9 receiver chain. To conduct these tests a Keysight vector signal generator (MXG) will be used to inject interference signals into the components while an Agilent E4440 spectrum analyzer is used to measure the response. All waveforms except the swept CW are created with a 200 Ms/sec sample rate.

Four interference waveforms will be tested:

- Swept CW (2590–2690 MHz, 1 MHz steps)
- 100 MHz wide additive white Gaussian noise (AWGN)
- Time gated 100 MHz wide AWGN (On 3.5 ms/Off 1.5 ms)
- Simulated 100 MHz wide 5G signal (256 QAM, PN-11, On 3.7 ms/Off 1.3 ms)

Three component configurations will be tested with each of these waveforms:

- Beam switch only
- STC only
- Beam switch and STC together

The spectrum analyzer will be configured with the following settings:

- $f_{\text{start}} = 2500$ MHz
- $f_{\text{stop}} = 2700$ MHz
- Resolution Bandwidth = 1 MHz
- Video Bandwidth = 3 MHz
- Points per Trace = 401
- Sweep Time = Analyzer's self-selecting default for the above settings
- Detector = Positive Peak
- First Trace Display Mode = Maximum Hold on Data Trace 01 (like, yellow)
- Second Trace Display Mode = Clear-Write on Data Trace 02 (like, blue or whatever)
- RF attenuation = 0 dB
- RF preamplifier = OFF
- Reference Level = Default with 0 dB attenuation running and no preamp

For each of the twelve total test conditions the power output of the MXG will be adjusted until third-order effects can be observed. This power level will be recorded, and the spectrum analyzer traces will be saved. Two more spectrum analyzer traces will be produced and saved with the MXG power adjusted [10 dB?] higher and lower. It is expected that nothing will be observed in the ASR band at the lower power level. With twelve test conditions tested at three power levels there will be a total of 36 bench test measurements. Each test should only take 5-10 minutes, so it should be possible to complete all these tests on September 24.

C.2 ASR-9 IF Characterization

During the previous testing at the FAA Tech Center, measurements were planned at all the test points, shown in red, in Figure C-1. One test point that was never measured was the IF output shown in Figure C-1 as Test Point 6. On September 25, measurements will be taken at this test point.

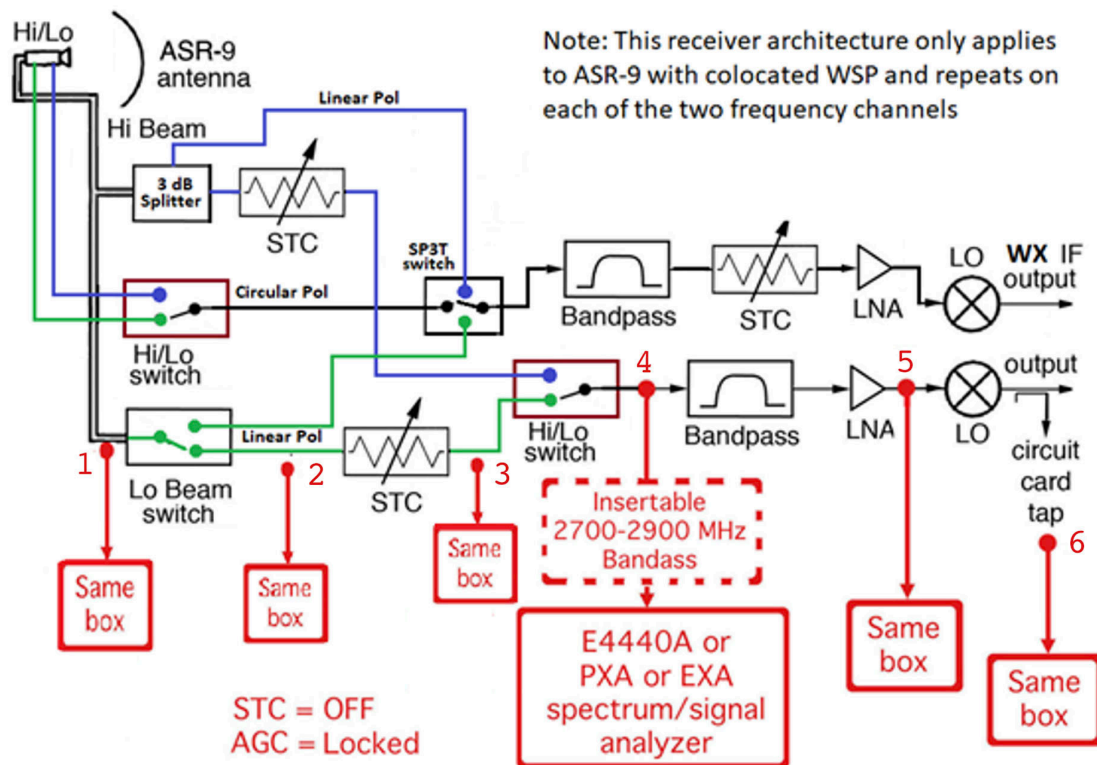


Figure C-1. Simplified block diagram of the ASR-9 with test points shown in red.

The spectrum analyzer will be connected to test point 6 and tests will be conducted using the same local 5G signal that was present for the testing in April 2024. Measurements will be conducted under 4 conditions:

- Normal configuration
- STC bypassed and beam switch active
- Beam switch bypassed and STC bypassed

- Both beam switch and STC bypassed

The spectrum analyzer will be configured with the following settings:

- $f_{\text{start}} = 28 \text{ MHz}$
- $f_{\text{stop}} = 34 \text{ MHz}$
- Frequency Span = 6 MHz.
- Resolution Bandwidth = 1 MHz (it is IMPORTANT that this bandwidth slightly exceeds the radar receiver's IF bandwidth of about 720 kHz!!)
- Video Bandwidth = 3 MHz
- Points per Trace = 1001
- Sweep Time = Analyzer's self-selecting default for the above settings
- Detector = Positive Peak
- First Trace Display Mode = Maximum Hold on Data Trace 01 (like, yellow)
- Second Trace Display Mode = Clear-Write on Data Trace 02 (like, blue or whatever)
- RF attenuation = 0 dB

The final test will be to determine how much the 5G signal needs to be attenuated to eliminate interference seen at the IF output. The ASR-9 will be configured in its normal operating condition, but with a step attenuator placed in front of the beam switch and STC. The IF output will be observed on the spectrum analyzer while the attenuation is increased. Traces will be recorded with 0, 10, 20, 30, 35, 40, 45, and 50 dB. Further traces will be recorded around the attenuation level where the interference effects disappear.

C.3 Additional Testing

If time permits, there are some additional tests that can be done. Controlled measurements of the ASR-9 receiver can be conducted using the MXG connected at Test Point 1 in Figure D-1. The MXG can be used to inject controlled signals into the receiver and the response can be measured using the spectrum analyzer at any of the other test points. Which waveforms to use and which monitor point can be determined at the site. Test Points 4 or 5 are probably the best monitoring point. It will not be possible to see the input test signal if Test Point 5 is used.

C.4 Test Matrix

Test	Type	Input Waveform	Power Level	Configuration
1	Bench	Swept CW	Low	Beam switch only
2	Bench	Swept CW	Mid	Beam switch only
3	Bench	Swept CW	high	Beam switch only
4	Bench	AWGN	Low	Beam switch only
5	Bench	AWGN	Mid	Beam switch only
6	Bench	AWGN	high	Beam switch only
7	Bench	Gated AWGN	Low	Beam switch only
8	Bench	Gated AWGN	Mid	Beam switch only
9	Bench	Gated AWGN	high	Beam switch only
10	Bench	Simulated 5G	Low	Beam switch only

Test	Type	Input Waveform	Power Level	Configuration
11	Bench	Simulated 5G	Mid	Beam switch only
12	Bench	Simulated 5G	high	Beam switch only
13	Bench	Swept CW	Low	STC only
14	Bench	Swept CW	Mid	STC only
15	Bench	Swept CW	high	STC only
16	Bench	AWGN	Low	STC only
17	Bench	AWGN	Mid	STC only
18	Bench	AWGN	high	STC only
19	Bench	Gated AWGN	Low	STC only
20	Bench	Gated AWGN	Mid	STC only
21	Bench	Gated AWGN	high	STC only
22	Bench	Simulated 5G	Low	STC only
23	Bench	Simulated 5G	Mid	STC only
24	Bench	Simulated 5G	high	STC only
25	Bench	Swept CW	Low	Beam Switch and STC
26	Bench	Swept CW	Mid	Beam Switch and STC
27	Bench	Swept CW	high	Beam Switch and STC
28	Bench	AWGN	Low	Beam Switch and STC
29	Bench	AWGN	Mid	Beam Switch and STC
30	Bench	AWGN	high	Beam Switch and STC
31	Bench	Gated AWGN	Low	Beam Switch and STC
32	Bench	Gated AWGN	Mid	Beam Switch and STC
33	Bench	Gated AWGN	high	Beam Switch and STC
34	Bench	Simulated 5G	Low	Beam Switch and STC
35	Bench	Simulated 5G	Mid	Beam Switch and STC
36	Bench	Simulated 5G	high	Beam Switch and STC
37	IF Char	Local 5G Signal	TBD	Normal Rx Config
38	IF Char	Local 5G Signal	TBD	Bypass beam switch
39	IF Char	Local 5G Signal	TBD	Bypass STC
40	IF Char	Local 5G Signal	TBD	Bypass STC and beam switch
41	IF Char	Local 5G Signal	TBD – 10	Normal with step attenuator
42	IF Char	Local 5G Signal	TBD – 20	Normal with step attenuator
43	IF Char	Local 5G Signal	TBD – 30	Normal with step attenuator
44	IF Char	Local 5G Signal	TBD – 35	Normal with step attenuator
45	IF Char	Local 5G Signal	TBD – 40	Normal with step attenuator
46	IF Char	Local 5G Signal	TBD – 45	Normal with step attenuator
47	IF Char	Local 5G Signal	TBD – 50	Normal with step attenuator
48	IF Char	Local 5G Signal	TBD – XXX	Normal with step attenuator
49	IF Char	Local 5G Signal	TBD – XXX	Normal with step attenuator
50	Add'l test	MXG signal	TBD	TBD

APPENDIX D: MEASUREMENTS DEMONSTRATING THE INTERFERENCE MECHANISM BETWEEN 5G BASE STATION TRANSMITTERS AND ASR-9 RECEIVERS

Following the Test Plan of Appendix C, three NTIA personnel⁶⁶ worked with FAA technical personnel⁶⁷ at the FAA Atlantic City Technical Center on September 24 and 25, 2024, to conclusively resolve the exact interference mechanism between B41 5G base stations and ASR-9 receivers. We provide here a readable, streamlined version of the work and its results.

Previous work had indicated that the core of the interference problem lay in the RF beam switch located in front of the STC stage, with the possibility that other RF beam switches could be problematic as well. All of these beam switches were (are) located in front of the radar receiver's RF bandpass filter. Somehow, it/they caused 5G input power, confined within the B41 channel (at frequencies below 2690 MHz), to spread across the radar receiver's radio spectrum band of 2700–2900 MHz. A second component, the STC stage, also needed to be examined.

The beam switches and STC stage are solid-state circuits, based on PIN diode technology. Their power overload points, where they would begin to behave non-linearly, were specified to be 0 dBm total power input. At the outset of the bench testing of these components, their overload points were measured and found to be a bit higher, +6 dBm total input power. Figure D-1 shows linearity of the switch output even at +8 dBm input power.

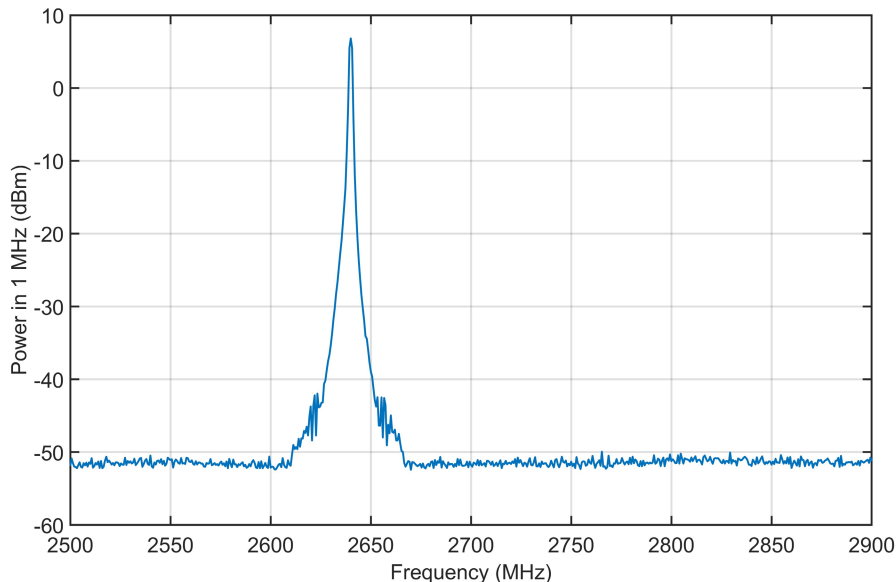


Figure D-1. The beam switch was well-behaved with a CW input as high as +8 dBm total power.

The 5G power levels that were spreading across the spectrum at the Atlantic City Technical Center location were -20 dBm/MHz peak, detected, or -30 dBm RMS average detected. This

⁶⁶ G. Sanders, B. Nelson, and J. Yoe

⁶⁷ A. Nandi and O. Valle-Colon

equated to total power input of 0 dBm across the 100-MHz wide B41 5G channel, or -10 dBm total power RMS average detected.

Peak or average, the input 5G power levels were well below the non-linear input thresholds. Leaving, still, the question of how the power was spreading out of the switches. Months earlier, we had observed that the spreading looked like the Fourier wave effect of chopping a carrier wave into pulses. We pursued this possibility with a series of bench tests that began with chopped carrier waves, and eventually progressed to chopping the actual, local 5G signals with both a bench-mounted beam switch and a beam switch inside the radar receiver.

The phenomenon of Fourier spectrum spreading is illustrated in Figure D-2. The mathematics of waves, and of the behavior of energy and time, dictate that localization of energy (or, equivalently, power) in time forces spreading in frequency. As drawn in Figure D-1, the waveform chopping can be purely mechanical, involving no circuits, electronics or batteries. Just turn a rotating shutter over a window in an otherwise impermeable wall, and the single-wave frequency that is going in on one side comes out of the other side as an infinitely large family of waves, of infinitely many frequencies and amplitudes. This is what the radar receivers' beam switches are doing when they send the input 5G signals down alternating pipes in the radars.

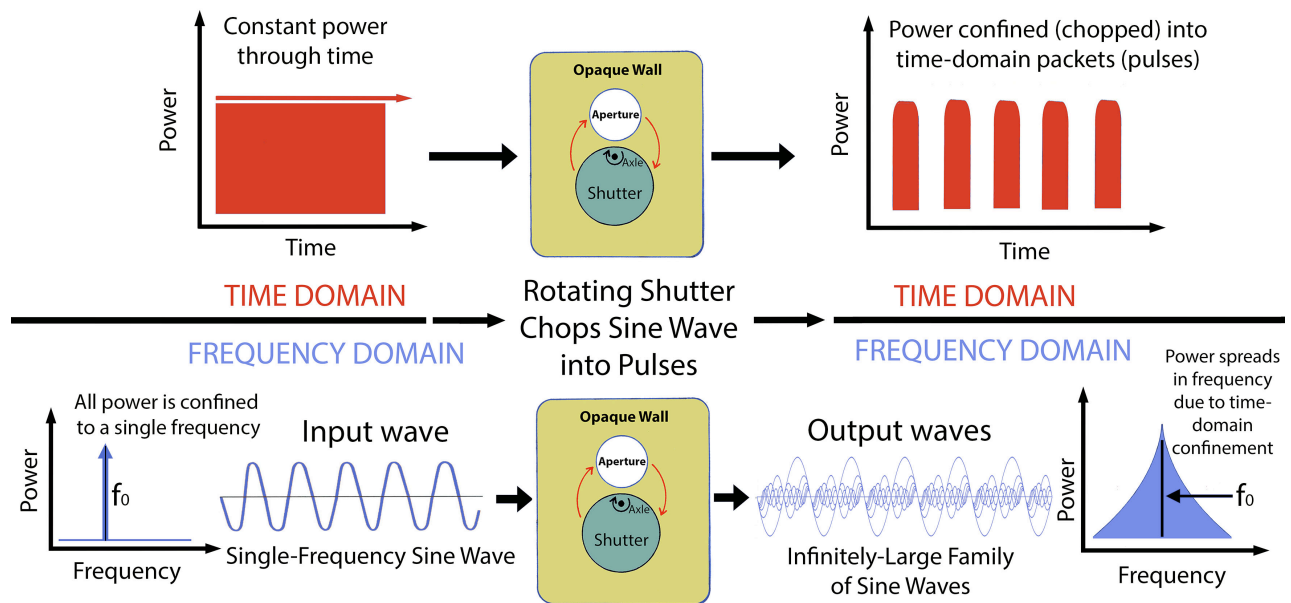


Figure D-2. Chopping a single-frequency wave into pulses in the time domain forces an infinitely large family of output waves to form across the entire spectrum.

We see the same spreading with a radar beam switch on a bench, when we go from OFF (no switching) to ON (switching activated), in Figure D-3.

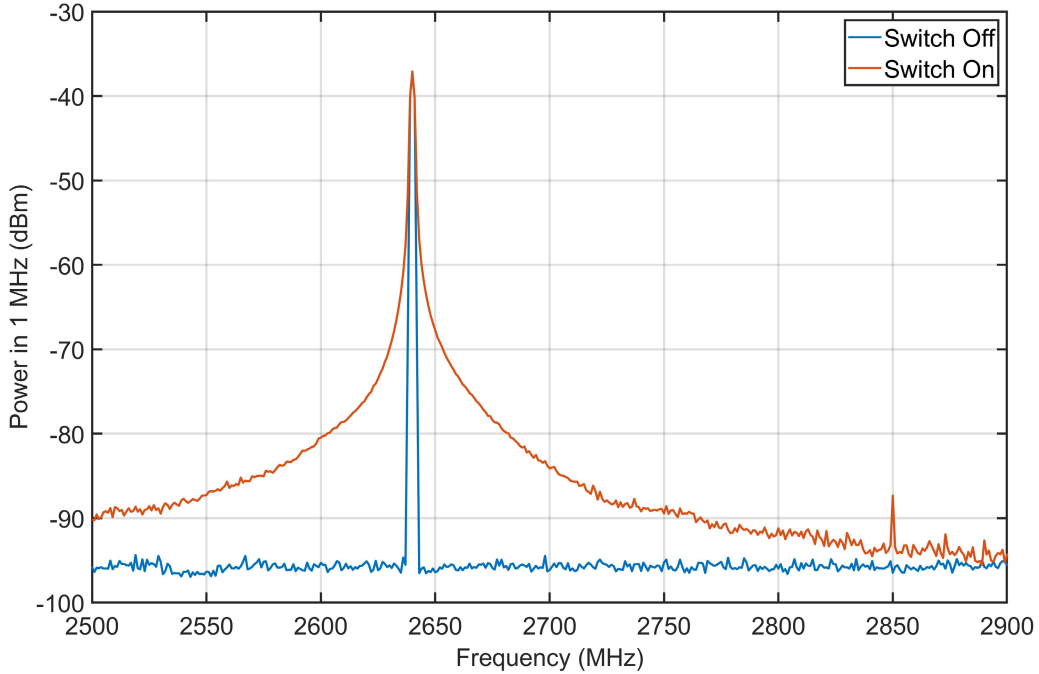


Figure D-3. A radar beam switch converts a carrier wave to a spread spectrum when it activates.

In our next step, we compared the CW spreading of the beam switch to the spreading of a carrier wave that we pulsed from a generator with the same characteristics as the switch’s operation, as shown in Figure D-4.

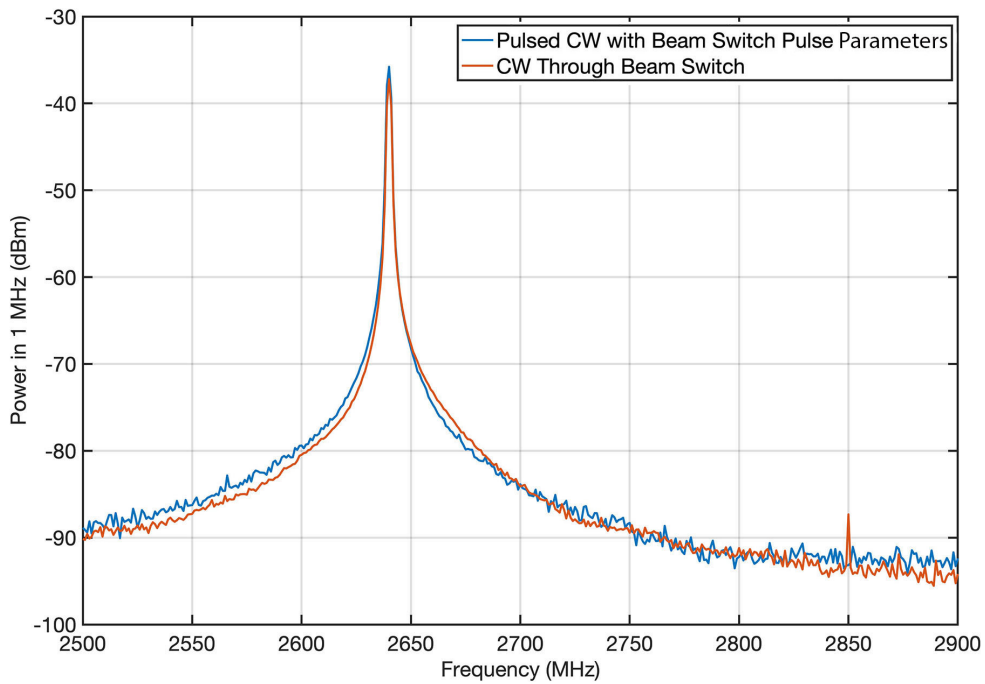


Figure D-4. Comparison of a time-gated (no beam switch) carrier wave’s Fourier spectrum spreading with the output of an ASR-9 beam switch with a CW input.

As a further check, we interchanged positions between the beam switch and STC, to mimic the ASR-9 non-WSP radar configuration of some sites. The 5G signal was injected directly into the STC, and the output of the STC was connected to the input of the beam switch. The result, which was null, is shown in Figure D-5.

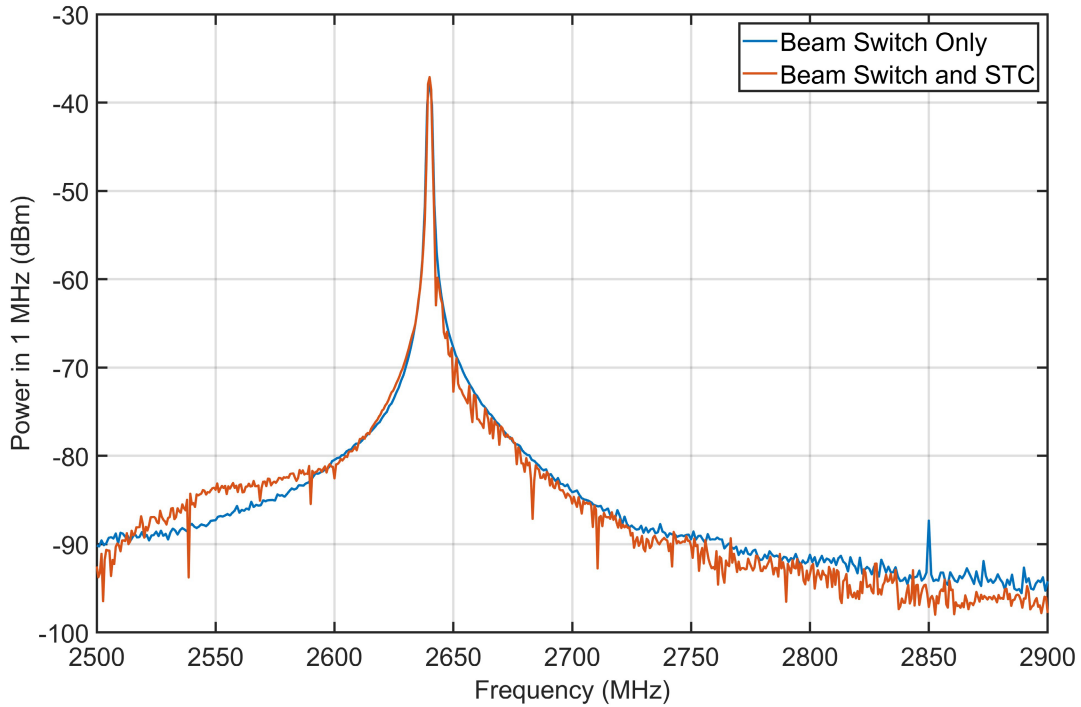


Figure D-5. Comparison of beam switch alone to switch plus STC. Null result.

We also examined the effect of changing the input power level on the beam switch Fourier spreading. The effect was linear, as shown in Figure D-6.

As a final demonstration of the Fourier spectrum spreading effect on the input 5G signal, we routed the 5G input from the radar antenna, when the antenna was locked on a local 5G base station tower, into the beam switch on the bench. The result is shown in Figure D-7.

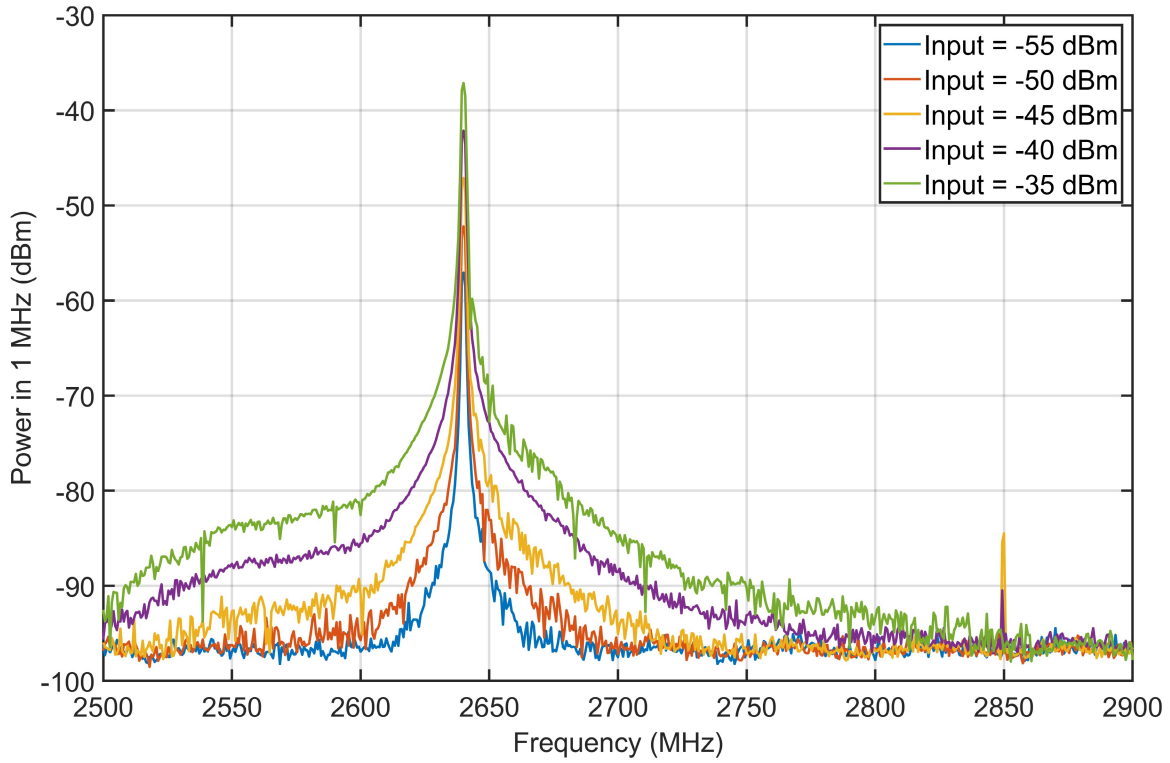


Figure D-6. Linearity of the Fourier spectrum spreading with input power levels.

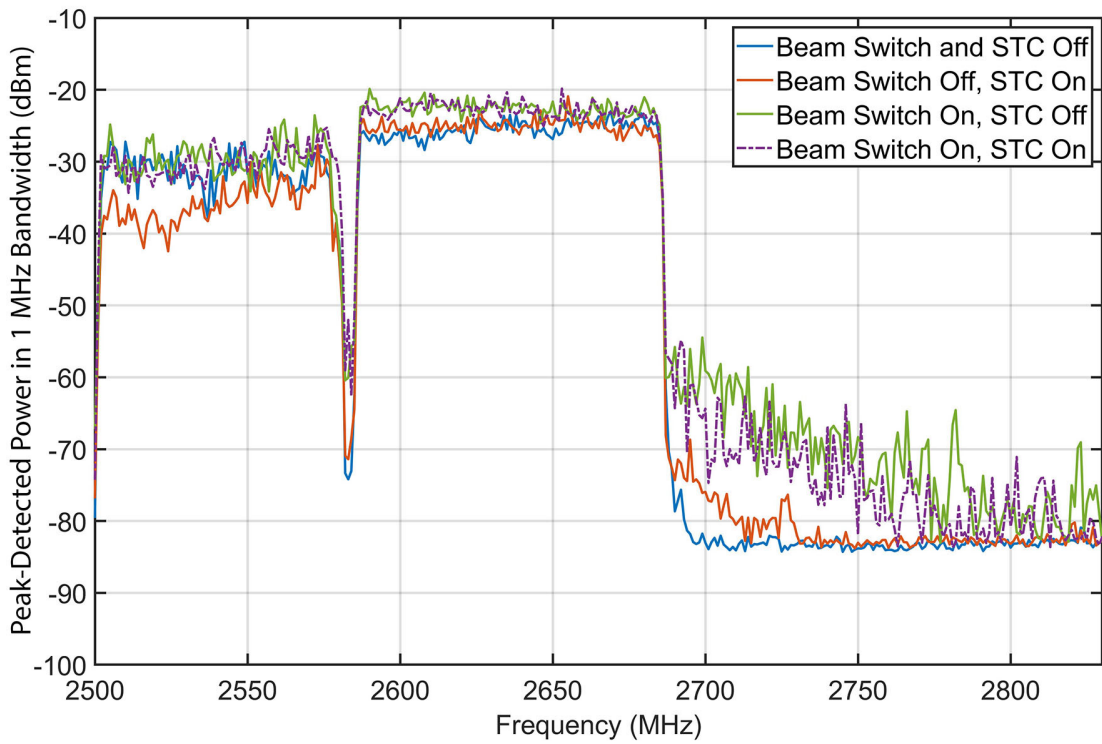


Figure D-7. Fourier spreading of a local, live 5G base station signal by a beam switch operated on the bench at the FAA Technical Center.

We conclude by noting that there are multiple RF beam switches in the ASR-9 receiver front ends. Depending upon the exact layout of a given ASR-9 station's circuits (i.e., with or without the weather system processor option), the 5G power which is being spectrum-spread by *each and all* of these switches can generate potentially confusing outputs when the interference is being analyzed (trouble-shot) during on-the-spot work at any given station. We believe we may have seen some-such confusing results ourselves, at one point or another at the Technical Center.

Putting such potential confusion aside, we note further that Fourier spectrum spreading must occur in each radar receiver beam switch, and the spectrum-spread power then moves downstream in the receiver from each switch, through the remaining receiver circuitry. All of the switches need to be protected, to prevent this problem from manifesting in the radars' target and weather displays.

APPENDIX E: 5G BASE STATION SPECTRUM CERTIFICATION MEASUREMENT DISCUSSION

5G base station transmitters’ RF spectrum emission certification measurements are described in FCC Laboratory Certification Test Reports.⁶⁸ These reports describe compliance measurements performed per requirements of the Code of Federal Regulations 47 (47 CFR), Parts 2 and 27. These measurements show the transmitters’ intentionally occupied bandwidths, channel-edge roll-offs, edge-of-band emissions and spurious emissions when the transmitters are in a variety of operational modes.

Two example certification measurement results, for one of the B41 5G base station models of this study, are shown in Figure E-1 and Figure E-2. Figure E-1 shows the edge-of-band emissions when this transmitter is in its (70 + 50) MHz mode. Figure E-2 shows the spurious emissions measurement across part of the FAA/DoD ASR-9/GPN-27 2700–2900 MHz band when the 5G base station is in that mode.

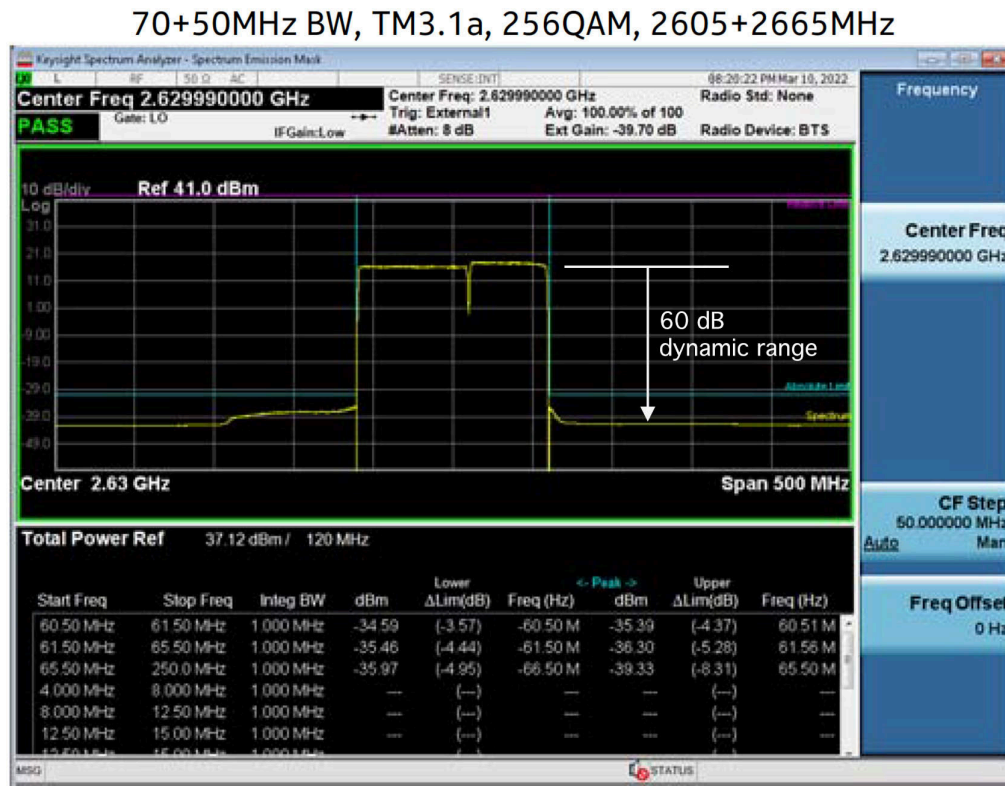


Figure E-1. Edge-of-band certification measurement for a 5G base station’s (70 + 50) MHz transmission mode. Dynamic range (60 dB) annotation added by the authors.

⁶⁸ We do not reference the specific FCC spectrum certification Test Reports for B41 5G base station models Radio-A and Radio-B in this NTIA Technical Report, to preserve the anonymity of these units’ identifications.

2.75GHz – 3GHz

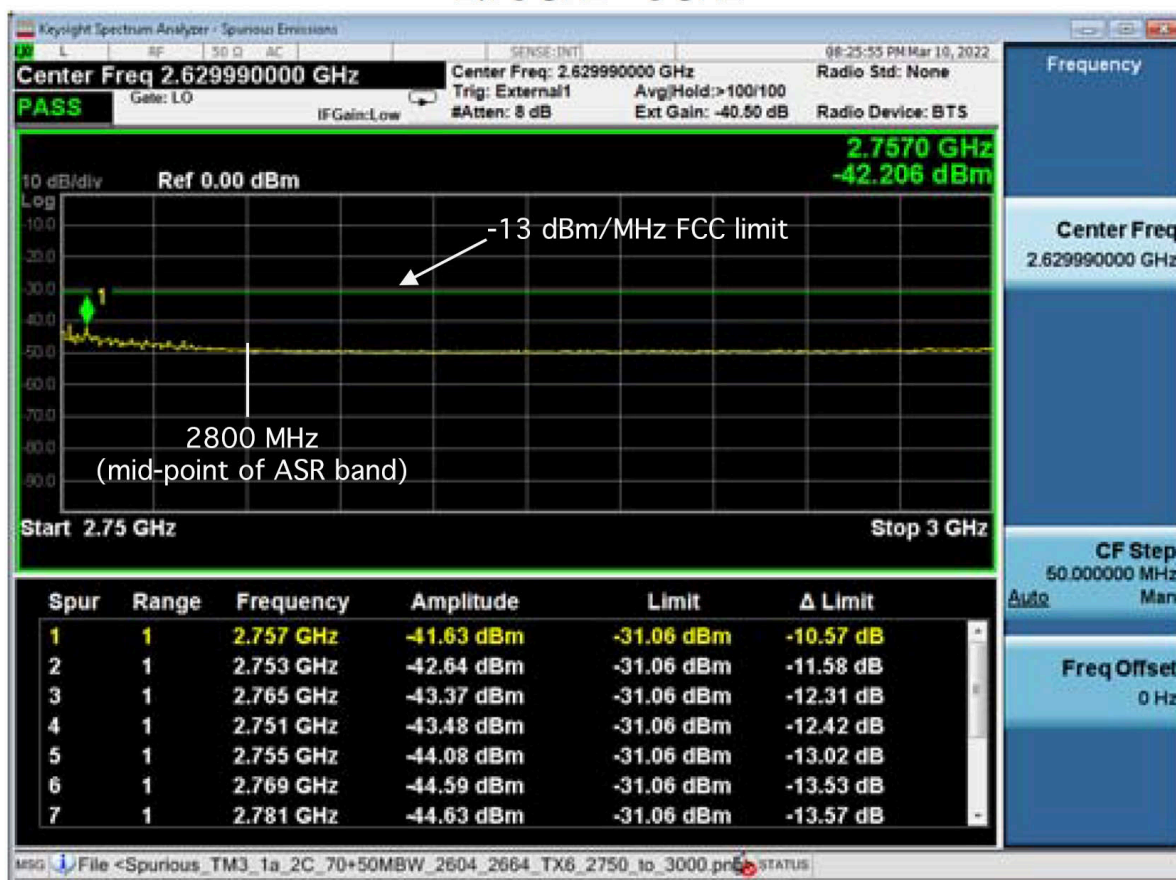


Figure E-2. Spurious emissions certification measurement result for the radio’s (70 + 50) MHz transmission mode. ASR-band frequency and FCC limit-level annotations added by the authors.

In the edge-of-band measurement, the available measurement dynamic range of 60 dB is adequate to demonstrate the transmitter’s occupied bandwidth and its sharp power roll-off on its channel edge. This is an excellent measurement, made with costly, state-of-the-art equipment. Emphasizing that we take no issue with the measurement (which we believe was well-performed), we note that the measurement machine’s dynamic range (DR) is six orders of magnitude in power, or 60 dB.

Sixty decibels was the DR limit of old-style analog spectrum analyzers in the 1970s. Half a century later, it is still the typical limit of even the best, now-current digital-type measurement equipment, as we see in this (typical) case. No performance improvement or technical progress has been made on this crucially important measurement parameter in more than five decades.

While 60 dB of DR is adequate for certification measurements such as specified in 47 CFR, Parts 2 and 27 (and we take no issue with those certification requirements and procedures), *60 dB is technically inadequate for many, perhaps most, EMC and spectrum coexistence technical analyses.* The reason 60 dB is inadequate is that interference can (and does) occur

between radio systems due to unwanted transmitter emissions that are more than 60 dB below those transmitters' intentional-emission power levels. For EMC and coexistence studies and analyses, we consider⁶⁹ that a DR of 100 dB is needed.

To phrase the situation colloquially, the 60 dB of DR that we see that the state-of-the-art measurement result of Figure E-1 cuts off our view of the transmitter's emissions just as things were about to get interesting. We needed another 40 dB of DR to see down where we need to go for EMC and spectrum coexistence studies and analyses.

There are ways to see further down into a transmitter's emissions. The approach is to use an RF bandpass filter that passes (and is tuned to) the transmitter's out-of-band (OoB) and spurious emissions⁷⁰ while rejecting the transmitter's intentional-radiation power.

In the NTIA/ITS RSMS, the bandpass filter is a yttrium-iron-garnet (YIG) technology design (Figure 19 showing it in the system's block diagram schematic) which passes signals on tuned measurement frequencies in the transmitter's OoB and spurious range, while decoupling the measurement system from other frequencies (of the transmitter's intentional emissions) with 70 dB or more of rejection. With this much rejection, the instantaneous DR of 60 dB in state-of-the-art spectrum analyzers and signal analyzers is extended by another 70 dB, to achieve as much as 130 dB of total dynamic range.

Noting that the 5G transmitters' Certification Test Reports state that these transmitters' emissions were reduced for spurious-emissions measurements,⁷¹ we take this to mean that a similar approach was used to extend the measurement system's DR downward, below the signal analyzer's instantaneous DR of 60 dB.

In Figure E-2, we see that some measurable unwanted emissions are in fact visible at frequencies as high as 2800 MHz, in the middle of the FAA/DoD ASR/GPN band (2700–2900 MHz).

Qualitatively, this FCC certification measurement result agrees with the radiated spectra that we measured at Table Mountain. To be useful in EMC and coexistence analyses and studies, however, we would need to know the power levels of those unwanted emissions relative to the transmitter's intentional emissions in the certification measurement. (This is what we have done with our own data in Section 3 of this report, where we have normalized many of our measurement results to 0 dB.)

In the certification measurement, the measured unwanted emissions are plotted relative to the FCC's limit of $(43 + 10\log(P, \text{ watts}))$ relative to the transmitter's intentional power $(10\log(P, \text{ watts}))$, which in all cases reduces to -13 dBm. (Specifically, the FCC limit is -13 dBm/MHz power density for 5G radio transmitters, as annotated in Figure E-2.)

⁶⁹ Based on over four decades of experience in these sorts of studies.

⁷⁰ OoB and spurious emissions are together referred to as unwanted emissions.

⁷¹ Quoting from one of the Certification Reports, "The RF output from the transmitter was reduced (to an amplitude usable by the receivers) using calibrated attenuators."

This FCC limit is graphed in Figure E-2 at a level of -31.06 dBm on the signal analyzer's display, in the analyzer's selected resolution bandwidth (which we believe to have been about 1 MHz).⁷² From a spectrum certification standpoint, this is an excellent result; we take no issue with it.

Unfortunately, the information provided in the certification testing and results reporting does not allow us to determine what the transmitter's unwanted emission levels, as shown in Figure E-2, were as compared to the radio's intentional radiation power level. This prevents us from quantitatively comparing our own field-measurement results of Section 3 of this report to the certification result of Figure E-2.

The upshot of this discussion is that, while 47 CFR spectrum-certification tests and measurements are well-adapted for flagging obvious (within 60 dB of the intended-emission transmit-power level (that is, within -60 dBc)) unwanted transmitter emissions that could cause interference to adjacent-band receivers, *detailed additional unwanted-emission measurements of transmitters are needed in cases where relatively low-power unwanted transmitter emissions may nevertheless cause interference to especially sensitive adjacent-band receivers.*

This happens to be the case in this study. Here, certification test results for high-power transmitters newly introduced in a previously quiet or nearly quiet band do not rule out unwanted emissions that are more than (i.e., beyond) -60 dBc. Such spectrum-test-compliant unwanted emissions outside the transmitters' band would, if co-channel to adjacent-band, sensitive receivers with high-gain antennas, cause interference to those receivers. Radar receivers may experience harmful interference effects at interference-to-noise (I/N) levels between -3 dB and -10 dB, and such levels may be reached by co-channel, unwanted transmitter emissions at levels of -60 dBc, and even lower levels than that, when produced by high-power transmitters in close physical proximity to such radar receivers.

It was a fortunate outcome that, in this case study, the adjacent-band coexistence issue or challenge has turned out to be primarily a receiver-internal effect from the licensed, on-tuned, in-band emissions of 5G base stations. Spectrum-certification test results with a DR of 60 dB would have been unlikely to have identified the other interference mechanism, co-channel interference to the receivers from 5G unwanted emissions, if that mechanism had occurred. It was that uncertainty that partly drove our need to perform the measurements of Section 3 in this Technical Report.

⁷² We do recommend including signal-analyzer resolution bandwidths in Test and Certification Reports, and in all such measurements in general. Readers should not have to guess the measurement bandwidths when they are reading data. Without analyzer measurement bandwidths, it is impossible to work out spectrum power-density values. We also recommend more-legible, higher-resolution graphs. It is frustrating to try to read nearly illegible graphs, with labels that verge on being unreadable. Also, graph scales should use counting divisions of twos, fives, or tens; and should have start, stop and center values that are in zeros, fives or tens. It is difficult, as in Figure E-1 for example, to read frequencies from a center-value of 2.63 GHz. A center value of 2.60 GHz, with higher-quality resolution, would have made that graph readable. This is what happens when signal analyzers are allowed to default to their own scale values, instead of being manually over-ridden by human-interpretable values, and/or the final, published data sets are not, at least, eventually re-graphed and presented legibly with human-readable scales.

Again emphasizing that we take no issue with existing FCC unwanted emission limits and 47 CFR certification and testing procedures, we state that, from a technical standpoint, additional (preferably radiated) transmitter emission measurements such as have been performed in this study, and which are described and presented in Section 3, may be necessary in the future to prevent (or correct) co-channel interference from unwanted transmitter emissions to sensitive receivers in an adjacent band.

BIBLIOGRAPHIC DATA SHEET

1. PUBLICATION NO. NTIA TR-25-577		2. Government Accession No.	3. Recipient's Accession No.
4. TITLE AND SUBTITLE NTIA Case Study: Adjacent-Band Coexistence Between 5G Base Station Transmitters and Air Traffic Control Radar Receivers		5. Publication Date December 24, 2024	
		6. Performing Organization Code NTIA/ITS-M	
7. AUTHOR(S) Frank H. Sanders, Geoffrey A. Sanders, Brian D. Nelson, Robert L. Sole, Oscar Valle-Colon		9. Project/Task/Work Unit No. 3172112-300 3170011-300	
8. PERFORMING ORGANIZATION NAME AND ADDRESS Institute for Telecommunication Sciences National Telecommunications & Information Administration U.S. Department of Commerce 325 Broadway Boulder, CO 80305		10. Contract/Grant Number.	
		12. Type of Report and Period Covered NTIA Technical Report	
11. Sponsoring Organization Name and Address National Telecommunications & Information Administration Herbert C. Hoover Building 14th & Constitution Ave., NW Washington, D.C. 20230			
14. SUPPLEMENTARY NOTES			
15. ABSTRACT (A 200-word or less factual summary of most significant information. If document includes a significant bibliography or literature survey, mention it here.) Introduction of Fifth Generation New Radio (5G NR) base station transmitters into 2590–2690 MHz in the U.S., adjacent to the spectrum band 2700–2900 MHz used by air traffic control radars, has resulted in interference effects in some safety-of-life Airport Surveillance Radar receivers, especially the Model 9 (ASR-9). This report describes work performed by the National Telecommunications and Information Administration (NTIA); the Federal Aviation Administration (FAA); the wireless carrier T-Mobile; and two 5G equipment manufacturers to understand and resolve this coexistence challenge. Although the problem initially appeared to be due to 5G unwanted emissions within the radar band, detailed work shows that this is not the typical case. Instead, a novel spectrum-spreading effect within the radar receivers generates power from adjacent-band 5G input signals on the receivers' tuned, radar-band frequencies. This occurs despite the receivers being equipped with robust radiofrequency (RF) bandpass filtering. The effect is generated by solid-state RF switches in the receivers. The spectrum spreading is due to ordinary physics of the switches' time-chopping of adjacent-band input 5G waveforms. Possible solutions are presented. This report is written as an illustrative case study, emphasizing not only the technical problem but also the study's underlying scientific and engineering process.			
16. Key Words (Alphabetical order, separated by semicolons) 5G; 5G NR; 5G emissions; 5G emission spectrum; 5G radiation; 5G spectrum bands; air traffic control radars; airport surveillance radars; electromagnetic coexistence; electromagnetic compatibility; national air space safety; radar receiver interference; radio spectrum coexistence; radio spectrum compatibility; wireless coexistence with radars			
17. AVAILABILITY STATEMENT <input checked="" type="checkbox"/> UNLIMITED. <input type="checkbox"/> FOR OFFICIAL DISTRIBUTION.		18. Security Class. (This report) Unclassified	20. Number of pages 128
		19. Security Class. (This page) Unclassified	21. Price: N/A

NTIA FORMAL PUBLICATION SERIES

NTIA MONOGRAPH (MG)

A scholarly, professionally oriented publication dealing with state-of-the-art research or an authoritative treatment of a broad area. Expected to have long-lasting value.

NTIA SPECIAL PUBLICATION (SP)

Conference proceedings, bibliographies, selected speeches, course and instructional materials, directories, and major studies mandated by Congress.

NTIA REPORT (TR)

Important contributions to existing knowledge of less breadth than a monograph, such as results of completed projects and major activities.

JOINT NTIA/OTHER-AGENCY REPORT (JR)

This report receives both local NTIA and other agency review. Both agencies' logos and report series numbering appear on the cover.

NTIA SOFTWARE & DATA PRODUCTS (SD)

Software such as programs, test data, and sound/video files. This series can be used to transfer technology to U.S. industry.

NTIA HANDBOOK (HB)

Information pertaining to technical procedures, reference and data guides, and formal user's manuals that are expected to be pertinent for a long time.

NTIA TECHNICAL MEMORANDUM (TM)

Technical information typically of less breadth than an NTIA Report. The series includes data, preliminary project results, and information for a specific, limited audience.

For information about NTIA publications, contact the NTIA/ITS Technical Publications Office at 325 Broadway, Boulder, CO, 80305 Tel. (303) 497-3572 or e-mail ITSinfo@ntia.gov.